

TÁCIA TAVARES DE AQUINAS LIGUORI

**Desenvolvimento de matrizes celulares para o tratamento
de cardiomiopatia dilatada**

**Novel regenerative medicine approach to treat
dilated cardiomyopathy**

Tese apresentada à Faculdade de Medicina da
Universidade de São Paulo e a Rijksuniversiteit
Groningen, para obtenção do título de dupla
titulação, título de Doutor em Ciências

Programa de Cirurgia Torácica e
Cardiovascular (Faculdade de Medicina da
Universidade de São Paulo - FMUSP)

Orientador: Prof. Dr. Luiz Felipe Pinho Moreira

Programa REGENERATE
(University Medical Center Groningen - UMCG)
Coorientador: Prof. Dr. Martin Conrad Harmsen

**SÃO PAULO
2020**

Dados Internacionais de Catalogação na Publicação (CIP)

Preparada pela Biblioteca da
Faculdade de Medicina da Universidade de São Paulo

©reprodução autorizada pelo autor

Liguori, Tácia Tavares de Aquinas

Desenvolvimento de matrizes celulares para o tratamento de cardiomiopatia dilatada = Novel regenerative medicine approach to treat dilated cardiomyopathy / Tácia Tavares de Aquinas Liguori -- São Paulo, 2020.

Tese(doutorado)--Faculdade de Medicina da Universidade de São Paulo.

Programa de Cirurgia Torácica e Cardiovascular.

Rijksuniversiteit Groningen. Programa REGENERATE.

Orientador: Luiz Felipe Pinho Moreira.

Orientador Estrangeiro: Martin Conrad Harmsen.

Descritores: 1.Hidrogel 2.Matriz extracelular 3.Medicina regenerativa
4.Células tronco mesenquimais 5.Secretoma 6.Insuficiência cardíaca 7.Modelos
animais 8.Células endoteliais 9.Fibroblastos cardíacos 10.Fibrose cardíaca.

USP/FM/DBD-113/20

Responsável: Erinalva da Conceição Batista, CRB-8 6755

DEDICATORY

Ao meu esposo, Gabriel,

Por ser meu companheiro, conselheiro e confidente durante todo esse caminho. Por compreender e apoiar meu amor aos animais. É uma honra dividir mais esse projeto com você.

Aos animais,

Que foram tão essenciais ao desenvolvimento dessa pesquisa. Espero ser capaz de contribuir para a cura de tantos outros através da medicina regenerativa.

ACKNOWLEDGMENTS

Motivos para agradecer não faltam!

Eu não poderia deixar de agradecer aos animais que tornaram possível a realização dessa tese. Como Médica Veterinária e adoradora dos animais, todos se preocupavam como seria essa vivência. Uma frase: Não é fácil! Nós ainda estamos longe de não precisarmos mais utilizá-los mas, com ética, integridade e muito humanismo podemos extinguir o sofrimento desse processo. Durante dois anos tive a oportunidade de conhecer mais dessa espécie tão cativante, e a palavra “rato” deixou de significar aquela imagem pejorativa e passou a ser sinônimo de olhinhos vermelhos, pêlos branquinhos e patinhas pequeninas. Eles foram de fundamental importância para a realização desse projeto. Um sinto muito, e um muito obrigada, ao Bones, e a todos os seus irmãozinhos.

Ao meu amigo, colega de profissão e esposo,

Para mim você será sempre o maior responsável por tudo isso! Obrigada por ter iniciado essa parceria internacional, por ter mostrado tanta dedicação tendo como consequência a abertura de portas para mim e para outros tantos que vieram e vão vir! Obrigada por me retificar, oito anos atrás: “Ao lado de um grande homem sempre tem...”. Foram anos de tanto aprendizado que, olhando para trás, a sensação é que se passaram décadas. Obrigada por apostar em mim, e me levar com você para esse mundo tão paralelo, louco e mágico que é a Medicina Regenerativa! Obrigada pela rigidez do início e pelo ombro amigo quando os experimentos não deram certo 1, 2, 3, 4 vezes (ninguém disse que seria fácil, mas também ninguém disse que, por vezes, seria muito difícil)... Em compensação, obrigada por vibrar comigo em cada vitória!

Em cada publicação, em cada apresentação bem sucedida. Eu, particularmente nunca vou esquecer a sensação de euforia e felicidade depois de meses de trabalho duro, debruçados em uma hipótese, horas realizando um Western Blot e vê-lo terminado com o melhor resultado possível. Bandas lindas e perfeitas, ilustrando exatamente o que esperávamos encontrar! Obrigada, por contribuir tanto com meu crescimento pessoal e profissional. Como costumo brincar com você, por ser meu “coaching de vida”, aquele que me impulsiona a ser mais, a ir além e alcançar nossos objetivos. Obrigada por uma vida repleta de experiências! Sobretudo, obrigada por ser aquele responsável pela concretização do meu maior sonho: Obrigada por ser minha família, e me proporcionar o amparo, a paz e segurança que você me traz. Eu serei sempre sua maior admiradora, seu alicerce e seu suporte durante toda essa caminhada linda que você ainda tem pela frente! Eu estarei sempre aqui.. te amo! Obrigada pelo privilégio de dormir e acordar todos os dias com você.

Obrigada às nossas famílias por terem nos apoiado em todos os momentos. Em especial aos meus pais, por saberem a importância de uma boa educação e, por mais difícil que fosse, apostarem no meu estudo. À minha irmã, por incentivar meus estudos, desde a época da tabuada. À Tati, ao Finnis, à Sniffa e, ao Pepe (por breves meses). Eles foram meus primeiros pacientes, e me moldaram a ser o que sou hoje. Foram 18 anos de amizade e companheirismos sem iguais! Eles estão em meu pensamento e ação no que quer que eu faça. Obrigada por terem me completado durante tantos anos.

Obrigada à USP, à University of Groningen e aos meus orientadores, Prof. Luiz Felipe e Marco. Obrigada pela oportunidade, pela paciência e pelo voto de confiança. De aceitarem orientar uma aluna sem experiência prévia na área, mas com muita vontade de aprender. Uma vez, alguém me disse que na vida o que conta é o que se faz com

as oportunidades que recebe e, hoje, gostaria de dizer que espero ter atendido as expectativas, pois dei meu máximo! Fiz e refiz, aprendi, li, me reconstruí para ser merecedora dessa oportunidade. Obrigada por tantas reuniões que foram moldando e lapidando o que esta tese é hoje. Obrigada pela liberdade de conduzir essa pesquisa da maneira como eu achava mais adequada. Obrigada pela oportunidade de divulgar os nossos estudos apresentando-os em congressos internacionais. Prof Luiz Felipe, obrigada pela amizade em tempos difíceis e por estar conosco torcendo sempre pelo melhor.

Gostaria de agradecer à minha banca de qualificação por apontarem pontos de melhorias e contribuindo para o aperfeiçoamento desta tese: Prof. Cristina Camargo, Prof. Paulo Cardoso e Prof. Denise Swartz. Em especial à última, que em um futuro breve, consigamos unir forças e contribuir na vida de muitos cães e gatos.

Obrigada a todos os colegas que contribuíram de maneira construtiva para esse trabalho. Ao Henk, pelo fornecimento de tantas células endoteliais, que me permitiram realizar grande parte dessa pesquisa. Ao Cristiano, Coutinho e Fernando por terem transmitido seu conhecimento para mim. Um obrigada especial ao nosso aluno e amigo, Viktor, que se virou em dois e me permitiu tê-lo um pouquinho como meu aluno também. Tudo sem muita pressão e nenhuma responsabilidade: “Viktor, você só não pode deixar contaminar. Mas de resto, tranquilo”.

Um obrigada a todos vocês e a Ele.

EPIGRAPH

“Change ... we don’t like it, we fear it. But we can’t stop it from coming. We either adapt to change, or we get left behind. It hurts to grow. Anybody who tells you it doesn’t, is lying. But here’s the truth: Sometimes, the more things change, the more they stay the same. And sometimes, oh, sometimes, change is good. Sometimes, change is ... everything!”

Shonda Lynn Rhimes

SUMMARY

| | |
|--|------|
| DEDICATORY (<i>Portuguese</i>) | i |
| ACKNOWLEDGEMENTS (<i>Portuguese</i>) | ii |
| EPIGRAPH | v |
| SUMMARY | vi |
| RESUMO/ABSTRACT | viii |
| GENERAL INTRODUCTION | 1 |
| CHAPTER 1 | 11 |

Fibroblast growth factor-2, but not the adipose tissue-derived stromal cells secretome, inhibits TGF- β 1-induced differentiation of human cardiac fibroblasts into myofibroblasts

Published in Scientific Reports. DOI: 10.1038/s41598-018-34747-3

| | |
|-----------------|----|
| CHAPTER 2 | 22 |
|-----------------|----|

Adipose tissue-derived stromal cells' conditioned medium modulates endothelial-mesenchymal transition induced by IL-1 β /TGF- β 2 but does not restore endothelial function

Published in Cell Proliferation. DOI: 10.1111/cpr.12629

CHAPTER 3 ----- 35

Bioactive decellularized cardiac extracellular matrix-based hydrogel as a sustained-release platform for human adipose tissue-derived stromal cell-secreted factors.

Submitted.

CHAPTER 4 ----- 69

Intrapericardial injection of hydrogels derived from decellularized cardiac extracellular matrix loaded with mesenchymal stromal cells and their secretome: a novel therapeutic approach to treat cytostatics-induced dilated cardiomyopathy.

To be submitted.

CRITICAL ANALYSIS AND FUTURE PERSPECTIVES ----- 119

Resumo

Liguori TTA. Desenvolvimento de matrizes celulares para o tratamento de cardiomiopatia dilatada [tese]. São Paulo: “Faculdade de Medicina, Universidade de São Paulo”, 2020.

Embora muito se tenha avançado no desenvolvimento de novas terapias para as cardiomiopatias, ainda não existe uma opção curativa que substitua a necessidade do transplante. A medicina regenerativa vem se consolidando pelo mundo ao trazer novas alternativas para doenças cardíacas crônicas. Embora os cardiomiócitos sejam afetados de maneira importante no processo de degeneração do órgão, sendo os responsáveis pela contração cardíaca, eles não são, na verdade, as células mais abundantes no coração de mamíferos. Esse lugar é ocupado pelos fibroblastos: células alongadas presentes entre as fibras musculares e que ajudam na manutenção do equilíbrio da matriz extracelular. Durante a insuficiência cardíaca, dois processos contribuem para o desbalanço desse equilíbrio e consequente fibrose e remodelamento do coração. O primeiro processo é a diferenciação de fibroblastos em miofibroblastos; o segundo é a transição de células endoteliais em mesenquimais (EndMT). Ambos os processos levam ao aumento de células responsáveis por depositar matriz extracelular e, portanto, à fibrose e remodelamento. Assim, abordagens direcionadas a impedir o progresso desses processos podem ser uma alternativa interessante para o tratamento das cardiomiopatias. Utilizando-se de células-tronco, biomateriais e fatores de crescimento, o objetivo desta tese é a criação de uma nova abordagem terapêutica que vise diminuir ou extinguir o processo de fibrose no tecido cardíaco, a fim de manter preservada a função do órgão. Para isso,

em nosso primeiro estudo, ***Fibroblast growth factor-2, but not the adipose tissue-derived stromal cells secretome, inhibits TGF- β 1-induced differentiation of human cardiac fibroblasts into myofibroblasts*** (Scientific Reports, 2018) fibroblastos cardíacos humanos primários, foram cultivados e sua diferenciação foi estimulada através do uso de *TGF- β 1 in vitro*. Como tentativa de prevenir sua transformação em miofibroblastos, foi realizada a coleta do secretoma de células estromais derivadas de tecido adiposo (ASC-CMed) e os fibroblastos foram tratados com tal secretoma. Neste trabalho, os resultados demonstraram que não foi possível inibir a diferenciação dos fibroblastos em miofibroblastos com o uso de ASC-CMed. Em nosso segundo estudo, ***Adipose tissue-derived stromal cells' conditioned medium modulates endothelial-mesenchymal transition induced by IL-1 β /TGF- β 2 but does not restore endothelial function*** (Cell Proliferation, 2019), induzimos a diferenciação de células endoteliais através de um ambiente pró-inflamatório e pró-fibrótico, utilizando IL-1 β e *TGF- β 1*, e buscamos impedir a diferenciação dessas utilizando ASC-CMed. Os resultados mostraram que, embora as células endoteliais não tenham retornado a um fenótipo funcional, nós conseguimos inibir o processo de EndMT. Nosso terceiro estudo, ***Bioactive decellularized cardiac extracellular matrix-based hydrogel as a sustained-release platform for human adipose tissue-derived stromal cell-secreted factors*** (submetido), teve como objetivo desenvolver uma plataforma baseada em um hidrogel derivado de matriz extracelular miocárdica para liberação do ASC-CMed, processo que foi testado utilizando em diferentes concentrações de secretoma (1x, 10x e 100x). Nossos resultados demonstraram que esse biomaterial demonstrou ser uma excelente plataforma para a liberação fatores de crescimento de maneira contínua. Finalizando a presente tese, com a utilização desse mesmo hidrogel, no quarto estudo, ***Intrapericardial injection***

of hydrogels derived from decellularized cardiac extracellular matrix loaded with mesenchymal stromal cells and their secretome: a novel therapeutic approach to treat cytostatics-induced dilated cardiomyopathy, nós levamos em consideração a resposta imune *in vivo*, ao realizarmos a aplicação intrapericárdica do hidrogel carregado de ASC e seu secretoma em um modelo crônico de cardiomiopatia dilatada em ratos. Neste estudo foi possível concluir que nossa terapia foi capaz de diminuir a fibrose cardíaca e reduzir o remodelamento, bem como melhorar a função cardíaca e parâmetros hemodinâmicos dos animais. Assim, o conteúdo da presente tese demonstra que a aplicação intrapericárdica de um hidrogel composto de matriz extracelular miocárdica carregada com células estromais derivadas de tecido adiposo e seus fatores de crescimento proporciona um ambiente que predispõe a regeneração cardíaca. Futuros estudos são necessários para melhor elucidar os mecanismos envolvidos nessa melhora de função, bem como o estudo em modelos animais que mais se assemelham aos humanos, objetivando, em um momento futuro, a aplicação dessa terapia em *clinical trials*.

Descritores: hidrogel, matriz extracelular, medicina regenerativa, células tronco mesenquimais, secretoma, insuficiência cardíaca, modelo animal, células endoteliais, fibroblastos cardíacos, fibrose cardíaca

Abstract

Liguori TTA. Development of cellular matrices for the treatment of dilated cardiomyopathy [thesis]. São Paulo: "Faculty of Medicine, University of São Paulo", 2020.

Although considerable progress has been made in the development of new therapies for cardiomyopathies, there is still no curative alternative to replace the need for transplantation. Regenerative medicine has been consolidated around the world by bringing new alternatives to chronic heart disease. Although cardiomyocytes are significantly affected in the cardiac degeneration process, being responsible for the muscle contraction, they are not, in fact, the most abundant cells in the heart of mammals. This place is occupied by fibroblasts: elongated cells present between the muscle fibers and which help to maintain the extracellular matrix balance. During heart failure, two processes contribute to the disruption of this balance and the consequent fibrosis and heart remodeling. The first process is the transdifferentiation of cardiac fibroblasts into myofibroblasts; the second is the endothelial-mesenchymal transition (EndMT). Both processes lead to an increase in the number of cells responsible for depositing extracellular matrix and, therefore, fibrosis and remodeling. Thus, approaches aimed at preventing the progress of these processes can be an interesting alternative for the treatment of cardiomyopathies. Using stem cells, biomaterials and growth factors, the objective of this thesis was to create a new therapeutic approach to decrease or extinguish the process of fibrosis in the cardiac tissue, in order to maintain the organ's function preserved. For that, in our first study, ***Fibroblast growth factor-2, but not the adipose tissue-derived stromal cells secretome, inhibits***

TGF- β 1-induced differentiation of human cardiac fibroblasts into myofibroblasts (Scientific Reports, 2018), primary human cardiac fibroblasts stimulated TGF- β 1 *in vitro* and their transdifferentiation was assessed. In an attempt to prevent its transformation into myofibroblasts, the secretome of adipose tissue-derived stromal cells (ASC-CMed) was collected and the fibroblasts were treated with it. In this work, the results demonstrated that it was not possible to inhibit the transdifferentiation of fibroblasts into myofibroblasts with the use of ASC-CMed. In our second study, ***Adipose tissue-derived stromal cells' conditioned medium modulates endothelial-mesenchymal transition induced by IL-1 β / TGF- β 2 but does not restore endothelial function*** (Cell Proliferation, 2019), we induced the differentiation of endothelial cells through a pro-inflammatory and pro-fibrotic environment, using IL-1 β and TGF- β 1, and we sought to prevent their differentiation using ASC-CMed. The results showed that, although the endothelial cells did not return to a functional phenotype, we were able to inhibit the EndMT process. Our third study, ***Bioactive decellularized cardiac extracellular matrix-based hydrogel as a sustained-release platform for human adipose tissue-derived stromal cell-secreted factors*** (submitted), aimed to develop a platform based on a hydrogel derived from myocardial extracellular matrix for the release of ASC-CMed, a process that was tested using different concentrations of secretome (1X, 10X and 100X). Our results demonstrated that this biomaterial proved to be an excellent platform for releasing growth factors in a sustained manner. Concluding the present thesis, using this same hydrogel, in the fourth study, ***Intrapericardial injection of hydrogels derived from decellularized cardiac extracellular matrix loaded with mesenchymal stromal cells and their secretome: a novel therapeutic approach to treat cytostatics-induced dilated cardiomyopathy***, we took into account the

immune response *in vivo*, when carrying out the intrapericardial application of the dECM hydrogel loaded with ASC and their secretome in a rat model of dilated cardiomyopathy. In this study it was possible to conclude that our therapy was able to decrease cardiac fibrosis and reduce remodeling, as well as improving cardiac function and hemodynamic parameters of the treated animals. Thus, the content of the present thesis demonstrates that the intrapericardial application of a myocardial extracellular matrix-derived hydrogel loaded with ASC and their growth factors constitutes a potential approach for cardiac regeneration. Further studies are necessary to better elucidate the mechanisms involved in the process, as well as to investigate the approach in large animal models that better resemble humans, aiming, in the future, the application of this therapy in clinical trials.

Descriptors: hydrogel, extracellular matrix, regenerative medicine, mesenchymal stem cells, secretome, heart failure, animal model, endothelial cells, cardiac fibroblasts, cardiac fibrosis

GENERAL INTRODUCTION

Dilated cardiomyopathy (DCM) is a health condition characterized by ventricular wall thinning and changes in ventricular chambers geometry to a more spherical, less elongated shape. Ultimately, the disease causes a loss of contractility and compromise ventricular function, leading to remodeling and, finally, heart failure (HF) (1–3). HF is an irreversible and potentially lethal clinical condition, affecting nearly 23 million people worldwide (1). The five-year survival is approximately 50%, and, naturally, it significantly impacts the quality of life of the patients, representing an increasing burden on society and health care.

DCM and, consequently, HF present as a consequence of adverse cardiac tissue remodeling after myocardial injury. In normal physiology, cardiac tissue is in homeostasis that is maintained by a well-regulated biochemical and biomechanical crosstalk between the parenchyma, composed of cardiomyocytes, and the supportive tissue stroma, which consists of endothelial cells, fibroblasts and the extracellular matrix (ECM). Myocardial injury disrupts cardiac tissue homeostasis. The ECM is a dynamic acellular network composed of structural proteins, such as collagen and elastin, proteoglycans, enzymes, and hundreds of other smaller proteins and macromolecules essential for cell adhesion, migration, and function (4,5). Once the healthy heart receives any kind of injury, this network suffers changes that affect the function of the cells it supports (6,7). Among the different types of injury, the heart tissue is susceptible to cardiomyocyte death by necrosis,

apoptosis, and autophagy. All these processes are followed by an increase in fibrosis - either localized or diffuse - through two main mechanisms: transdifferentiation of cardiac fibroblasts to myofibroblasts (Figure 1) (8–10) and endothelial-mesenchymal transition (EndMT, Figure 2) (10–13), both contributing to a progressive depletion of cardiac function (5,7,10,14).

Patophysiology – Myofibroblast Differentiation

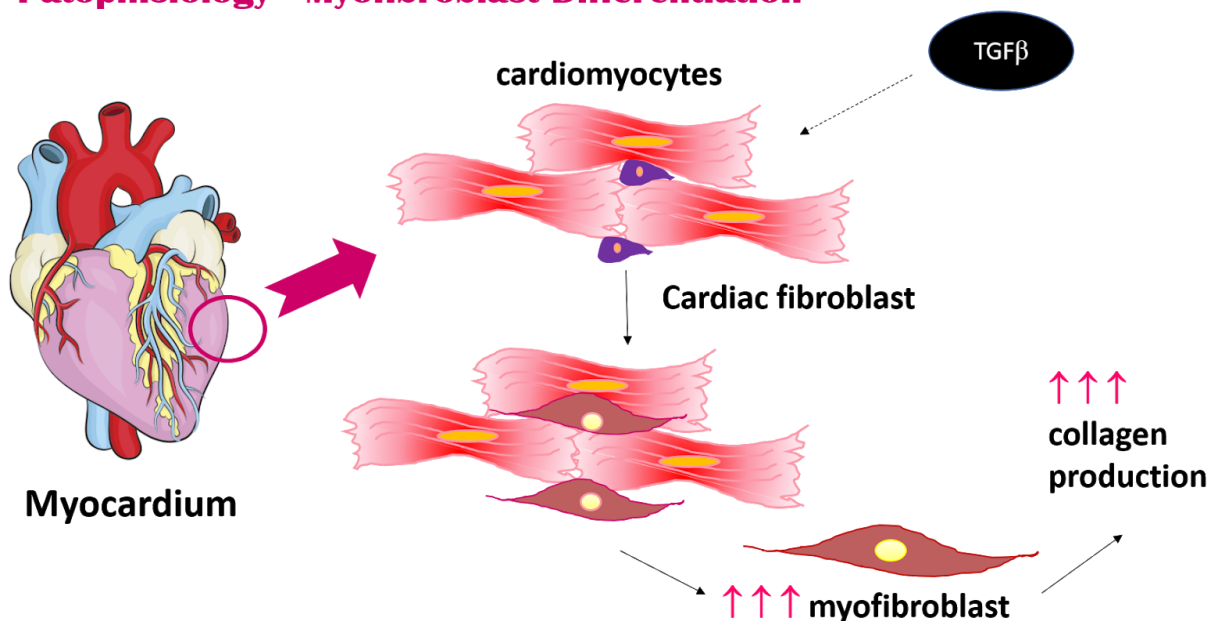


Figure 1. Schematic explanation of the transdifferentiation of cardiac fibroblasts to myofibroblasts.

Patophysiology - Endomt

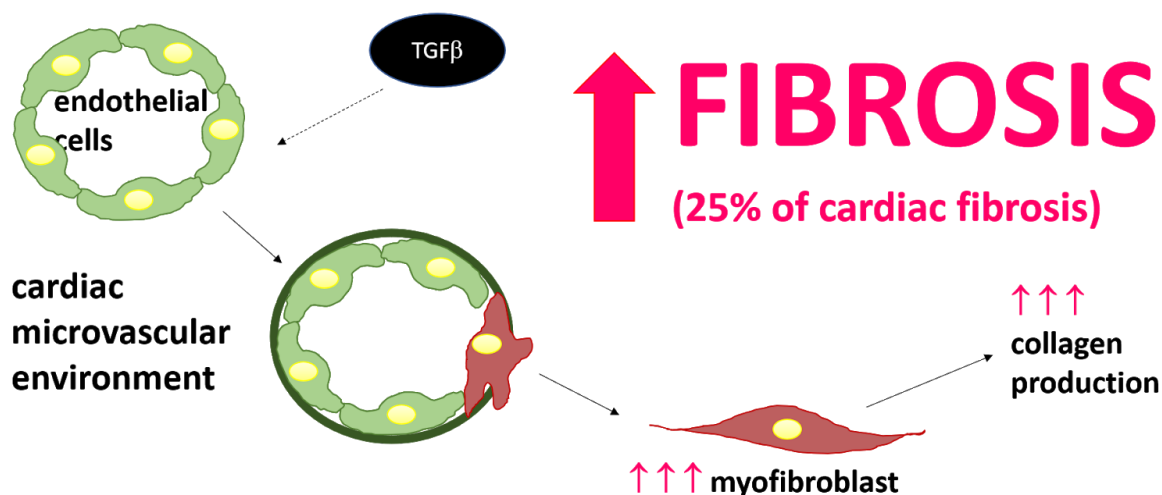


Figure 2. Schematic explanation of endothelial-mesenchymal transition (EndMT)

These processes are activated mostly via three main pathways, the TGFβ canonical and non-canonical pathways (10), and the MAPK/ERK pathway (10,15). Injured cardiomyocytes and endothelial cells secrete TGFβ (7) which activates such pathways. Both processes culminate in the increase of myofibroblasts, a cell that expresses mesenchymal markers, present a contractile phenotype, deposit ECM proteins (mostly collagen), and is capable of secreting inflammatory cytokines that lead to positive feedback on damage development (5).

Targeting the above-mentioned mechanisms of cardiac degeneration would be a potential approach to treat several cardiomyopathies. Taking the TGFβ signaling as a starting point, the use of therapies capable of blocking such pathways could represent a treatment option for several cardiac diseases (16,17). It is known

that some types of stem cells, namely mesenchymal stromal cells (MSC), secrete paracrine factors that can interact with the TGF β pathways to inhibit it (18–21). Among the different subtypes of mesenchymal stromal cells, adipose tissue-derived stromal cells remain one of the most interesting due to their abundance, easiness to acquire and ability to secrete dozens of clinically relevant trophic factors (22). Thus, the use of cell therapy for cardiovascular regeneration presents a fundamental and theoretical foundation.

Not only the use of cells themselves but also of combinations of cells with their secreted factors (secretome) has been proposed and shown capable of restoring the degenerated cardiac tissue through the promotion of angiogenesis and the decrease of apoptosis (23). Part of these results is related to the secretion of pro-regenerative, pro-angiogenic and anti-inflammatory trophic factors such as HGF, VEGF (23–26), SDF (23,24), IGF-1 (25,27,28), and PDGF (27). The positive effects observed from cell therapy, however, seem to be related not solely to the cell type or their secretome, but to the balance between all secreted factors and their interplay between cells, factors and the microenvironment surrounding them (24).

Several animal models have been used to study the therapeutic effect of stem cells in cardiac diseases such as dilated cardiomyopathy (23) (25,29,30), infarction (29,31–33), heart failure (34,35), myocarditis (29,34,36,37) and cardiac hypertrophy (29). A few clinical trials were also performed in this respect (38–40). Still, there are issues to be solved to increase the long-term efficacy of using stem cells to treat cardiovascular disease and allow the translation of such therapies to the

clinical practice. Among the aspects that remain to be wholly understood are the choice of cell type and amount, the right time to deliver them (41), the best route of administration (42), and how to avoid early cell migration from the transplanted region (43), to improve stem cell survival and to better integrate these cells to the native tissue (44). Being able to keep a high amount of live cells for a prolonged time in the damaged tissue, so that cells can exert a relevant effect, is a critical step towards the clinical application of cardiovascular cell therapy (24).

Recently, new tools have emerged in the cardiovascular regenerative field to address some of these requirements. One of the highest relevance is the use of smart biomaterials together with the cells or their secretome (44). There are plenty of biomaterial options, natural and synthetic. Some of these biomaterials are capable of acting as hydrogels (45). Such hydrogels can provide an interesting alternative for cardiovascular cell therapies because they can be molded and injected (45,46), facilitating cell delivery (42). Among the several biomaterials that can be used as hydrogels, there are those derived from the decellularized extracellular matrix, which mimics the native environment to the cells (45,47). Such hydrogels present the same mechanical and cell signaling properties of the original tissue (48), leading to enhanced cell engraftment and binding with regenerative growth factors (49).

The present thesis will elaborate on, first, the impact of ASC and their secretome on the two mechanisms involved in cardiac degeneration, i.e., the transdifferentiation of cardiac fibroblasts to myofibroblasts and the endothelial-mesenchymal transition, *in vitro*; second, the use hydrogels derived from

decellularized cardiac tissue as a delivery platform for the sustained release of trophic factors in the context of cardiovascular cell therapy; and third, the application of such platforms loaded with ASC and their secretome as a regenerative approach on an animal model of dilated cardiomyopathy.

REFERENCES

1. Bui AL, Horwich TB, Fonarow GC. Epidemiology and risk profile of heart failure. *Nat Rev Cardiol*. 2010;8(1):30–41.
2. Benjamin EJ, Blaha MJ, Chiuve SE, Cushman M, Das SR, Deo R, et al. Heart Disease and Stroke Statistics-2017 Update: A Report From the American Heart Association. *Circulation*. 2017 Mar 7;135(10):e146–603.
3. Masarone D, Kaski JP, Pacileo G, Elliott PM, Bossone E, Day SM, et al. Epidemiology and Clinical Aspects of Genetic Cardiomyopathies. *Heart Fail Clin*. 2018 Apr;14(2):119–28.
4. Rienks M, Papageorgiou A-P, Frangogiannis NG, Heymans S. Myocardial extracellular matrix: an ever-changing and diverse entity. *Circ Res*. 2014 Feb 28;114(5):872–88.
5. Fan D, Takawale A, Lee J, Kassiri Z. Cardiac fibroblasts, fibrosis and extracellular matrix remodeling in heart disease. *Fibrogenesis Tissue Repair*. 2012 Sep 3;5(1):15.
6. Frangogiannis NG. The extracellular matrix in myocardial injury, repair, and remodeling. *J Clin Invest*. 2017 May 1;127(5):1600–12.
7. Frangogiannis NG. The Extracellular Matrix in Ischemic and Nonischemic Heart Failure. *Circ Res*. 2019 Jun 21;125(1):117–46.
8. Humeres C, Frangogiannis NG. Fibroblasts in the Infarcted, Remodeling, and Failing Heart. *JACC Basic Transl Sci*. 2019 Jun;4(3):449–67.
9. Tarbit E, Singh I, Peart JN, Rose-Meyer RB. Biomarkers for the identification of cardiac fibroblast and myofibroblast cells. *Heart Fail Rev*. 2019 Jan;24(1):1–15.
10. Schirone L, Forte M, Palmerio S, Yee D, Nocella C, Angelini F, et al. A Review of the Molecular Mechanisms Underlying the Development and Progression of Cardiac Remodeling. *Oxid Med Cell Longev*. 2017 Jul 2;2017:3920195.
11. Gogiraju R, Bochenek ML, Schäfer K. Angiogenic Endothelial Cell Signaling in Cardiac Hypertrophy and Heart Failure. *Front Cardiovasc Med*. 2019 Mar

6;6:20.

12. Yoshimatsu Y, Watabe T. Roles of TGF- β signals in endothelial-mesenchymal transition during cardiac fibrosis. *Int J Inflam*. 2011 Nov 30;2011:724080.
13. Kovacic JC, Dimmeler S, Harvey RP, Finkel T, Aikawa E, Krenning G, et al. Endothelial to Mesenchymal Transition in Cardiovascular Disease: JACC State-of-the-Art Review. *J Am Coll Cardiol*. 2019 Jan 22;73(2):190–209.
14. Houser SR, Margulies KB, Murphy AM, Spinale FG, Francis GS, Prabhu SD, et al. Animal models of heart failure: a scientific statement from the American Heart Association. *Circ Res*. 2012 Jun 22;111(1):131–50.
15. Kehat I, Molkentin JD. Molecular pathways underlying cardiac remodeling during pathophysiological stimulation. *Circulation*. 2010 Dec 21;122(25):2727–35.
16. Man S, Sanchez Duffhues G, Ten Dijke P, Baker D. The therapeutic potential of targeting the endothelial-to-mesenchymal transition. *Angiogenesis*. 2019 Feb;22(1):3–13.
17. Fernández-Colino A, Iop L, Ventura Ferreira MS, Mela P. Fibrosis in tissue engineering and regenerative medicine: treat or trigger? *Adv Drug Deliv Rev* [Internet]. 2019 Jul 8; Available from: <http://dx.doi.org/10.1016/j.addr.2019.07.007>
18. Golpanian S, Wolf A, Hatzistergos KE, Hare JM. Rebuilding the Damaged Heart: Mesenchymal Stem Cells, Cell-Based Therapy, and Engineered Heart Tissue. *Physiol Rev*. 2016 Jul;96(3):1127–68.
19. Si Y-L, Zhao Y-L, Hao H-J, Fu X-B, Han W-D. MSCs: Biological characteristics, clinical applications and their outstanding concerns. *Ageing Res Rev*. 2011 Jan;10(1):93–103.
20. L PK, Kandoi S, Misra R, S V, K R, Verma RS. The mesenchymal stem cell secretome: A new paradigm towards cell-free therapeutic mode in regenerative medicine. *Cytokine Growth Factor Rev*. 2019 Apr;46:1–9.
21. Harrell CR, Fellabaum C, Jovicic N, Djonov V, Arsenijevic N, Volarevic V. Molecular Mechanisms Responsible for Therapeutic Potential of Mesenchymal Stem Cell-Derived Secretome. *Cells* [Internet]. 2019 May 16;8(5). Available from: <http://dx.doi.org/10.3390/cells8050467>
22. Riis S, Stensballe A, Emmersen J, Pennisi CP, Birkelund S, Zachar V, et al. Mass spectrometry analysis of adipose-derived stem cells reveals a significant effect of hypoxia on pathways regulating extracellular matrix. *Stem Cell Res Ther*. 2016 Apr 14;7(1):52.
23. Bagno L, Hatzistergos KE, Balkan W, Hare JM. Mesenchymal Stem Cell-Based Therapy for Cardiovascular Disease: Progress and Challenges. *Mol Ther*. 2018 Jul 5;26(7):1610–23.

24. Vizoso FJ, Eiro N, Cid S, Schneider J, Perez-Fernandez R. Mesenchymal Stem Cell Secretome: Toward Cell-Free Therapeutic Strategies in Regenerative Medicine. *Int J Mol Sci* [Internet]. 2017 Aug 25;18(9). Available from: <http://dx.doi.org/10.3390/ijms18091852>
25. Nagaya N, Kangawa K, Itoh T, Iwase T, Murakami S, Miyahara Y, et al. Transplantation of mesenchymal stem cells improves cardiac function in a rat model of dilated cardiomyopathy. *Circulation*. 2005 Aug 23;112(8):1128–35.
26. Daltro PS, Barreto BC, Silva PG, Chenaud Neto P, Sousa PH, Santana Neta D, et al. Therapy with mesenchymal stromal cells or conditioned medium reverse cardiac alterations in a high-fat diet–induced obesity model [Internet]. Vol. 19, *Cytotherapy*. 2017. p. 1176–88. Available from: <http://dx.doi.org/10.1016/j.jcyt.2017.07.002>
27. Hodgkinson CP, Bareja A, Gomez JA, Dzau VJ. Emerging Concepts in Paracrine Mechanisms in Regenerative Cardiovascular Medicine and Biology. *Circ Res*. 2016 Jan 8;118(1):95–107.
28. Mohammadi Gorji S, Karimpor Malekshah AA, Hashemi-Soteh MB, Rafiei A, Parivar K, Aghdami N. Effect of mesenchymal stem cells on Doxorubicin-induced fibrosis. *Cell J*. 2012 Aug 31;14(2):142–51.
29. Ou L, Li W, Liu Y, Zhang Y, Jie S, Kong D, et al. Animal models of cardiac disease and stem cell therapy. *Open Cardiovasc Med J*. 2010 Nov 26;4:231–9.
30. Jiao R, Liu Y, Yang W-J, Zhu X-Y, Li J, Tang Q-Z. Effects of stem cell therapy on dilated cardiomyopathy. *Saudi Med J*. 2014 Dec;35(12):1463–8.
31. Li G, Chen J, Zhang X, He G, Tan W, Wu H, et al. Cardiac repair in a mouse model of acute myocardial infarction with trophoblast stem cells. *Sci Rep*. 2017 Mar 15;7:44376.
32. Min J-Y, Yang Y, Sullivan MF, Ke Q, Converso KL, Chen Y, et al. Long-term improvement of cardiac function in rats after infarction by transplantation of embryonic stem cells. *J Thorac Cardiovasc Surg*. 2003 Feb;125(2):361–9.
33. Lalu MM, Mazzarello S, Zlepzig J, Dong YYR, Montroy J, McIntyre L, et al. Safety and Efficacy of Adult Stem Cell Therapy for Acute Myocardial Infarction and Ischemic Heart Failure (SafeCell Heart): A Systematic Review and Meta-Analysis. *Stem Cells Transl Med*. 2018 Dec;7(12):857–66.
34. Zhang C, Zhou G, Cai C, Li J, Chen F, Xie L, et al. Human umbilical cord mesenchymal stem cells alleviate acute myocarditis by modulating endoplasmic reticulum stress and extracellular signal regulated 1/2-mediated apoptosis. *Mol Med Rep*. 2017 Jun;15(6):3515–20.
35. Jayaraj JS, Janapala RN, Qaseem A, Usman N, Fathima N, Kashif T, et al. Efficacy and Safety of Stem Cell Therapy in Advanced Heart Failure Patients: A Systematic Review with a Meta-analysis of Recent Trials Between 2017 and

2019. *Cureus*. 2019 Sep 6;11(9):e5585.
36. Ohnishi S, Yanagawa B, Tanaka K, Miyahara Y, Obata H, Kataoka M, et al. Transplantation of mesenchymal stem cells attenuates myocardial injury and dysfunction in a rat model of acute myocarditis. *J Mol Cell Cardiol*. 2007 Jan;42(1):88–97.
 37. Silva DN, de Freitas Souza BS, Azevedo CM, Vasconcelos JF, Carvalho RH, Soares MBP, et al. Intramyocardial transplantation of cardiac mesenchymal stem cells reduces myocarditis in a model of chronic Chagas disease cardiomyopathy. *Stem Cell Res Ther*. 2014 Jul 1;5(4):81.
 38. Rong S-L, Wang Z-K, Zhou X-D, Wang X-L, Yang Z-M, Li B. Efficacy and safety of stem cell therapy in patients with dilated cardiomyopathy: a systematic appraisal and meta-analysis. *J Transl Med*. 2019 Jul 11;17(1):221.
 39. Chakravarty T, Makkar RR, Ascheim DD, Traverse JH, Schatz R, DeMaria A, et al. ALLogeneic Heart STem Cells to Achieve Myocardial Regeneration (ALLSTAR) Trial: Rationale and Design. *Cell Transplant*. 2017 Feb 16;26(2):205–14.
 40. del Corso C, Campos de Carvalho AC. Cell therapy in dilated cardiomyopathy: from animal models to clinical trials. *Braz J Med Biol Res*. 2011 May;44(5):388–93.
 41. Harding J, Roberts RM, Mirochnitchenko O. Large animal models for stem cell therapy. *Stem Cell Res Ther*. 2013 Mar 28;4(2):23.
 42. Lemcke H, Voronina N, Steinhoff G, David R. Recent Progress in Stem Cell Modification for Cardiac Regeneration. *Stem Cells Int*. 2018 Jan 16;2018:1909346.
 43. van den Akker F, Feyen DAM, van den Hoogen P, van Laake LW, van Eeuwijk ECM, Hoefler I, et al. Intramyocardial stem cell injection: go(ne) with the flow. *Eur Heart J*. 2017 Jan 14;38(3):184–6.
 44. Wang X, Rivera-Bolanos N, Jiang B, Ameer GA. Advanced Functional Biomaterials for Stem Cell Delivery in Regenerative Engineering and Medicine. *Adv Funct Mater*. 2019 Jun 13;29(23):1809009.
 45. Kc P, Hong Y, Zhang G. Cardiac tissue-derived extracellular matrix scaffolds for myocardial repair: advantages and challenges. *Regen Biomater*. 2019 Aug;6(4):185–99.
 46. Kim H, Kim S-HL, Choi Y-H, Ahn Y-H, Hwang NS. Biomaterials for Stem Cell Therapy for Cardiac Disease. *Adv Exp Med Biol*. 2018;1064:181–93.
 47. Cutts J, Nikkhah M, Brafman DA. Biomaterial Approaches for Stem Cell-Based Myocardial Tissue Engineering. *Biomark Insights*. 2015 Jun 1;10(Suppl 1):77–90.

48. Segers VFM, Lee RT. Biomaterials to enhance stem cell function in the heart. *Circ Res.* 2011 Sep 30;109(8):910–22.
49. Ferrini A, Stevens MM, Sattler S, Rosenthal N. Toward Regeneration of the Heart: Bioengineering Strategies for Immunomodulation. *Front Cardiovasc Med.* 2019 Mar 21;6:26.

CHAPTER 1

Fibroblast growth factor-2, but not the adipose tissue-derived stromal cells secretome, inhibits TGF- β 1-induced differentiation of human cardiac fibroblasts into myofibroblasts

Tácia Tavares de Aquinas Liguori^{1,2}, Gabriel Romero Liguori^{1,2}, Luiz Felipe Pinho Moreira², Martin C. Harmsen¹


1. Department of Pathology and Medical Biology, University of Groningen and University Medical Center Groningen, Groningen, Netherlands
2. Heart Institute (InCor), Hospital das Clinicas HCFMUSP, Faculdade de Medicina, Universidade de Sao Paulo, Sao Paulo, Brazil

Published

Scientific Reports, 2018 - DOI: 10.1038/s41598-018-34747-3

Link: <https://www.nature.com/articles/s41598-018-34747-3>

SCIENTIFIC REPORTS



OPEN

Fibroblast growth factor-2, but not the adipose tissue-derived stromal cells secretome, inhibits TGF- β 1-induced differentiation of human cardiac fibroblasts into myofibroblasts

Tácia Tavares Aquinas Liguori^{1,2}, Gabriel Romero Liguori^{1,2}, Luiz Felipe Pinho Moreira¹ & Martin Conrad Harmsen²

Transforming growth factor- β 1 (TGF- β 1) is a potent inducer of fibroblast to myofibroblast differentiation and contributes to the pro-fibrotic microenvironment during cardiac remodeling. Fibroblast growth factor-2 (FGF-2) is a growth factor secreted by adipose tissue-derived stromal cells (ASC) which can antagonize TGF- β 1 signaling. We hypothesized that TGF- β 1-induced cardiac fibroblast to myofibroblast differentiation is abrogated by FGF-2 and ASC conditioned medium (ASC-CMed). Our experiments demonstrated that TGF- β 1 treatment-induced cardiac fibroblast differentiation into myofibroblasts, as evidenced by the formation of contractile stress fibers rich in α SMA. FGF-2 blocked the differentiation, as evidenced by the reduction in gene (*TAGLN*, $p < 0.0001$; *ACTA2*, $p = 0.0056$) and protein (α SMA, $p = 0.0338$) expression of mesenchymal markers and extracellular matrix components gene expression (*COL1A1*, $p < 0.0001$; *COL3A1*, $p = 0.0029$). ASC-CMed did not block myofibroblast differentiation. The treatment with FGF-2 increased matrix metalloproteinases gene expression (*MMP1*, $p < 0.0001$; *MMP14*, $p = 0.0027$) and decreased the expression of tissue inhibitor of metalloproteinase gene *TIMP2* ($p = 0.0023$). ASC-CMed did not influence these genes. The proliferation of TGF- β 1-induced human cardiac fibroblasts was restored by both FGF-2 ($p = 0.0002$) and ASC-CMed ($p = 0.0121$). The present study supports the anti-fibrotic effects of FGF-2 through the blockage of cardiac fibroblast differentiation into myofibroblasts. ASC-CMed, however, did not replicate the anti-fibrotic effects of FGF-2 *in vitro*.

Fibroblasts are the most abundant cell type in the heart and regulate the homeostasis of the extracellular matrix (ECM). The ECM provides the architecture of cardiac tissue, it supports the structural integrity and it regulates cellular communication and function. A major component of the ECM is collagen which is deposited primarily by cardiac fibroblasts¹. Pathological stimuli, such as myocardial infarction, disrupt the cardiac tissue homeostasis² which predisposes the onset and progression of fibrosis^{3,4} by the activation and differentiation of fibroblasts into myofibroblasts^{1,5}. Cardiac fibrosis features the production and deposition of excessive amounts of extracellular matrix by cardiac myofibroblasts. Fibroblast activation and subsequent differentiation into myofibroblasts are primarily driven by transforming growth factor- β (TGF- β) and contributes to the pro-fibrotic cardiac microenvironment^{6–10}.

¹Laboratório de Cirurgia Cardiovascular e Fisiopatologia da Circulação (LIM-11), Instituto do Coração (InCor), Hospital das Clínicas HCFMUSP, Faculdade de Medicina, Universidade de São Paulo, São Paulo, SP, Brazil. ²University of Groningen, University Medical Center Groningen, Department of Pathology and Medical Biology, Groningen, The Netherlands. Tácia Tavares Aquinas Liguori and Gabriel Romero Liguori contributed equally. Correspondence and requests for materials should be addressed to M.C.H. (email: m.c.harmsen@umcg.nl)

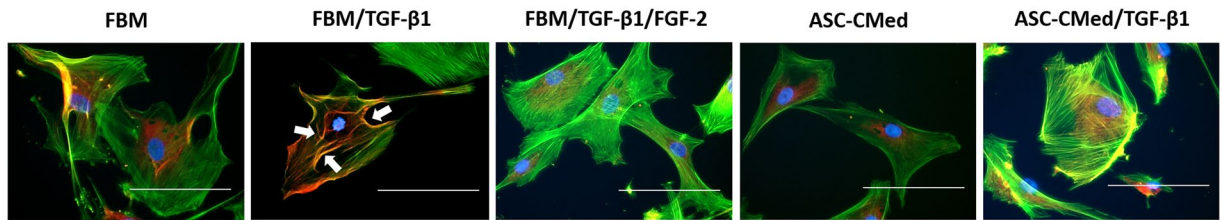


Figure 1. Formation of F-actin stress fibers in differentiating NHCF-V is refractory to suppression by ASC-CMed. Representative immunofluorescence micrographs of human cardiac fibroblasts (NHCF-V) under stimulation with TGF- β 1 or co-stimulation with TGF- β 1 and FGF-2, both in FBM and ASC-CMed, for 5 days. Upon TGF- β 1 stimulation, cells developed transcellular α SMA-expressing stress fibers (arrows). ASC-CMed did not inhibit the development of stress fibers. Blue: DAPI; Green: phalloidin; Red: α SMA. Scale reference: 100 μ m.

To date, no therapies exist that prevent or reverse fibrosis *in vivo*, yet it is possible to antagonize TGF- β signaling with specific growth factors such as FGF-2. Fibroblast growth factor 2 (FGF-2) is relevant in wound healing processes *in vivo*^{11–13} and *in vitro*^{14–17} to stimulate proliferation of tissue cells, connective tissue fibroblasts and promote angiogenesis, while it suppresses apoptosis. Moreover, FGF-2 antagonizes TGF- β signaling and thus affects fibrosis, albeit in early stages¹⁸. In fibroblasts of various origins, FGF-2 suppressed the expression of *TGF β 1*¹⁹ and its protein^{16,20}, that also suppressed the deposition of collagen^{21,22}. All these studies suggest that FGF-2 is an attractive molecule to target in TGF- β regulated fibrotic disease.

Mesenchymal stromal cells (MSC), such as adipose tissue-derived stromal cells (ASC), as well as their conditioned medium, have been shown to improve cardiac remodeling and thus to modulate cardiac fibrosis^{23–30}. Because ASC release a series of anti-fibrotic factors, among which are FGF, IGF and HGF^{31–34}, a possible mechanism underlying their anti-fibrotic effect could be to antagonize TGF- β signaling and thus the inhibition of the transformation of fibroblasts into myofibroblasts as well as the reduction of extracellular matrix production.

In a previous study, we demonstrated that TGF- β 1-induced differentiation of dermal fibroblasts to myofibroblasts could be modulated by adipose tissue-derived stromal cells' conditioned medium (ASC-CMed)³⁵. Therefore, we hypothesized that cardiac fibroblast differentiation into myofibroblast could also be abrogated by ASC-CMed.

Results

Formation of F-actin stress fibers in differentiating NHCF-V is refractory to suppression by ASC-CMed. After five days of pro-fibrotic stimulus, NHCF-V undergo myofibroblast differentiation, phalloidin detected F-actin and cells had an increase in α SMA expression (Fig. 1). Human cardiac fibroblast without TGF- β 1 stimuli had a mild phalloidin staining distributed all over the cytoplasm, on the other hand, the TGF- β 1 stimulated cells had the detection of phalloidin in the contractile fibers which had colocalization with the α SMA staining. FGF-2, but not ASC-CMed, could inhibit the phalloidin and α SMA in the contractile fibers. The expression of α SMA seems to be more evident in the TGF- β 1 stimulated cells. As expected, TGF- β 1 induced myofibroblast differentiation of cardiac fibroblasts which leads to the formation of smooth actin fibers at cytoskeletal level. Only FGF-2 inhibited the formation of these fibers.

FGF-2, but not ASC-CMed, inhibits the expression of mesenchymal markers in NHCF-V stimulated with TGF- β 1. The expression of mesenchymal genes *TAGLN*, encoding SM22 α , and *ACTA2*, encoding α SMA, was increased TGF- β 1 stimulated fibroblasts, irrespective of ASC-CMed (Fig. 2). FGF-2 suppressed the expression of *TAGLN* (One-way ANOVA, $p < 0.0001$; Sidak's multiple comparison test, $p < 0.0001$) and *ACTA2* in cardiac fibroblasts stimulated with TGF- β 1 (One-way ANOVA, $p = 0.0007$; Sidak's multiple comparison test, $p = 0.0056$). The influence of ASC-CMed no more than tended to decrease *TAGLN* expression (One-way ANOVA, $p < 0.0001$; Sidak's multiple comparison test, $p = 0.0820$) but not *ACTA2* expression.

TGF- β 1 upregulated the expression of α SMA in human cardiac fibroblasts which was blocked by FGF-2 (Fig. 3) (One-way ANOVA, $p = 0.0413$; Sidak's multiple comparison test, $p = 0.0338$). ASC-CMed did not alter the upregulation of α SMA by TGF- β 1 (Fig. 3). Under these culture conditions, cardiac fibroblasts had a basal expression of SM22 α which increased 1.4-fold after TGF- β 1 stimulation. Thus, although FGF-2 inhibits the production of α SMA, it could not reverse the expression of the already formed SM22 α .

FGF2, but not ASC-CMed, modulates extracellular matrix production in NHCF-V stimulated with TGF- β 1. The gene expression of collagens, as well as of matrix metalloproteinases (MMPs) - enzymes responsible for ECM degradation - and the tissue inhibitors of metalloproteinases (TIMPs), was analyzed. The stimulation with TGF- β 1 upregulated the transcription of both *COL1A1* and *COL3A1*, genes responsible for the protein synthesis of the alpha-1 chain of collagens I and III respectively (Fig. 4A,B). This increase was more pronounced for *COL1A1*. Treatment with FGF-2 in samples stimulated by TGF- β 1 was responsible for a statistically significant downregulation in *COL1A1* (One-way ANOVA, $p < 0.0001$; Sidak's multiple comparison test, $p < 0.0001$) and *COL3A1* (One-way ANOVA, $p = 0.0572$; Sidak's multiple comparison test, $p = 0.0290$), demonstrating the strong inhibition of NHCF-V towards the myofibroblast phenotype.

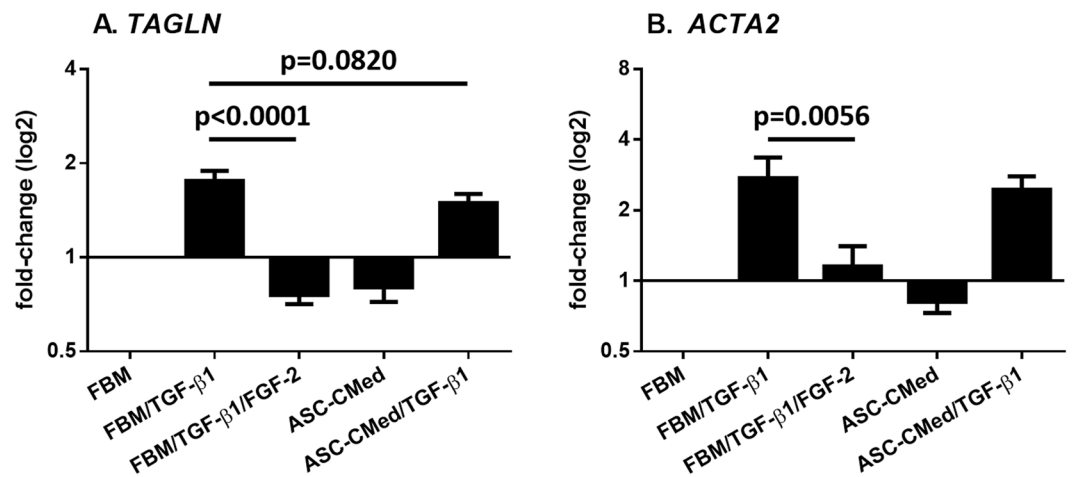


Figure 2. FGF-2, but not ASC-CMed, inhibits the gene expression of mesenchymal markers. (A) TAGLN, and (B) ACTA2, by RT-qPCR of NHCF-V after stimulation with TGFβ1 or co-stimulation with TGF-β1 and FGF-2, both in FBM and ASC-CMed, for five days. Data were analyzed by One-way ANOVA with Sidak's multiple comparison test for the groups FBM/TGF-β1 vs. FBM/TGF-β1/FGF-2 and FBM/TGF-β1 vs. ASC-CMed/TGF-β1; p-values for the Sidak's multiple comparison test are shown in the figure. Values represent mean ± SEM of 3 independent experiments in duplicate.

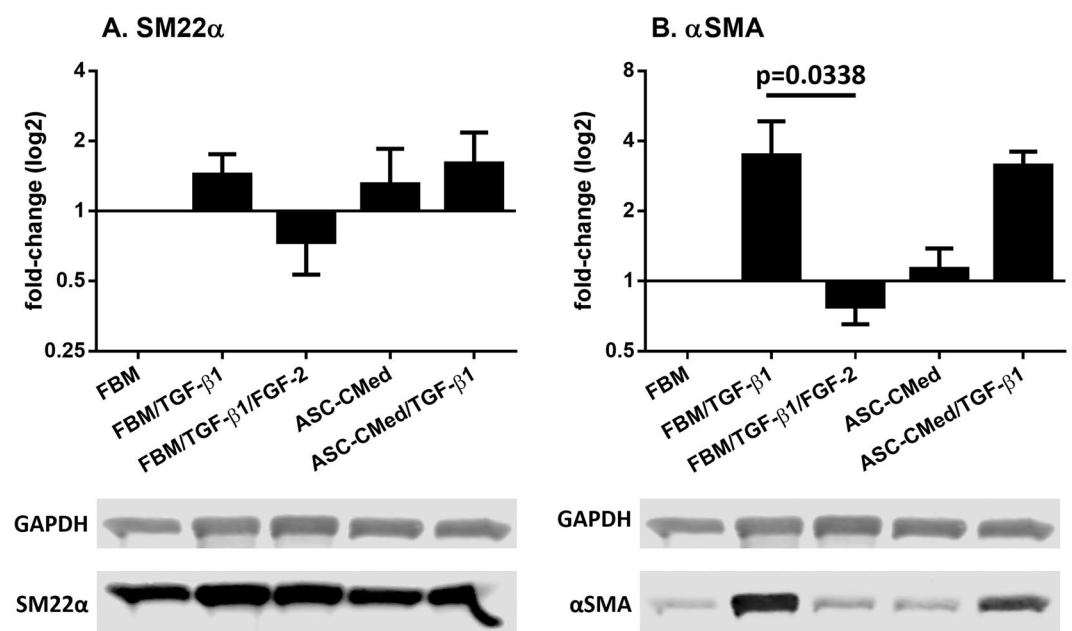


Figure 3. FGF-2, but not ASC-CMed, inhibits the protein expression of mesenchymal markers. (A) SM22α, and (B) αSMA, by immunoblotting of NHCF-V after stimulation with TGFβ1 or co-stimulation with TGF-β1 and FGF-2, both in FBM and ASC-CMed, for five days. Data were analyzed by One-way ANOVA with Sidak's multiple comparison test for the groups FBM/TGF-β1 vs. FBM/TGF-β1/FGF-2 and FBM/TGF-β1 vs. ASC-CMed/TGF-β1; p-values for the Sidak's multiple comparison test are shown in the figure. Values represent mean ± SEM of 3 independent experiments.

The gene expression of MMPs and TIMPs did not change irrespective of treatment, except for FGF-2 (Fig. 4C–G). Expression of *MMP1*, encoding matrix metalloproteinase 1 *i.e.* collagenase, was downregulated by TGF-β1. In contrast, FGF-2 upregulated *MMP1* expression compared to control groups and TGF-β1 stimulation (One-way ANOVA, $p < 0.0001$; Sidak's multiple comparison test, $p < 0.0001$). Treatment with ASC-CMed did not affect the TGF-β-induced downregulation of *MMP1* in NHCF-V. The expression of *MMP2* gene was not regulated by TGF-β, FGF or ASC-CMed (co)stimulation of NHCF-V. Although TGF-β1 did not affect the expression of *MMP14*, FGF-2 upregulated its expression (One-way ANOVA, $p < 0.0001$; Sidak's multiple comparison test, $p = 0.0027$). Treatment with ASC-CMed tended to increase the expression of *MMP14*.

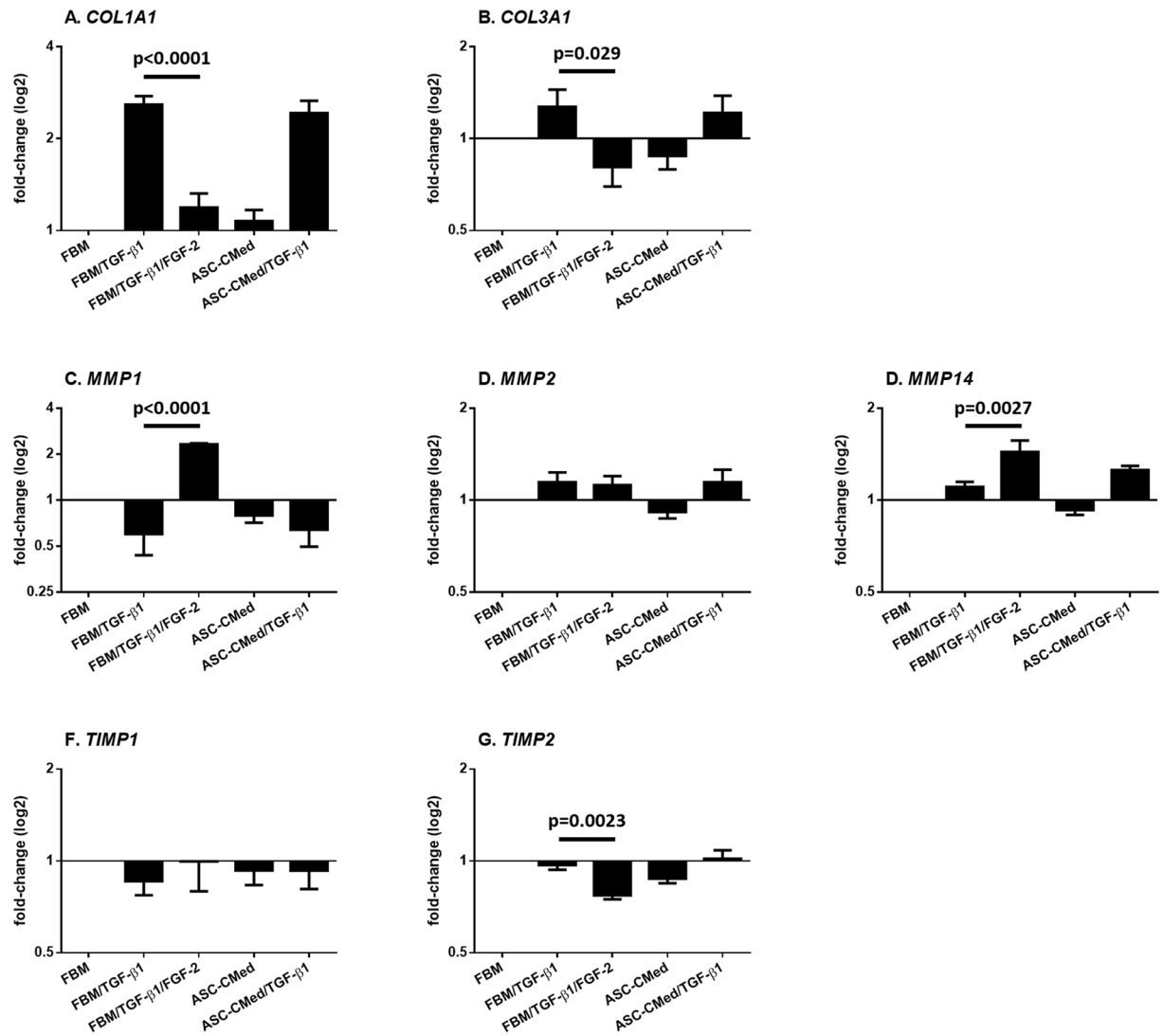


Figure 4. FGF2, but not ASC-CMed, modulates the expression of extracellular matrix-related genes. (A) *COL1A1*, (B) *COL3A1*, (C) *MMP1*, (D) *MMP2*, (E) *MMP14*, (F) *TIMP1*, and (G) *TIMP2* by RT-qPCR of NHCF-V after stimulation with TGF- β 1 or co-stimulation with TGF- β 1 and FGF-2, both in FBM and ASC-CMed, for five days. Data were analyzed by One-way ANOVA with Sidak's multiple comparison test for the groups FBM/TGF- β 1 vs. FBM/TGF- β 1/FGF-2 and FBM/TGF- β 1 vs. ASC-CMed/TGF- β 1; p-values for the Sidak's multiple comparison test are shown in the figure. Values represent mean \pm SEM of 3 independent experiments in duplicate.

Expression of TIMPs genes *TIMP1* and *TIMP2* which are regulators of MMP activity had differential expression. Expression of *TIMP1*, remained unchanged irrespective of TGF- β 1 or ASC-CMed treatment. Expression of *TIMP2* was decreased by FGF-2 (One-way ANOVA, $p = 0.0005$; Sidak's multiple comparison test, $p = 0.0023$), while neither TGF- β 1 nor ASC-CMed affected its expression. Interestingly, *TIMP2* is a co-factor of membrane-bound *MMP14*, which is e.g. responsible for activation of ECM-bound MMPs.

Immunofluorescence microscopy of intracellular collagen I demonstrated an increase in the protein content for all the groups stimulated with TGF- β 1 (Fig. 5). FGF-2 could not decrease the intracellular collagen I at the microscopical level, so that virtually all the TGF- β 1 stimulated cells and ASC-CMed/TGF- β 1 expressed the protein in their cytoplasm. Both groups without TGF- β 1 stimulation showed a very limited expression of collagen I.

FGF2 and ASC-CMed restore the TGF- β 1-inhibited proliferation of NHCF-V. NHCF-V proliferation was measured after five days of stimulation with TGF- β 1. The pro-fibrotic stimulus led to a decrease in cell proliferation, as detected by Ki-67 staining. TGF- β 1 suppressed the proliferation of human cardiac fibroblasts; control cells had 40.8% of proliferating cells compared to 22.3% in TGF- β 1 stimulated cells (Fig. 6). Treatment with FGF-2, recovered the proliferation to 37.8% (One-way ANOVA, $p < 0.0001$; Sidak's multiple comparison test, $p = 0.0002$) while the proliferation of fibroblasts cells stimulated with TGF- β 1 was virtually rescued by

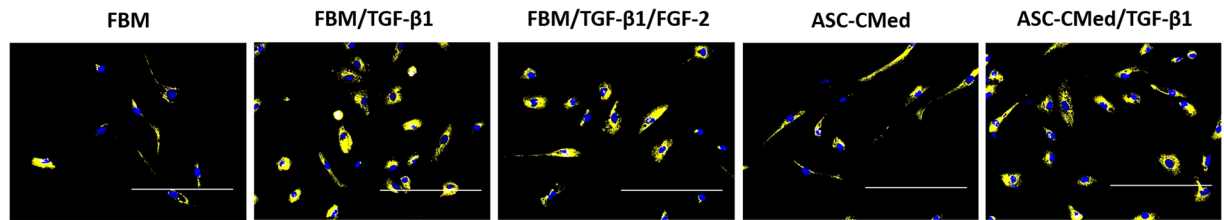


Figure 5. Pro-collagen production in cardiac fibroblasts. Immunofluorescence analysis of expression of pro-collagen in human cardiac fibroblasts undergoing myofibroblast differentiation for five days. Collagen I was upregulated upon TGF- β 1 stimuli and neither ASC-CMed nor FGF-2 inhibited the process. Minor expression of collagen I was showed in cultured cells without TGF- β 1 stimuli. Blue: DAPI; Yellow: collagen I. Scale reference: 200 μ m.

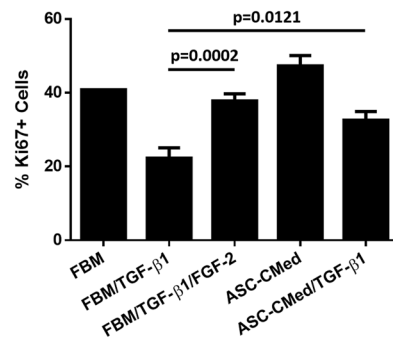
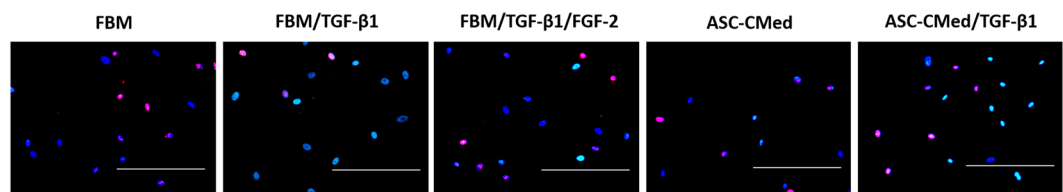


Figure 6. FGF2 and ASC-CMed restore the TGF- β 1-inhibited proliferation of NHCF-V. Immunofluorescence proliferation analysis of human cardiac fibroblasts undergoing myofibroblast differentiation for five days. TGF- β 1 stimuli downregulated the proliferation of cardiac fibroblasts. ASC-CMed and FGF-2 upregulated the proliferation. Blue: DAPI; Red: Ki-67. Scale reference: 200 μ m. Data were analyzed by One-way ANOVA with Sidak's multiple comparison test for the groups FBM/TGF- β 1 vs. FBM/TGF- β 1/FGF-2 and FBM/TGF- β 1 vs. ASC-CMed/TGF- β 1; p-values for the Sidak's multiple comparison test are shown in the figure. Values represent mean \pm SEM of 3 independent experiments in quadruplicate.

ASC-CMed (32.6%) (One-way ANOVA, $p < 0.0001$; Sidak's multiple comparison test, $p = 0.0121$). Treatment of nonstimulated cardiac fibroblasts with ASC-CMed increased proliferation to 47.3%.

Wound healing is not affected by NHCF-V stimulation with TGF- β 1. Wound healing was examined with a scratch assay and assessed after 24 hours. The percentage of gap closure did not differ among all groups (One-way ANOVA, $p = 0.3716$). Still, the treatment with FGF-2 or ASC-CMed tended to increase wound healing potential (Fig. 7).

Discussion

We demonstrated that FGF-2 - but not the secreted factors of adipose tissue-derived stromal cells - downmodulate TGF- β 1-induced fibroblast into myofibroblast differentiation. Our results show that FGF-2 reduced differentiation via the reduction of mesenchymal gene expression (*TAGLN* and *ACTA2*), and the reduction of α SMA expression subsequently. Concomitantly, we demonstrated that FGF-2 downregulated expression of collagens (*COL1A1* and *COL3A1*), upregulate expression of matrix metalloproteinases (*MMP1* and *MMP14*), and downregulated expression of inhibitor of metalloproteinase *TIMP2*. Finally, we showed that not only FGF-2 but also ASC-CMed restored the proliferation of TGF- β 1-impaired fibroblasts.

TGF- β 1 signaling is a pivotal mechanism of the activation of fibroblasts into myofibroblasts and, thus, fibrosis⁶⁻¹⁰. The ability of FGF-2 to antagonize TGF- β signaling, in turn, has been demonstrated in a series of studies^{17,36-39}, each of these suggesting different mechanisms of interference on the TGF- β pathway. Among these suggested mechanisms are: the activation of ERK and JNK pathways¹⁷; the expression of *let-7* miRNA, TGF β

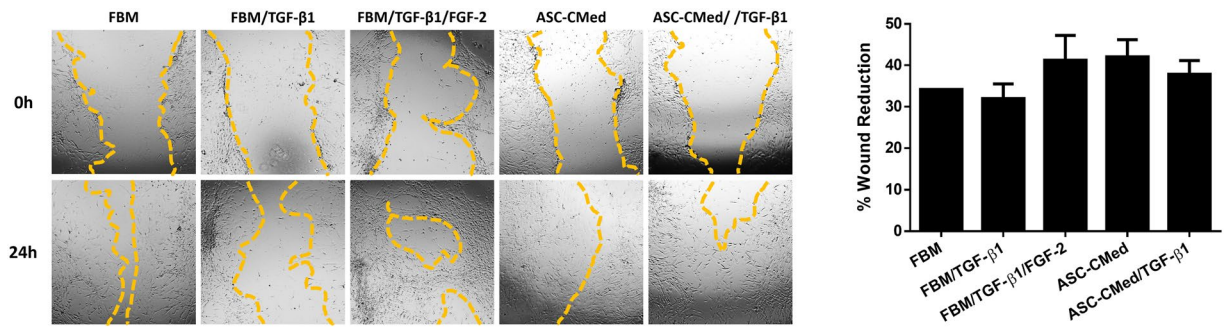


Figure 7. Wound healing is not affected by NHCF-V stimulation with TGF- β 1. Wound healing assay (24h) in NHCF-V under stimulation with TGF- β 1 or co-stimulation with TGF- β 1 and FGF-2, both in FBM and ASC-CMed. Original magnification: 4x. Values represent mean \pm SEM of 3 independent experiments in triplicate.

receptor suppressor^{38,39}; the expression of miRNA-20a, another repressor of the TGF β receptor complex³⁶; and the inhibition of the transcriptional regulator of muscle differentiation myf-5⁴⁰.

We hypothesized that, because ASC are known to secrete pro-regenerative growth factors such as FGF-2, treatment of human cardiac fibroblasts with ASC-CMed would abrogate TGF- β 1-induced differentiation into myofibroblasts. Both gene and protein expression of mesenchymal and extracellular matrix-related markers showed that, differently than expected, ASC-CMed did not exert a noticeable effect on TGF- β 1-induced myofibroblast activation. We did find, however, that ASC-CMed restored fibroblast proliferation impaired by TGF- β 1 stimulation. This finding might point to potential differences between the FGF-2 thresholds required for restoring proliferation and blocking differentiation. However, another possibility is that ASC produce other growth factors that also impact proliferation but are not involved in the differentiation process. In this regard, it has been previously shown that epidermal growth factor (EGF) from ASC was capable to enhance the proliferation of skin fibroblasts *in vitro*⁴¹.

To our knowledge, this is the first report to investigate the effects of conditioned medium from mesenchymal stromal cells - here ASC - in the TGF- β 1-induced differentiation of cardiac fibroblasts into myofibroblasts. Several other studies, however, have investigated the effects of MSC secretome in the spontaneous differentiation of cardiac fibroblasts^{42–46}. Thus, although our findings oppose to many of the results described in these studies, there are important differences - which deserve attention - between published data and our current work (Table 1).

Three out of the five studies reported anti-fibrotic effects of MSC conditioned-medium on cardiac fibroblasts, including a reduction in expression of α SMA, collagens and TIMPs and increased MMPs expression and/or activity^{43,45,46}. These studies were all performed with rat - not human - cardiac fibroblasts and none of these included a control group treated with Fibroblast Growth Medium (FGM), a medium capable to inhibit the spontaneous differentiation of fibroblasts, as we did. Thus, in this respect our results are not comparable to these studies for several reasons, the main being that the induction of cardiac fibroblast differentiation with TGF- β 1 is a much more effective and powerful mechanism than the spontaneous differentiation, being consequently much more difficult to be blocked or reversed. Furthermore, both other studies which investigated the effects of MSC conditioned-medium on the spontaneous differentiation of cardiac fibroblasts reported either no differences⁴² or even a trend towards the pro-fibrotic phenotype, with reduced MMP2 and MMP9 protein expression and activity and increased TIMP1 protein expression⁴⁴. An important observation is that the concentration of FGF-2 in the ASC-CMed could be too low to counteract TGF- β 1 action, while it is enough to block spontaneous differentiation. Previous studies demonstrated that the concentration of FGF-2 in ASC-CMed was less than 150 pg/mL^{33,34}, much lower than the FGF-2 concentration necessary to block the TGF- β 1-induced differentiation in this study. Another point which deserves attention is the variety of factors secreted by ASC which could interfere with FGF-2 activity. Among the factors that might be involved in the FGF-2 blockage of TGF- β 1 signaling are inflammatory factors, as INF α , TNF α , and IL-1 β , which block the FGF receptor and, thus, do not allow FGF-2 to inhibit TGF- β 1 action³⁹. In fact, studies demonstrated that ASC may release TNF α and IL-1 β , besides many other interleukins^{33,47,48}. These factors, together, could abrogate the effect of FGF-2 in the low doses it is found in ASC-CMed. Still, it is essential to highlight the fact that ASC also produce TGF- β , as demonstrated by several studies^{33,34,49,50}. In this regard, Rehman *et al.* showed that ASC produce around ten times more TGF- β than FGF-2³⁴. The conjoint action of all these factors, which are contained in the ASC secretome, could explain, in part, the insufficiency of ASC-CMed to block the fibrotic stimule.

Still, in our view, the partial recapitulation *in vitro* of the fibroblast-related component of cardiac fibrosis, with the use of primary human cardiac fibroblast cultured in FGM and induced with TGF- β 1 is a suitable *in vitro* model of the natural conditions in the fibrotic heart. Thus, considering the controversial findings between the studies using the spontaneous differentiation in addition to the results of the present study, we consider that in TGF- β -driven cardiac fibrosis ASC-CMed may not suffice as a sole therapeutic modality to block or reverse ongoing fibrosis. FGF-2, however, corroborating with the findings of two previous studies^{21,22}, did block TGF- β 1-induced pro-fibrotic conversion of cardiac human fibroblasts.

The present study supports the anti-fibrotic effects of FGF-2 through the blockage of NHCF-V differentiation into myofibroblasts, as demonstrated by the modulation of gene and/or protein expression in a series of

| Study | Fibroblast type | Fibroblast culture medium | MSC conditioned medium | Differentiation induction | Findings |
|---------------------------------------|--|---------------------------|---|---------------------------|---|
| Ohnishi <i>et al.</i> ⁴² | primary SD rat atrial fibroblast | αMEM (10% FBS) | αMEM (10% FBS)-based CM from Lewis rat BM-MSC cultured for 48 h | spontaneous | = proliferation = <i>COL1A1</i> and <i>COL3A1</i> gene expression |
| Mias <i>et al.</i> ⁴³ | primary Lewis rat cardiac ^(NS) fibroblast | DMEM/F12 (10% FBS) | MEM (10% FBS)-based CM from Lewis rat BM-MSC cultured for 24 h* | spontaneous | ↓ αSMA protein expression ↓ collagens I and III deposition ↑ MMP2 and MMP9 activity ↓ <i>TIMP2</i> gene expression |
| Wang <i>et al.</i> ⁴⁴ | primary SD rat ventricular fibroblast** | DMEM (10% FBS) | transwell co-culture with SD rat BM-MSC in DMEM (10% FBS) | spontaneous | ↓ MMP2 protein expression = MMP9 protein expression ↓ MMP2 activity = MMP9 activity ↑ TIMP1 protein expression |
| Mao <i>et al.</i> ⁴⁵ | primary SD rat ventricular fibroblast | DMEM (10% FBS) | DMEM (10% FBS)-based CM from SD rat BM-MSC cultured for 72 h and concentrated*** | spontaneous | ↓ <i>ACTA2</i> gene expression ↓ <i>COL1A1</i> and <i>COL3A1</i> gene expression ↑ <i>MMP2</i> and <i>MMP9</i> gene expression ↓ <i>TIMP1</i> and <i>TIMP2</i> gene expression |
| Li <i>et al.</i> ⁴⁶ | primary SD rat ventricular fibroblast | DMEM (10% FBS) | gap mode co-culture with human ASC in MSC growth medium ^(NS) | spontaneous | ↓ αSMA expression |
| Liguori <i>et al.</i> (current paper) | primary human ventricular fibroblast | FGM (10% FBS) | DMEM (10% FBS)-based CM from human ASC cultured for 24 h, concentrated 30X, and resuspended in FGM (2% FBS) | 5 ng/mL of TGF-β1 | = <i>TAGLN</i> and <i>ACTA2</i> gene expression = SM22α and αSMA protein expression = <i>COL1A1</i> and <i>COL3A1</i> gene expression = <i>MMP1</i> , <i>MMP2</i> and <i>MMP14</i> gene expression = <i>TIMP1</i> and <i>TIMP2</i> gene expression ↑ proliferation = wound healing potential |

Table 1. Overview of the studies investigating the effects of MSC conditioned medium in cardiac fibroblasts. MSC: mesenchymal stromal cells; SD: Sprague-Dawley; αMEM: α-Minimal Essential Medium; FBS: fetal bovine serum; CM: conditioned medium; BM-MSC: bone marrow mesenchymal stromal cells; DMEM: Dulbecco's Modified Eagle Media; MEM: Minimal Essential Medium; ASC: adipose tissue-derived stromal cells; FGM: Fibroblast Growth Medium; NS: not specified. *Used the same medium, not conditioned, as control. **Fibroblasts pre-conditioned under hypoxia. ***Concentration ratio and resuspension method (if any) not described.

| Group | Description |
|------------------|---|
| FBM | NHCF-V culture with FGM2, without added factors. |
| FBM/TGF-β1 | NHCF-V culture with FGM2 added with TGF-β1. |
| FBM/TGF-β1/FGF-2 | NHCF-V culture with FGM2 added with TGF-β1 and FGF-2 |
| ASC-CMed | NHCF-V culture with ASC conditioned media, without added factors. |
| ASC-CMed/TGF-β1 | NHCF-V culture with ASC conditioned media added with TGF-β1 |

Table 2. Experimental Groups. FBM: Fibroblast media; FGM2: Fibroblast growth media with 2% of fetal bovine serum; NHCF-V: Ventricular normal human cardiac fibroblasts; FGF-2: Fibroblast growth factor 2; TGF-β1: transforming growth factor-beta 1; ASC-CMed: Conditioned Medium derived from Adipose tissue-derived stromal cells.

mesenchymal and extracellular matrix-related markers. ASC-CMed, however, could not demonstrate the same effects found with FGF-2.

Methods

Experimental groups. Ventricular normal human cardiac fibroblasts (NHCF-V) were allocated into 5 groups with different induction/FGF-2/ASC-CMed combinations, as described in Table 2.

Cell sources, cell culture, and conditioned medium. Ventricular normal human cardiac fibroblasts were purchased from Lonza (NHCF-V; #CC-2904, Lonza, Basel, Switzerland) and cultured with Fibroblast Growth Medium-3 with 10% of fetal bovine serum (FBS) (FGM3; #CC-4526, Lonza, Basel, Switzerland) added with 500 ng/mL Amphotericin B (#15290018, Gibco Invitrogen, Carlsbad, USA) at 37 °C in a humidified incubator with 5% CO₂. The medium was refreshed every 3 days. Cells were passed at a ratio of 1:3 after reaching confluency. NHCF-V were used between passages 3–5.

At day 0 of the experiment, NHCF-V were seeded at a 10,000 cells/cm² density. After 24 hours, NHCF-V were allocated into the 5 distinct groups and cultured for 5 days. Fibroblast growth factor 2 (FGF-2; #100-18C, PeproTech, Inc., Rocky Hill, N.J.) and human transforming growth factor-beta 1 (TGF-β1; #100-21, PeproTech, New Jersey, USA) were used at a concentration of 10 ng/mL and 5 ng/mL, respectively, in all experiments.

Human ASC were isolated as described previously⁵¹. Briefly, human abdominal fat was obtained by liposuction, washed with phosphate-buffered saline (PBS) and digested enzymatically with 0.1% collagenase A (#11088793001, Roche Diagnostic, Mannheim, Germany) in PBS with 1% bovine serum albumin (BSA; #A9647, Sigma-Aldrich, Boston, USA). The tissue was shaken constantly at 37 °C for 2 h. After this, the digested tissue

was mixed with 1% PBS/BSA, filtered, centrifuged and the cell pellet was resuspended in Dulbecco's Modified Eagle's Medium (DMEM; #12-604F, Lonza, Basel, Switzerland) with 10% fetal bovine serum (FBS; #F0804, Sigma-Aldrich, Missouri, United States), 1% penicillin/streptomycin (#15140122, Gibco Invitrogen, Carlsbad, USA) and 1% L-glutamine (#17-605E, Lonza Biowhittaker, Verviers, Belgium). Cells were cultured at 37°C in a humidified incubator with 5% CO₂. The medium was refreshed every 2 days. Cells were passed at a ratio of 1:3 after reached confluency.

ASC conditioned medium (ASC-CMed) was obtained from confluent cultures of ASC between passages 3 and 6 from at least 3 different donors. For ASC-CMed, cells were cultured in DMEM without serum. Cells were kept at 37°C with a minimum relative humidity of 95% and an atmosphere of 5% CO₂ in the air. The conditioned medium was harvested after 24 hours, passed through a 0.22 µm filter and stored at -20°C until use. Before the experiment, the conditioned medium was concentrated 30 times using Amicon® Ultra 15 mL filters (UFC900324, Merck, Darmstadt, Germany) and resuspended to the initial volume using Fibroblast Growth Medium-2 (FGM2; #CC-3132, Lonza, Basel, Switzerland).

Immunofluorescence, gene expression, and immunoblotting. *Immunofluorescence.* NHCF-V were cultured in 48 well tissue culture plates. After 5 and 21 days of induction, cells were fixed at room temperature with 2% paraformaldehyde (PFA) for 30 minutes. Cells were permeabilized with 1% Triton-X100 in PBS for 15 minutes at room temperature and blocked with 5% donkey serum in PBS and 1% BSA for another 15 minutes at room temperature. Subsequently, cells were incubated with primary antibodies diluted in 5% donkey serum in PBS for 2 hours at room temperature. The following primary antibodies were used: mouse anti-αSMA (1:400; #ab5694, Abcam, Cambridge, UK), rabbit anti-collagen I (1:200, #ab34710, Abcam, Cambridge, UK), rabbit anti-collagen III (1:200, #ab34710, Abcam, Cambridge, UK) and rabbit anti Ki-67 (1:400; #ab15580, Abcam, Cambridge, UK). Controls were incubated with 5% donkey serum in PBS. Next, cells were washed with 0.05% Tween-20 in PBS and incubated with secondary antibodies in 5% donkey serum in PBS with 4',6-diamidino-2-phenylindole (DAPI; 1:5000; #D9542-5MG, Sigma-Aldrich, Missouri, United States) and Alexa Fluor® 488 phalloidin (1:400; #A12379, Life Technologies, Carlsbad, United States) for 1 hour at room temperature. The following secondary antibodies were used: donkey anti-rabbit IgG (H + L) Alexa Fluor® 594 (1:400; #A-21207, Life Technologies, Carlsbad, United States) and donkey anti-mouse IgG (H + L) Alexa Fluor® 647 (1:400; #A-31571, Life Technologies, Carlsbad, United States). Finally, cells were washed 3 times with PBS and the plates were imaged with Evos FL System (Thermo Fisher Scientific, Waltham, United States) using Texas Red (TXR), Cy5, DAPI and Green Fluorescent Protein (GFP) channels with 20x magnification.

Gene expression analysis. NHCF-V were cultured in 25 cm² flasks. After 5 days of induction, RNA isolation was performed using TRIzol reagent (#15596018, Invitrogen Corp, Carlsbad, United States) according to the manufacturer's protocol. RNA concentration and purity were determined using NanoDrop technology (Thermo Scientific, Hemel Hempstead, United Kingdom). Between 300 ng and 500 ng of total RNA was used for cDNA synthesis, which was performed using RevertAid™ First Strand cDNA Synthesis Kit (Thermo Fisher Scientific, Waltham, United States) according to the manufacturer's protocol. The cDNA-equivalent of 5 ng total RNA was used per single qPCR reaction. PCR was performed using SYBR Green (Bio-Rad, Hercules, United States) with the ViiA7 Real-Time PCR system (Applied Biosystems, Foster City, United States). Each analysis was done in duplicate for each one of the independent experiments. The primers used are listed in the Supplementary Table S1. Data were analyzed using ViiA7 software (Applied Biosystems, Foster City, United States) and normalized with the ΔC_T method, using the geometrical mean of 18S ribosomal RNA (18S RNA) cycle threshold (C_T) values. The fold-change in gene expression versus the no treatment control group (ECM) was calculated using the ΔΔC_T method.

Immunoblotting analysis. NHCF-V were cultured in 25 cm² flasks. After 5 days of induction, cells were rinsed with cold PBS and lysed in 100 µL of cold lysis buffer (RIPA; #89900, Thermo Fisher Scientific, Waltham, United States) containing 1% protease inhibitor cocktail (PIC; #P8340, Sigma Aldrich, St. Louis, United States) and 1% Halt™ phosphatase inhibitor cocktail (#78420, Thermo Fisher Scientific, Waltham, United States). The lysed cells were collected in 2 mL microcentrifuge tubes and the contents homogenized by sonication at 30 W for 30 seconds and centrifuged at 7,500 g at 4°C for 5 minutes. The supernatant was collected for the protein concentration determination using the Bio-Rad DC protein assay (#5000112; Bio-Rad, Hercules, United States) according to the manufacturer's protocol. Gels (12%) were loaded with 4–10 µg of protein. After electrophoresis, gels were blotted onto nitrocellulose membranes (#170-4270; Bio-Rad, Hercules, United States). Blots were blocked with Odyssey® Blocking Buffer (#927-40000, LI-COR, Lincoln, USA) in a dilution of 1:1 with PBS overnight at 4°C. Afterward, blots were incubated with the primary antibodies overnight. The following primary antibodies were used: rabbit anti-SM22α (1:1000; #ab14106, Abcam, Cambridge, UK), mouse anti-αSMA (1:1000; #ab5694, Abcam, Cambridge, UK) and rabbit anti-GAPDH (1:1000; #ab9485, Abcam, Cambridge, UK). Then, the membranes were washed during 30 minutes with Tris-buffered saline with 0.1% Tween-20 (TBST) and incubated for 1 hour with the Odyssey® secondary antibodies goat anti-rabbit IRDye 680LT (1:10000; #926-68021, LI-COR, Lincoln, USA) and goat anti-mouse IRDye 800CW (1:10,000; #926-32210, LI-COR, Lincoln, USA). Non-bound secondary antibodies were removed by washing with TBST for 30 minutes. Then, blots were washed for 5 minutes with Tris-buffered saline (TBS) and scanned with Odyssey® Infrared Imaging System (LI-COR, Lincoln, USA).

Wound healing assay. NHCF-V were seeded in 48-well tissue culture plates at a density of 15,000 cells/cm² and cultured in FGM3, 37°C, and 5% CO₂ until 70% confluence was reached. Then, cells were divided into 5 groups and stimulated for 5 days, as prescribed previously. After this period, the confluent monolayers were scored with a 10 µl sterile pipette tip to leave a scratch of approximately 0.4–0.5 mm in width. Culture medium

was, then, immediately removed and cells were carefully washed with PBS - to remove any dislodged cells - and the medium was replaced with fresh FGM2. Pictures were taken immediately after the scratch and, again, after 24 hours. The percentage of wound reduction was evaluated in ImageJ.

Statistical analysis. All data were obtained from at least three independent experiments, performed in duplicate or triplicate. Data are presented as mean \pm standard error of the mean (SEM). Graphs and statistical analysis were done using GraphPad Prism (Version 6.01; GraphPad Software, Inc., La Jolla, United States). Differences among multiple groups were analyzed by One-way ANOVA with Sidak's multiple comparison test for the following groups: FGM2/TGF- β 1 vs. FGM2/TGF- β 1/FGF-2 and FGM2/TGF- β 1 vs. ASC-CMed/TGF- β 1.

Data Availability Statement

The datasets generated during and/or analyzed during the current study are available from the corresponding author on reasonable request.

References

- Kong, P., Christia, P. & Frangogiannis, N. G. The pathogenesis of cardiac fibrosis. *Cell. Mol. Life Sci.* **71**, 549–574 (2014).
- Edgley, A. J., Krum, H. & Kelly, D. J. Targeting fibrosis for the treatment of heart failure: a role for transforming growth factor- β . *Cardiovasc. Ther.* **30**, e30–40 (2012).
- Piera-Velazquez, S., Li, Z. & Jimenez, S. A. Role of endothelial-mesenchymal transition (EndoMT) in the pathogenesis of fibrotic disorders. *Am. J. Pathol.* **179**, 1074–1080 (2011).
- Zeisberg, E. M. & Kalluri, R. Origins of cardiac fibroblasts. *Circ. Res.* **107**, 1304–1312 (2010).
- Travers, J. G., Kamal, F. A., Robbins, J., Yutzey, K. E. & Blaxall, B. C. Cardiac Fibrosis: The Fibroblast Awakens. *Circ. Res.* **118**, 1021–1040 (2016).
- Biernacka, A., Dobaczewski, M. & Frangogiannis, N. G. TGF- β signaling in fibrosis. *Growth Factors* **29**, 196–202 (2011).
- Piersma, B., Bank, R. A. & Boersema, M. Signaling in Fibrosis: TGF- β , WNT, and YAP/TAZ Converge. *Front. Med.* **2**, 59 (2015).
- Dobaczewski, M., Chen, W. & Frangogiannis, N. G. Transforming growth factor (TGF)- β signaling in cardiac remodeling. *J. Mol. Cell. Cardiol.* **51**, 600–606 (2011).
- Pohlars, D. *et al.* TGF- β and fibrosis in different organs — molecular pathway imprints. *Biochimica et Biophysica Acta (BBA) - Molecular Basis of Disease* **1792**, 746–756 (2009).
- Leask, A. TGF β , cardiac fibroblasts, and the fibrotic response. *Cardiovasc. Res.* **74**, 207–212 (2007).
- Spyrou, G. E. & Naylor, I. L. The effect of basic fibroblast growth factor on scarring. *Br. J. Plast. Surg.* **55**, 275–282 (2002).
- Akasaka, Y., Ono, I., Yamashita, T., Jimbow, K. & Ishii, T. Basic fibroblast growth factor promotes apoptosis and suppresses granulation tissue formation in acute incisional wounds. *J. Pathol.* **203**, 710–720 (2004).
- Nunes, Q. M., Li, Y., Sun, C., Kinnunen, T. K. & Fernig, D. G. Fibroblast growth factors as tissue repair and regeneration therapeutics. <https://doi.org/10.7287/peerj.preprints.1378v1> (2015).
- Gallego-Muñoz, P. *et al.* Effects of TGF β 1, PDGF-BB, and bFGF, on human corneal fibroblasts proliferation and differentiation during stromal repair. *Cytokine* **96**, 94–101 (2017).
- Song, Q. H., Klepeis, V. E., Nugent, M. A. & Trinkaus-Randall, V. TGF-beta1 regulates TGF-beta1 and FGF-2 mRNA expression during fibroblast wound healing. *Mol. Pathol.* **55**, 164–176 (2002).
- Maltseva, O., Folger, P., Zekaria, D., Petridou, S. & Masur, S. K. Fibroblast growth factor reversal of the corneal myofibroblast phenotype. *Invest. Ophthalmol. Vis. Sci.* **42**, 2490–2495 (2001).
- Dolivo, D. M., Larson, S. A. & Dominko, T. FGF2-mediated attenuation of myofibroblast activation is modulated by distinct MAPK signaling pathways in human dermal fibroblasts. *J. Dermatol. Sci.* **88**, 339–348 (2017).
- Dolivo, D. M., Larson, S. A. & Dominko, T. Fibroblast Growth Factor 2 as an Antifibrotic: Antagonism of Myofibroblast Differentiation and Suppression of Pro-Fibrotic Gene Expression. *Cytokine Growth Factor Rev.* **38**, 49–58 (2017).
- Song, Q. H. TGF-beta1 regulates TGF-beta1 and FGF-2 mRNA expression during fibroblast wound healing. *Mol. Pathol.* **55**, 164–176 (2002).
- Tiede, S. *et al.* Basic fibroblast growth factor: a potential new therapeutic tool for the treatment of hypertrophic and keloid scars. *Ann. Anat.* **191**, 33–44 (2009).
- Svystonyuk, D. A. *et al.* Fibroblast growth factor-2 regulates human cardiac myofibroblast-mediated extracellular matrix remodeling. *J. Transl. Med.* **13** (2015).
- Park, D. S. J. *et al.* Heparin Augmentation Enhances Bioactive Properties of Acellular Extracellular Matrix Scaffold. *Tissue Eng. Part A* **24**, 128–134 (2018).
- Mazo, M. *et al.* Treatment of Reperfused Ischemia With Adipose-Derived Stem Cells in a Preclinical Swine Model of Myocardial Infarction. *Cell Transplant.* **21**, 2723–2733 (2012).
- Yu, L. H. *et al.* Improvement of cardiac function and remodeling by transplanting adipose tissue-derived stromal cells into a mouse model of acute myocardial infarction. *Int. J. Cardiol.* **139**, 166–172 (2010).
- Perin, E. C. *et al.* Adipose-derived regenerative cells in patients with ischemic cardiomyopathy: The PRECISE Trial. *Am. Heart J.* **168**, 88–95.e2 (2014).
- Mazo, M. *et al.* Transplantation of adipose derived stromal cells is associated with functional improvement in a rat model of chronic myocardial infarction. *Eur. J. Heart Fail.* **10**, 454–462 (2008).
- Tano, N. *et al.* Epicardial placement of mesenchymal stromal cell-sheets for the treatment of ischemic cardiomyopathy; *in vivo* proof-of-concept study. *Mol. Ther.* **22**, 1864–1871 (2014).
- Araña, M. *et al.* Epicardial delivery of collagen patches with adipose-derived stem cells in rat and minipig models of chronic myocardial infarction. *Biomaterials* **35**, 143–151 (2014).
- He, J., Cai, Y., Luo, L. M. & Liu, H. B. Hypoxic adipose mesenchymal stem cells derived conditioned medium protects myocardial infarct in rat. *Eur. Rev. Med. Pharmacol. Sci.* **19**, 4397–4406 (2015).
- Jiang, Y. *et al.* Intramyocardial injection of hypoxia-preconditioned adipose-derived stromal cells treats acute myocardial infarction: an *in vivo* study in swine. *Cell Tissue Res.* **358**, 417–432 (2014).
- Kapur, S. K. & Katz, A. J. Review of the adipose derived stem cell secretome. *Biochimie* **95**, 2222–2228 (2013).
- Salgado, A. J. B. O. G., Reis, R. L. G., Sousa, N. J. C. & Gimble, J. M. Adipose tissue derived stem cells secretome: soluble factors and their roles in regenerative medicine. *Curr. Stem Cell Res. Ther.* **5**, 103–110 (2010).
- Du, W. J. *et al.* Heterogeneity of proangiogenic features in mesenchymal stem cells derived from bone marrow, adipose tissue, umbilical cord, and placenta. *Stem Cell Res. Ther.* **7**, 163 (2016).
- Rehman, J. *et al.* Secretion of angiogenic and antiapoptotic factors by human adipose stromal cells. *Circulation* **109**, 1292–1298 (2004).
- Spiekman, M. *et al.* Adipose tissue-derived stromal cells inhibit TGF- β 1-induced differentiation of human dermal fibroblasts and keloid scar-derived fibroblasts in a paracrine fashion. *Plast. Reconstr. Surg.* **134**, 699–712 (2014).

36. Correia, A. C. P., Moonen, J.-R. A. J., Brinker, M. G. L. & Krenning, G. FGF2 inhibits endothelial-mesenchymal transition through microRNA-20a-mediated repression of canonical TGF- β signaling. *J. Cell Sci.* **129**, 569–579 (2016).
37. Papetti, M., Shujath, J., Riley, K. N. & Herman, I. M. FGF-2 antagonizes the TGF-beta1-mediated induction of pericyte alpha-smooth muscle actin expression: a role for myf-5 and Smad-mediated signaling pathways. *Invest. Ophthalmol. Vis. Sci.* **44**, 4994–5005 (2003).
38. Chen, P.-Y., Qin, L., Li, G., Tellides, G. & Simons, M. Smooth muscle FGF/TGF β cross talk regulates atherosclerosis progression. *EMBO Mol. Med.* **8**, 712–728 (2016).
39. Chen, P.-Y. *et al.* FGF regulates TGF- β signaling and endothelial-to-mesenchymal transition via control of let-7 miRNA expression. *Cell Rep.* **2**, 1684–1696 (2012).
40. Papetti, M., Shujath, J., Riley, K. N. & Herman, I. M. FGF-2 Antagonizes the TGF- β 1-Mediated Induction of Pericyte α -Smooth Muscle Actin Expression: A Role for Myf-5 and Smad-Mediated Signaling Pathways. *Investigative Ophthalmology & Visual Science* **44**, 4994 (2003).
41. Zhao, J., Hu, L., Liu, J., Gong, N. & Chen, L. The effects of cytokines in adipose stem cell-conditioned medium on the migration and proliferation of skin fibroblasts *in vitro*. *Biomed Res. Int.* **2013**, 578479 (2013).
42. Ohnishi, S., Sumiyoshi, H., Kitamura, S. & Nagaya, N. Mesenchymal stem cells attenuate cardiac fibroblast proliferation and collagen synthesis through paracrine actions. *FEBS Lett.* **581**, 3961–3966 (2007).
43. Mias, C. *et al.* Mesenchymal stem cells promote matrix metalloproteinase secretion by cardiac fibroblasts and reduce cardiac ventricular fibrosis after myocardial infarction. *Stem Cells* **27**, 2734–2743 (2009).
44. Wang, Y. *et al.* Effects of mesenchymal stem cells on matrix metalloproteinase synthesis in cardiac fibroblasts. *Exp. Biol. Med.* **236**, 1197–1204 (2011).
45. Mao, Q., Lin, C.-X., Liang, X.-L., Gao, J.-S. & Xu, B. Mesenchymal stem cells overexpressing integrin-linked kinase attenuate cardiac fibroblast proliferation and collagen synthesis through paracrine actions. *Mol. Med. Rep.* **7**, 1617–1623 (2013).
46. Li, X. *et al.* Direct intercellular communications dominate the interaction between adipose-derived MSCs and myofibroblasts against cardiac fibrosis. *Protein Cell* **6**, 735–745 (2015).
47. Kilroy, G. E. *et al.* Cytokine profile of human adipose-derived stem cells: expression of angiogenic, hematopoietic, and pro-inflammatory factors. *J. Cell. Physiol.* **212**, 702–709 (2007).
48. Pritchard, H. L., Reichert, W. & Klitzman, B. IFATS collection: Adipose-derived stromal cells improve the foreign body response. *Stem Cells* **26**, 2691–2695 (2008).
49. Nakagami, H. *et al.* Novel autologous cell therapy in ischemic limb disease through growth factor secretion by cultured adipose tissue-derived stromal cells. *Arterioscler. Thromb. Vasc. Biol.* **25**, 2542–2547 (2005).
50. Cui, L. *et al.* Expanded Adipose-Derived Stem Cells Suppress Mixed Lymphocyte Reaction by Secretion of Prostaglandin E2. *Tissue Eng.* **13**, 1185–1195 (2007).
51. Tuin, A., Kluijtmans, S. G., Bouwstra, J. B., Harmsen, M. C. & Van Luyn, M. J. A. Recombinant gelatin microspheres: novel formulations for tissue repair? *Tissue Eng. Part A* **16**, 1811–1821 (2010).

Author Contributions

T.T.A.L. has contributed to the conception and design of the work, data collection, data analysis and interpretation, drafting the article, critical revision of the article and final approval of the version to be published. G.R.L. has contributed to the conception and design of the work, data collection, data analysis and interpretation, drafting the article, critical revision of the article and final approval of the version to be published. L.F.P.M. has contributed to the data analysis and interpretation, critical revision of the article and final approval of the version to be published. M.C.H. has contributed to the conception and design of the work, data analysis and interpretation, critical revision of the article and final approval of the version to be published.

Additional Information

Supplementary information accompanies this paper at <https://doi.org/10.1038/s41598-018-34747-3>.

Competing Interests: The authors declare no competing interests.

Publisher's note: Springer Nature remains neutral with regard to jurisdictional claims in published maps and institutional affiliations.



Open Access This article is licensed under a Creative Commons Attribution 4.0 International License, which permits use, sharing, adaptation, distribution and reproduction in any medium or format, as long as you give appropriate credit to the original author(s) and the source, provide a link to the Creative Commons license, and indicate if changes were made. The images or other third party material in this article are included in the article's Creative Commons license, unless indicated otherwise in a credit line to the material. If material is not included in the article's Creative Commons license and your intended use is not permitted by statutory regulation or exceeds the permitted use, you will need to obtain permission directly from the copyright holder. To view a copy of this license, visit <http://creativecommons.org/licenses/by/4.0/>.

© The Author(s) 2018

CHAPTER 2

Adipose tissue-derived stromal cells' conditioned medium modulates endothelial-mesenchymal transition induced by IL-1 β /TGF- β 2 but does not restore endothelial function

Tácia Tavares de Aquinas Liguori^{1,2}, Gabriel Romero Liguori^{1,2}, Luiz Felipe Pinho Moreira², Martin C. Harmsen¹

1. Department of Pathology and Medical Biology, University of Groningen and University Medical Center Groningen, Groningen, Netherlands
2. Heart Institute (InCor), Hospital das Clinicas HCFMUSP, Faculdade de Medicina, Universidade de Sao Paulo, Sao Paulo, Brazil

Published

Cell Proliferation, 2018 - DOI: 10.1111/cpr.12629

Link: <https://onlinelibrary.wiley.com/doi/full/10.1111/cpr.12629>



Adipose tissue-derived stromal cells' conditioned medium modulates endothelial-mesenchymal transition induced by IL-1 β /TGF- β 2 but does not restore endothelial function

Tácia Tavares Aquinas Liguori^{1,2} | Gabriel Romero Liguori^{1,2} | Luiz Felipe Pinho Moreira¹ | Martin Conrad Harmsen²

¹Laboratório de Cirurgia Cardiovascular e Fisiopatologia da Circulação (LIM-11), Faculdade de Medicina, Instituto do Coração (InCor), Hospital das Clínicas HCFMUSP, Universidade de São Paulo, São Paulo, Brazil

²Department of Pathology and Medical Biology, University of Groningen, University Medical Center Groningen, Groningen, The Netherlands

Correspondence

Martin Conrad Harmsen, Department of Pathology and Medical Biology, University of Groningen, University Medical Center Groningen, Hanzeplein 1 - EA11, 9713 GZ Groningen, the Netherlands.
Email: m.c.harmsen@umcg.nl

Abstract

Objectives: Endothelial cells undergo TGF- β -driven endothelial-mesenchymal transition (EndMT), representing up to 25% of cardiac myofibroblasts in ischaemic hearts. Previous research showed that conditioned medium of adipose tissue-derived stromal cells (ASC-CMed) blocks the activation of fibroblasts into fibrotic myofibroblasts. We tested the hypothesis that ASC-CMed abrogates EndMT and prevents the formation of adverse myofibroblasts.

Materials and methods: Human umbilical vein endothelial cells (HUVEC) were treated with IL-1 β and TGF- β 2 to induce EndMT, and the influence of ASC-CMed was assessed. As controls, non-treated HUVEC or HUVEC treated only with IL-1 β in the absence or presence of ASC-CMed were used. Gene expression of inflammatory, endothelial, mesenchymal and extracellular matrix markers, transcription factors and cell receptors was analysed by RT-qPCR. The protein expression of endothelial and mesenchymal markers was evaluated by immunofluorescence microscopy and immunoblotting. Endothelial cell function was measured by sprouting assay.

Results: IL-1 β /TGF- β 2 treatment induced EndMT, as evidenced by the change in HUVEC morphology and an increase in mesenchymal markers. ASC-CMed blocked the EndMT-related fibrotic processes, as observed by reduced expression of mesenchymal markers *TAGLN* ($P = 0.0008$) and *CNN1* ($P = 0.0573$), as well as *SM22 α* ($P = 0.0501$). The angiogenesis potential was impaired in HUVEC undergoing EndMT and could not be restored by ASC-CMed.

Conclusions: We demonstrated that ASC-CMed reduces IL-1 β /TGF- β 2-induced EndMT as observed by the loss of mesenchymal markers. The present study supports the anti-fibrotic effects of ASC-CMed through the modulation of the EndMT process.

Tácia Tavares Aquinas and Gabriel Romero Liguori equally contributed to the manuscript.

This is an open access article under the terms of the Creative Commons Attribution License, which permits use, distribution and reproduction in any medium, provided the original work is properly cited.

© 2019 The Authors. Cell Proliferation Published by John Wiley & Sons Ltd

1 | INTRODUCTION

Heart failure (HF) is an irreversible and potentially lethal clinical condition that affects nearly 23 million people worldwide.¹ The five-year survival is approximately 50%. Obviously, HF impacts significantly on the quality of life and is an increasing burden on society and health care. Heart failure presents as various forms of idiopathic or heritable cardiomyopathy and as the consequence of adverse cardiac tissue remodelling after acute myocardial infarction.

In normal physiology, cardiac tissue is in homeostasis that is maintained by a well-regulated biochemical and biomechanical crosstalk between the parenchyma and the supportive tissue stroma. Cardiac parenchyma comprises cardiomyocytes, while the stroma consists of vasculature, fibroblasts and their product, the extracellular matrix (ECM). The ECM provides structural support and architecture and instructs adhered tissue cells.² HF disrupts the cardiac tissue homeostasis. A prominent feature is the proliferation of myofibroblasts and their excessive deposition and accumulation of fibrotic ECM. Thus, HF is a process of cardiac fibrosis. Differentiation of cardiac fibroblasts to myofibroblasts is a major contribution to HF.^{3,4} Several other cell types, both endogenous in the heart and exogenous, also contribute to cardiac fibrosis.⁵ The heart is particularly rich in capillaries and thus endothelial cells. Under pathological conditions, endothelial cells contribute to adverse wound healing and tissue remodelling via endothelial-mesenchymal transition (EndMT) and contribute significantly to cardiac fibrosis and development of heart failure.^{6,7} After acute myocardial infarction in mice, up to 25% of cardiac myofibroblasts are the consequence of EndMT.⁸ Irrespective of the source, *for example*, fibroblasts or endothelial cells, the resulting myofibroblasts are indistinguishable with respect to proliferation and ECM remodelling. Interestingly, EndMT is pivotal during cardiogenesis, when EndMT underlies the development of heart valves.⁹ In contrast, in adult life, EndMT is related to pathophysiological phenomena such as cardiac fibrosis,¹⁰⁻¹² after myocardial infarction,^{8,13} diabetic cardiomyopathy^{14,15} and hypertensive heart disease.^{11,16} Therefore, inhibition or reversal of cardiac EndMT is a therapeutic option to interfere with heart failure.

Endothelial-to-mesenchymal transition is a relatively slow de-differentiation process (days to weeks) that is driven by pro-fibrotic growth factors of the TGF- β superfamily,^{17,18} such as TGF- β 2. Several processes coincide: endothelial cells lose cell-to-cell contacts and the downregulated endothelial markers. This causes the cells to transit from their characteristic cobblestone morphology to a spindle-like shape. Simultaneously, a progressive upregulation of mesenchymal markers occurs, such as smooth muscle protein 22 alpha (SM22 α), calponin and alpha-smooth muscle actin (α SMA). Similar to myofibroblasts, the EndMT process renders cells highly migratory and proliferative, while these become resistant to apoptosis too. The process of EndMT also coincides with the increased production and deposition of extracellular matrix, which contributes to the development and progression of cardiac fibrosis including the increased stiffness of the failing heart.^{19,20}

The TGF- β superfamily is important during embryogenesis, but also for wound healing, and thus influences cell growth, proliferation, differentiation and migration.²¹ In addition, TGF- β members are strong regulators of ECM remodelling, in particular, through upregulation of constructive proteins such as collagens. All three TGF- β isoforms stimulate EndMT.²²⁻²⁸ In cardiovascular wound healing, fibrosis coincides with inflammation. In fact, EndMT is synergized by TGF- β 2 and IL-1 β .^{29,30} Heart failure is also associated with pro-fibrotic stimuli by members of the TGF- β superfamily, inflammation and reactive oxygen species (ROS). These three triggers are tightly interrelated because TGF- β promotes inflammatory activation via TAK1, similar to ROS, and with it, EndMT.³¹ We have shown that pro-fibrotic stimuli and pro-inflammatory stimuli synergize EndMT,^{29,30} and other studies showed that ROS mediates the EndMT process through the TGF- β superfamily.^{32,33}

Cardiac stem cell therapy with mesenchymal stem/stromal cells (MSC) has shown to improve remodelling after acute myocardial infarction. This suggests that MSC affect myofibroblast formation and function. The intramyocardial administration of mesenchymal stromal cells (MSC), which include adipose tissue-derived stromal cells (ASC), has benefit for cardiac function and remodelling in a variety of cardiac diseases.³⁴⁻⁴² As a matter of fact, injection of conditioned medium of MSC (CMed) also improved cardiac function.^{43,44} Previous research in our laboratory showed that ASC secrete paracrine factors that abrogate TGF- β -induced differentiation of dermal fibroblasts to myofibroblasts which is a mesenchymal transition too.⁴⁵ In general, ASC and their secreted bioactive factors harbour pro-regenerative⁴⁶⁻⁴⁸ and anti-inflammatory potential.^{49,50} In addition, ASC promote angiogenesis. Therefore, we hypothesized that the formation of myofibroblasts from endothelial cells via EndMT, which also is a TGF- β -driven process and synergized by IL-1 β , is down-modulated by the paracrine action of ASC while it would rescue their endothelial phenotype. We tested our hypothesis *in vitro*, by assessing the influence of adipose tissue-derived stromal cells' conditioned medium (ASC-CMed) on pro-fibrotic and pro-inflammatory-induced EndMT.

2 | EXPERIMENTAL

2.1 | Cell sources, cell culture, conditioned medium and experimental groups

Human umbilical vein endothelial cells (HUVEC) were obtained from the endothelial cell culture facility of our institution and comprised pools of at least three donors. Cells were seeded on gelatin-coated plates (1% gelatin solution in PBS) at a density of 35 000 cells/cm² and cultured until confluency in endothelial cell medium (ECMed) composed of RPMI 1640 basal medium (#BE04-558F, Lonza) with 10% heat-inactivated foetal bovine serum (FBS; #F0804, Sigma-Aldrich), 1% penicillin/streptomycin (#15140122, Gibco Invitrogen), 1% L-glutamine (#17-605E, Lonza BioWhittaker), 5 U/mL heparin (LEO Laboratories Limited) and 50 μ g/mL bovine brain extract (BBE, home-made preparation). HUVEC between passages 3 and 6 were used for the experiments. Confluent HUVEC were divided into six groups with

TABLE 1 Experimental groups

| Group | Description |
|---------------------------------------|---|
| ECMed | HUVEC culture only with endothelial cell medium |
| ECMed/IL-1 β | HUVEC culture with endothelial cell medium added with IL-1 β |
| ECMed/IL-1 β /TGF- β 2 | HUVEC culture with endothelial cell medium added with IL-1 β and TGF- β 2 |
| ASC-CMed | HUVEC culture only with ASC conditioned media |
| ASC-CMed/IL-1 β | HUVEC culture with ASC conditioned media added with IL-1 β |
| ASC-CMed/IL-1 β /TGF- β 2 | HUVEC culture with ASC conditioned media added with IL-1 β and TGF- β 2 |

ASC, adipose tissue-derived stromal cells; ASC-CMed, conditioned media from adipose tissue-derived stromal cells; ECMed, endothelial culture medium; IL-1 β , human recombinant interleukin-1 beta; TGF- β 2, human transforming growth factor beta 2; UVEC, human umbilical vein endothelial cells.

different induction/ASC-CMed combinations, as described in Table 1, and cultured for 5 days. Human recombinant interleukin-1 β (IL-1 β ; #200-01B, PeproTech) and human transforming growth factor beta 2 (TGF- β 2; #100-35B, PeproTech) were used to stimulate the EndMT process at a concentration of 10ng/mL in all experiments.

Human ASC were isolated as described previously.⁵¹ Briefly, human abdominal fat was obtained by liposuction. Tissue was washed with phosphate-buffered saline (PBS) and then enzymatically digested with 0.1% collagenase A (#11088793001, Roche Diagnostic, Mannheim, Germany) in PBS with 1% bovine serum albumin (BSA; #A9647, Sigma-Aldrich). The tissue was shaken constantly at 37°C for 2 hours. After this, the digested tissue was washed in 1% BSA in PBS and filtered using 70 μ m cell strainers. The filtered suspension was centrifuged at 600 g for 10 minutes, and the cell pellet was resuspended in lysis buffer containing ammonium chloride to remove red blood cells, centrifuged again and resuspended in Dulbecco's modified Eagle's medium (DMEM; #12-604F, Lonza) with 10% foetal bovine serum (FBS; #F0804, Sigma-Aldrich), 1% penicillin/streptomycin (#15140122, Gibco Invitrogen) and 1% L-glutamine (#17-605E, Lonza BioWhittaker). Cells were cultured at 37°C in a humidified incubator with 5% CO₂. The medium was refreshed every 2 days. Cells were passed at a ratio of 1:3 after reached confluency. The characterization of the cells was routinely performed as previously described by our group and confirmed the required marker pattern and biological behaviour of ASC.⁵²

After the second passage, ASC were maintained in ECMed. ASC-CMed was obtained from confluent cultures of ASC between passages 3 and 6 from 3 different donors. For ASC-CMed, cells were cultured in ECMed and the conditioned medium was harvested after 48 hours, filtered in 0.22 μ m filters and stored at -20°C until use. The expression of fibroblast growth factor 1 (FGF-1) and vascular endothelial growth factor (VEGF) was determined in the medium

collected from ASC. For this purpose, Magnetic Luminex Human Premixed Multi-Analyte Kit (R&D Systems) was used according to the manufacturer's protocol. DMEM only was used as negative control.

2.2 | Immunofluorescence, Gene Expression and Immunoblotting

2.2.1 | Immunofluorescence

HUVEC were cultured in 96-well tissue culture plates in ECMed. After 5 days of EndMT induction, cells were fixed at room temperature with 2% paraformaldehyde (PFA) for 30 minutes. Cells were permeabilized with 1% Triton-X 100 in PBS at room temperature for 15 minutes and blocked with 5% donkey serum in PBS and 1% BSA at room temperature for 15 minutes. Subsequently, cells were incubated with primary antibodies diluted in 5% donkey serum in PBS at room temperature for 2 hours. The following primary antibodies were used: rabbit anti-SM22 α (1:400; #ab14106, Abcam) and mouse anti-human PECAM-1 (1:200; #MAB9381, R&D Systems, Oxon). Controls were incubated with 5% donkey serum in PBS instead of primary antibody. Next, cells were washed with 0.05% Tween-20 in PBS and incubated with secondary antibodies in 5% donkey serum in PBS with 4',6-diamidino-2-phenylindole (DAPI; 1:5000; #D9542-5MG, Sigma-Aldrich) and Alexa Fluor® 488 phalloidin (1:400; #A12379, Life Technologies) at room temperature for 1 hour. The following secondary antibodies were used: donkey anti-rabbit IgG (H + L) Alexa Fluor® 594 (1:400; #A-21207, Life Technologies) and donkey anti-mouse IgG (H + L) Alexa Fluor® 594 (1:400; #ab150108, Abcam). Finally, cells were washed three times with PBS and the plates were imaged with EVOS FL System (Thermo Fisher Scientific) using Texas Red (TXR), DAPI and Green Fluorescent Protein (GFP) channels with 20 \times magnification.

2.2.2 | Gene expression analysis

HUVEC were cultured in 75 cm² flasks. After 5 days of induction, total RNA was isolated using TRIzol reagent (#15596018, Invitrogen Corp) according to the manufacturer's protocol. RNA concentration and purity were determined using a NanoDrop Spectrophotometer (Thermo Scientific). Between 300 ng and 5000 ng of total RNA was used for cDNA synthesis, which was performed using RevertAid™ First Strand cDNA Synthesis Kit (Thermo Fisher Scientific) according to the manufacturer's protocol. The cDNA equivalent of 12 ng total RNA was used per single qPCR. PCR was performed using SYBR Green (Bio-Rad, Hercules) with the ViiA7 Real-Time PCR System (Applied Biosystems). Each analysis was done in duplicate for each one of the independent experiments. The primers used are listed in Table S1. Data were analysed using ViiA7 software (Applied Biosystems) and normalized with the ΔC_t method, using the geometrical mean of 18S ribosomal RNA (18S RNA) cycle threshold (C_t) values. The fold-change in gene expression vs the no treatment control group (ECMed) was calculated using the $\Delta\Delta C_t$ method.

2.2.3 | Immunoblotting analysis

HUVEC were cultured in 75 cm² flasks. After 5 days of induction, cells were rinsed with ice-cold PBS and lysed in 100 µL of ice-cold lysis buffer (RIPA; #89900, Thermo Fisher Scientific) containing 1% protease inhibitor cocktail (PIC; #P8340, Sigma-Aldrich) and 1% Halt™ Phosphatase Inhibitor Cocktail (#78420, Thermo Fisher Scientific). The lysed cells were collected in 2 mL microcentrifuge tubes, and the contents were homogenized by sonication at 30 W for 30 seconds and centrifuged at 7500 g at 4°C for 5 minutes. The supernatant was collected for the protein concentration determination using the Bio-Rad DC Protein Assay (#5000112; Bio-Rad, Hercules) according to the manufacturer's protocol. Gels (12%) were loaded with 25–30 µg of protein per lane. After electrophoresis, gels were blotted onto nitrocellulose membranes (#170-4270; Bio-Rad, Hercules). Blots were blocked with Odyssey® Blocking Buffer (#927-40000, LI-COR, Lincoln) in a dilution of 1:1 with PBS at 4°C overnight. Afterwards, blots were incubated with the primary antibodies overnight. The following primary antibodies were used: rabbit anti-SM22α (1:1000; #ab14106, Abcam), rabbit anti-VE-cadherin (1:500; #2500S, Cell Signalling), and mouse anti-GAPDH (1:1000; #ab9484, Abcam). Then, the membranes were washed with Tris-buffered saline (TBS) with 0.1% Tween-20 (TBST) 30 minutes and incubated with the Odyssey® secondary antibodies goat anti-rabbit IRDye 680LT (1:10000; #926-68021, LI-COR, Lincoln) and goat anti-mouse IRDye 800CW (1:10,000; #926-32210, LI-COR, Lincoln) for 1 hour. Non-bound secondary antibodies were removed by washing with TBST for 30 minutes. Then, blots were washed with TBS for 5 minutes and scanned with Odyssey® Infrared Imaging System (LI-COR, Lincoln).

2.2.4 | Endothelial sprouting assay

HUVEC were cultured in 25 cm² flasks. After 5 days of induction, cells were detached from the flasks and counted, and, for each group, 15 000 cells were resuspended in 50 µL of ECMed. Subsequently, cells were seeded in wells of a µ-Slide Angiogenesis Plate (Ibidi GmbH) previously coated and incubated at 37°C with 10 µL of Matrigel® (#356231, BD Biosciences) for 2 hours. The sprouting was allowed to proceed for 8 hours. Every condition was done in duplicate, and the experiment was performed three times independently. Formation of sprouting networks was imaged with a DM2000 LED Inverted Microscope (Leica) using 2.5× magnification and analysed using ImageJ software. The number of nodes,

branches, segments, total length, number of meshes and mean mesh size were analysed.

2.3 | Statistical analysis

All data were obtained from at least three independent experiments performed in duplicate. Data are presented as the mean ± SE of the mean (SEM). Graphs and statistical analysis were done using GraphPad Prism (version 6.01; GraphPad Software, Inc). Differences among multiple groups were analysed by one-way ANOVA with Sidak's multiple comparison test for the two groups of interested in each scenario.

3 | RESULTS

3.1 | ASC secrete fibroblast growth factor 1 (FGF-1) and vascular endothelial growth factor (VEGF)

The growth factor release from ASC was determined by the measurement of FGF-1 and VEGF, in the medium collected from the cells, using the Magnetic Luminex Human Premixed Multi-Analyte Kit. The concentration of growth factors was 21.7 ± 0.7 pg/mL for FGF-1 and 95.6 ± 3.1 pg/mL for VEGF. DMEM only showed growth factor concentrations close to zero (Figure 1).

3.2 | HUVEC undergoing EndMT present conformational changes

All cells started the experiment as a cobblestone morphology (Figure 2). After two days, the cells receiving inflammatory stimuli had disrupted intercellular adhesions. During this same period, co-stimulation with pro-inflammatory and pro-fibrotic factors, that is, induction of EndMT, part of the HUVEC showed more pronounced disruption of intercellular adhesions and had altered from their characteristic cobblestone morphology into spindle-shaped cells (Figure 2). The cells cultured with ASC-CMed retained their cobblestone morphology, but it did not inhibit the disruption of intercellular adhesions, in the cells neither with only inflammatory stimulation nor with both inflammatory and pro-fibrotic stimulation (Figure 2). Control cells kept their morphology for the entire duration of the experiment. The inflammatory environment did not change the cells compared to the second day. In EndMT-induced HUVEC, all intercellular adhesions were disrupted, while all cells were spindle-shaped at day 5 (Figure 2). Although these changes could be seen both in the groups cultured only with IL-1β and those

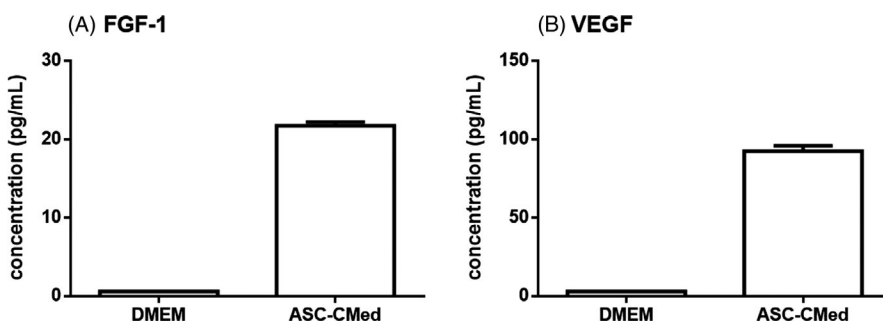


FIGURE 1 Concentration of growth factors released by ASC in the conditioned medium. A, FGF-1 B, VEGF

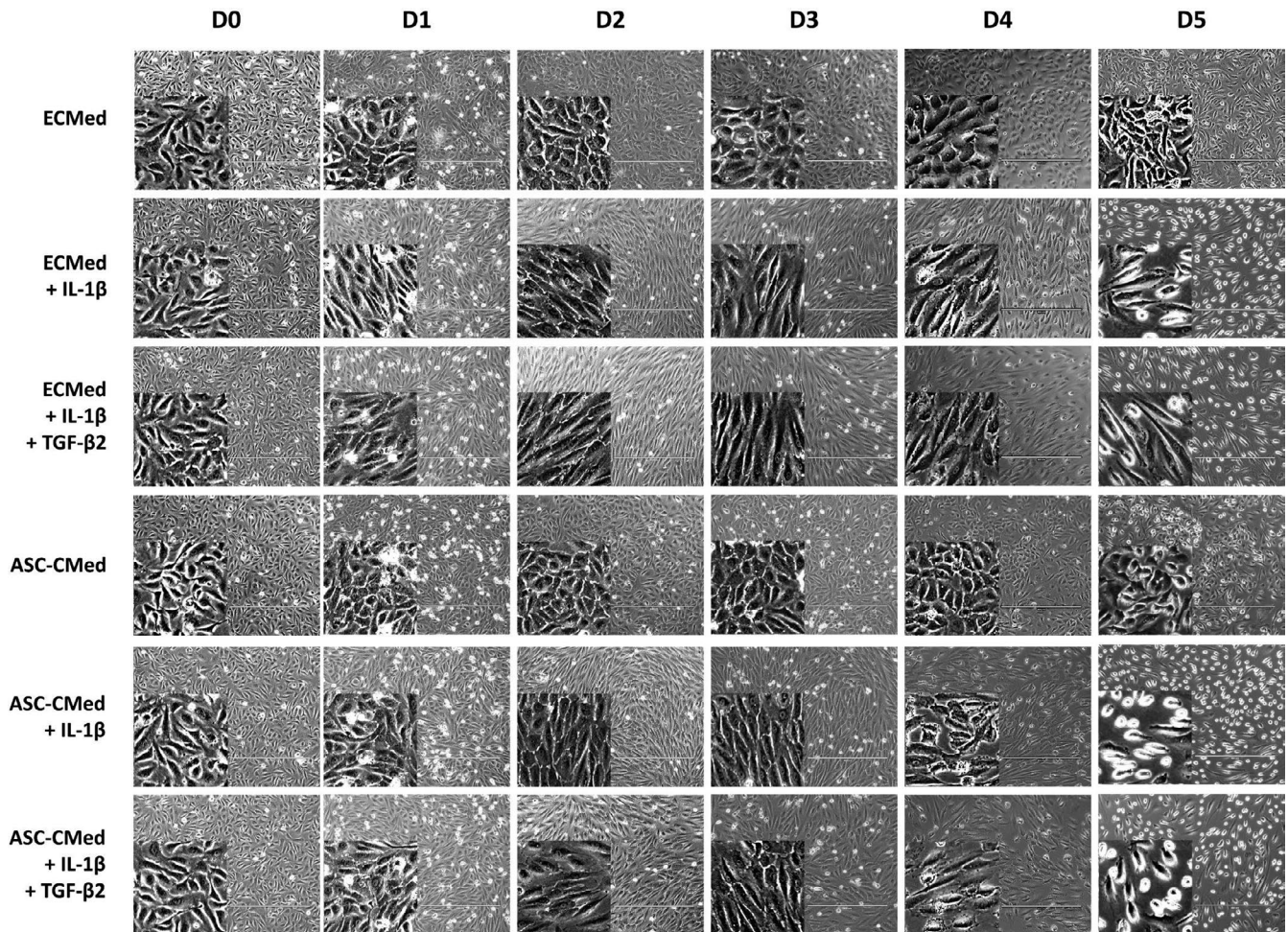


FIGURE 2 Conformational changes in HUVEC under stimulation with IL-1 β or co-stimulation with IL-1 β /TGF- β 2, both in ECMed and in ASC-CMed, for five days. Scale reference: 400 μ m

undergoing co-stimulation with IL-1 β and TGF- β 2, the latter showed a more explicit transformation. The use of ASC-CMed did not prevent cell-to-cell adhesion disruption or morphology changes to occur.

3.3 | Inflammatory gene expression in activated HUVEC is refractory to ASC-secreted factors

Pro-inflammatory stimulation of HUVEC with IL-1 β upregulated expression of *IL8*, *ICAM1* and *VCAM1*, which encode respectively chemoattractant and adhesion molecules required for endothelial transmigration of activated leucocytes (Figure 3). This upregulation was refractory to simultaneous treatment with ASC-CMed (Figure 3). Also, IL-1 β stimulation upregulated expression of two pro-inflammatory cytokine genes, *IL1B* and *IL6*, which was unaffected by ASC-CMed, except for *IL6* that was slightly upregulated by ASC-CMed (one-way ANOVA, $P = 0.0075$; Sidak's multiple comparison test, $P = 0.0683$). The influence of TGF- β 2 on IL-1 β -stimulated HUVEC was negligible with respect to the expression of these inflammatory activation-related genes, neither did co-stimulation with ASC-CMed affect these genes. However, the expression of *IL6* was normalized compared to stimulation of HUVEC with IL-1 β and ASC-CMed.

3.4 | Mesenchymal gene expression in EndMT-induced HUVEC is suppressed by ASC-secreted factors while extracellular matrix genes are not

Pro-inflammatory stimulation of HUVEC with IL-1 β did not change the expression of *PECAM1* and *CDH5* (Figure 4A-B) which are endothelial intercellular adhesion molecules that support the maintenance of the endothelial barrier. As expected, this pro-inflammatory activation abolished eNOS (*NOS3*) gene expression (Figure 4C). Similarly, endothelial co-stimulation with IL-1 β and TGF- β 2 did not affect the expression of *PECAM1* and *CDH5*, while *NOS3* expression was abolished too (Figure 4A-C). Though TGF- β 2 has anti-inflammatory effects, it could not alleviate the strong influence of IL-1 β on *NOS3* downregulation. The expression of these endothelial-specific genes was unaffected by ASC-CMed neither in unstimulated controls nor after cytokine activation (Figure 4A-C). The expression of *TAGLN* and *CCN1*, mesenchymal genes typical for EndMT, was unaffected in HUVEC after pro-inflammatory stimulation (Figure 4D-E). As expected, co-stimulation with IL-1 β and TGF- β 2 upregulated expression of *TAGLN* and *CCN1*. Endothelial gene expression (*PECAM1*, *CDH5*, and *NOS3*) was not

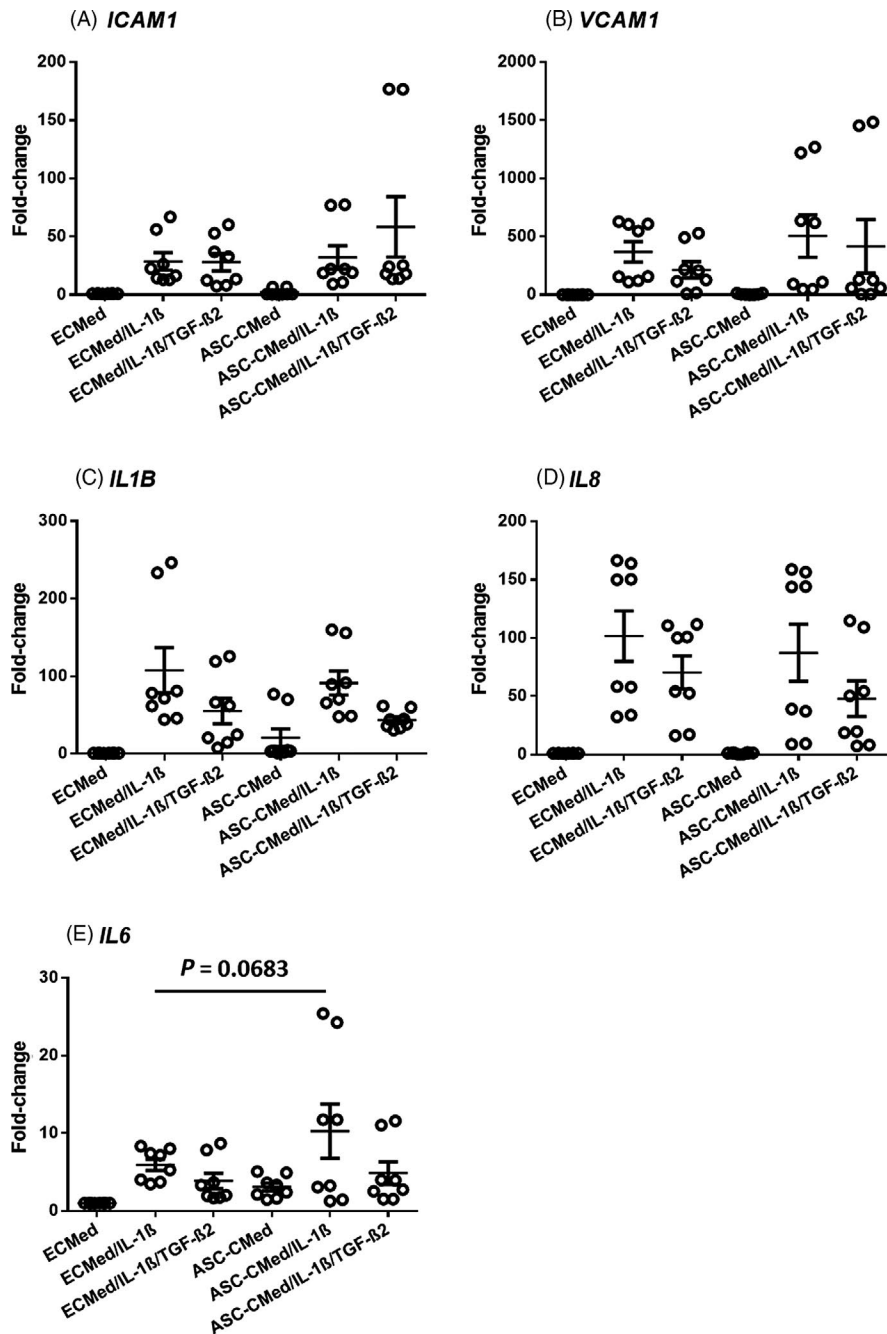


FIGURE 3 Gene expression (mRNA) of inflammatory markers A, *ICAM1*, B, *VCAM1*, C, *IL1B*, D, *IL8*, and E, *IL6* by semi-quantitative RT-qPCR of HUVEC after stimulation with IL-1 β or co-stimulation with IL-1 β /TGF- β 2, both in ECMed and in ASC-CMed, for five days. Data were analysed by one-way ANOVA with Sidak's multiple comparison test for the groups ECMed/IL-1 β vs ASC-CMed/IL-1 β ; *P*-values for the Sidak's multiple comparison test are shown in the figure. Values represent mean \pm SEM of 4 independent experiments in duplicate

affected by ASC-CMed in controls or cytokine-stimulated HUVEC. On the other hand, ASC-CMed normalized expression of *TAGLN* (Figure 4D, one-way ANOVA, $P < 0.0001$; Sidak's multiple comparison test, $P = 0.0008$) and, albeit to a lesser extent, of *CCN1* (Figure 4E, one-way ANOVA, $P = 0.0976$; Sidak's multiple comparison test, $P = 0.0573$) in HUVEC that were induced to undergo EndMT, that is, co-stimulation with IL-1 β and TGF- β 2 (Figure 4D-E). Over the five-day period of the pro-inflammatory induction or the induction of EndMT, the expression of representative fibrosis-related extracellular matrix genes *COL1A1* and *COL3A1* was upregulated after co-stimulation with both cytokines (Figure 4F-G). In contrast to the structural mesenchymal genes *TAGLN* and *CCN1*,

the upregulation of *COL1A1* and *COL3A1* was refractory to treatment with ASC-CMed (Figure 4F-G).

To corroborate the gene expression results, protein expression was assessed by immunoblotting of the endothelial marker VE-cadherin (CD144, *CDH5* gene) and the mesenchymal marker SM22 (transgelin, *TAGLN* gene) (Figure 5). The expression of both proteins did not change in upon pro-inflammatory stimulation, nor was it affected by co-treatment with ASC-CMed. The expression of VE-cadherin, however, was slightly increased by ASC-CMed, irrespective of cytokine treatment (Figure 5A, one-way ANOVA, $P = 0.1990$; Sidak's multiple comparison test, $P = 0.0673$). The upregulated expression of SM22 after stimulation with both cytokines was suppressed by ASC-CMed

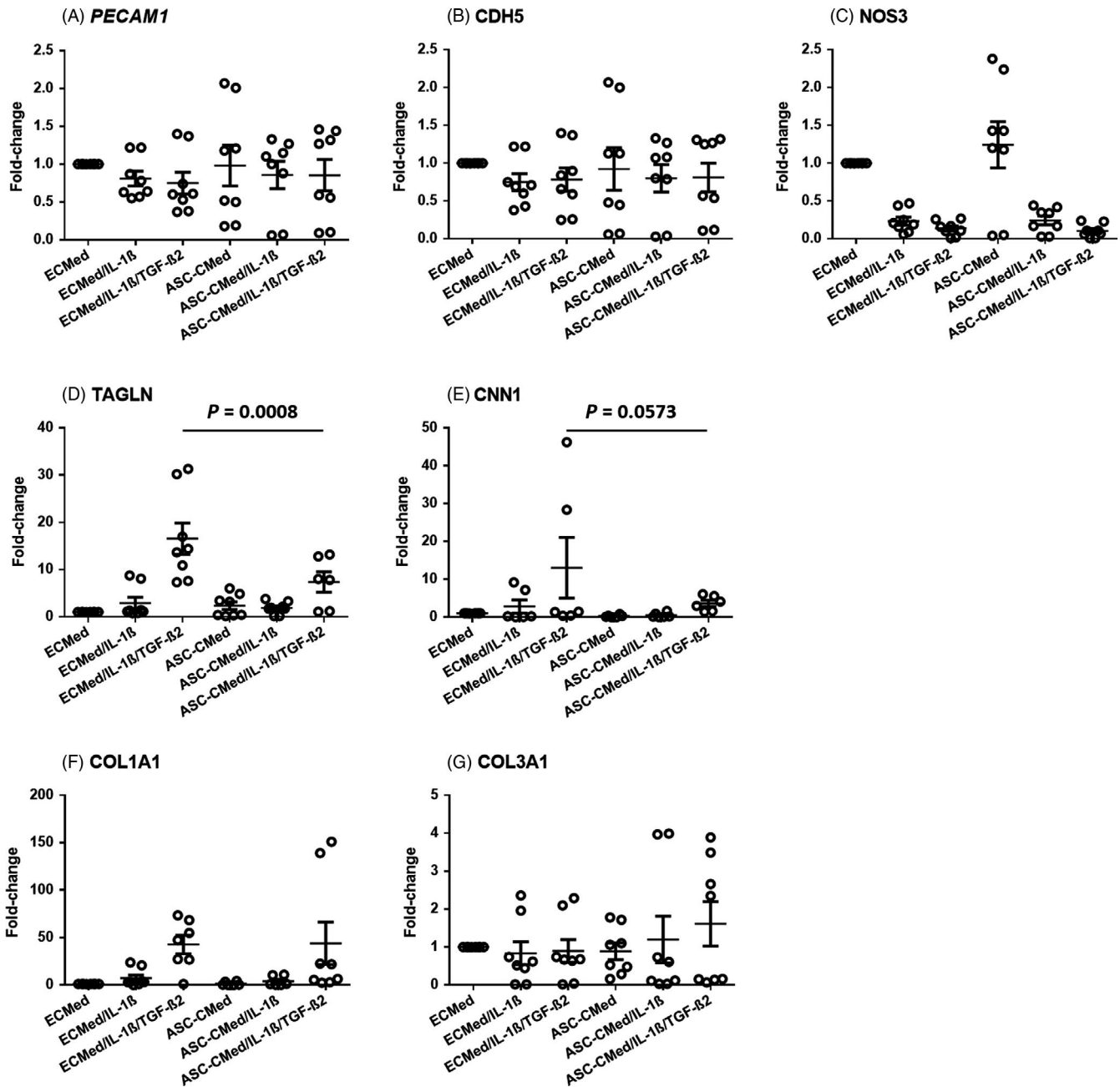


FIGURE 4 Gene expression (mRNA) of endothelial markers A, *PECAM1*, B, *CDH5* and C, *NOS3*; mesenchymal markers D, *TAGLN* and E, *CNN1*; and collagens F, *COL1A1* and G, *COL3A1* by semi-quantitative RT-qPCR of HUVEC under stimulation with IL-1 β or co-stimulation with IL-1 β /TGF- β 2, both in ECMed and in ASC-CMed, for five days. Data were analysed by one-way ANOVA with Sidak's multiple comparison test for the groups ECMed/IL-1 β /TGF- β 2 vs ASC-CMed/IL-1 β /TGF- β 2; P-values for the Sidak's multiple comparison test are shown in the figure. Values represent mean \pm SEM of four independent experiments in duplicate

(Figure 5B, one-way ANOVA, $P = 0.0064$; Sidak's multiple comparison test, $P = 0.0501$).

Immunofluorescence staining for the endothelial marker PECAM (CD31) showed that none of the cytokine treatments, nor the co-treatment with ASC-CMed, affected its expression (Figure 6, top row panels). In contrast to immunoblotting, in situ immunostaining of SM22 α proved less sensitive, yet it was detectable after stimulation with IL-1 β alone or together with TGF- β 2. Upon co-treatment with ASC-CMed, SM22 α expression was below detectable levels,

irrespective of treatment (Figure 6, middle row panels). This indicates that ASC secrete factors that suppress SM22 α in cytokine-stimulated HUVEC. The five-day pro-inflammatory activation of HUVEC induced hypertrophy as judged by F-actin detection with phalloidin staining (Figure 6, the lower row of panels). The hypertrophy was stronger and associated with transcellular stress fibres in HUVEC induced to undergo EndMT. Co-treatment with ASC-CMed, at least qualitatively, reduced the hypertrophy and intracellular stress fibres in HUVEC induced that underwent EndMT.

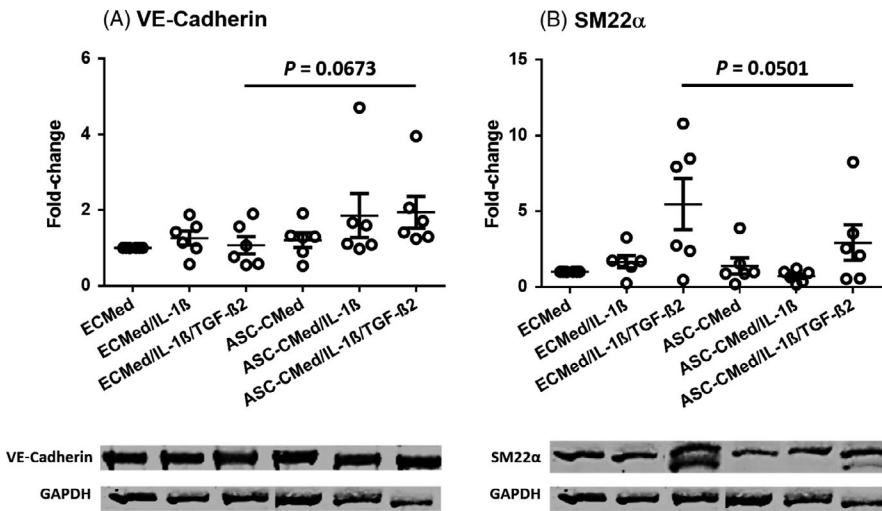


FIGURE 5 Protein expression of A, VE-cadherin and B, SM22 α by Western blot of HUVEC under stimulation with IL-1 β or co-stimulation with IL-1 β /TGF- β 2, both in ECMed and in ASC-CMed, for five days. Data were analysed by one-way ANOVA with Sidak's multiple comparison test for the groups ECMed/IL-1 β /TGF- β 2 vs ASC-CMed/IL-1 β /TGF- β 2; P-values for the Sidak's multiple comparison test are shown in the figure. Values represent mean \pm SEM of 6 independent experiments

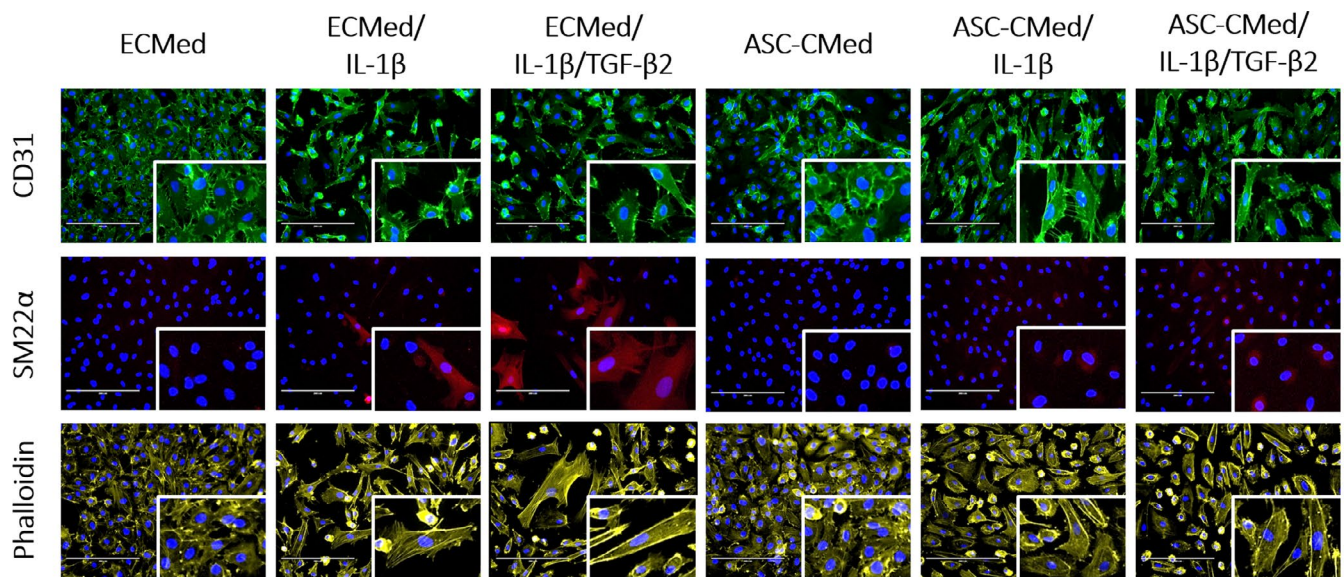


FIGURE 6 Fluorescence microscopy for phalloidin, SM22 α , and CD31 of HUVEC after stimulation with IL-1 β or co-stimulation with IL-1 β /TGF- β 2, both in ECMed and in ASC-CMed, for five days. Scale reference: 100 μ m

Downstream TGF- β signalling in EndMT is governed by the complex of the canonical TGF- β type II receptor (*TGFBR2*) and the TGF- β type I receptor *ALK5* (*ALK5*) that activate any of the transcription factors Snail (*SNAI1*), Slug (*SNAI2*) or Twist (*TWIST1*). The expression of *TGFBR2* remained unchanged, irrespective of cytokine treatment or co-treatment with ASC-CMed (Figure S1 A). However, as we published before, *ALK5* expression increased upon stimulation of EndMT for five days, albeit not significantly (Figure S1 B). The co-treatment with ASC-CMed did not influence the expression of *ALK5* irrespective of cytokine treatment. Expression of the most relevant downstream EndMT-associated transcription factor *SNAI1* paralleled the expression pattern of *ALK5*, that is, upregulation by co-stimulation with IL-1 β and TGF- β 2, while ASC-CMed had no influence on its expression (Figure S1 C). The expression of the second relevant transcription factor *SNAI2* was unaffected except for treatment with both cytokines

and the ASC-CMed (Figure S1 D, one-way ANOVA, $P = 0.0463$; Sidak's multiple comparison test, $P = 0.0244$). Expression of *TWIST1* was unchanged but tended to be upregulated in the presence of ASC-CMed (Figure S1 E).

3.5 | Factors secreted by ASC fail to restore impaired sprouting capacity of HUVEC undergoing EndMT

Endothelial cell function was assessed by short-term sprouting on Matrigel® and quantified through determination of nodes, segments, branches, total length, meshes and mean mesh size (Figure 7). Pro-inflammatory activated (5d, IL-1 β) HUVEC or HUVEC undergoing EndMT (5d, IL-1 β /TGF- β 2), largely lost their sprouting capacity, although this was more explicit in the latter group (Figure 7). Treatment with ASC-CMed did not restore the sprouting capacity of

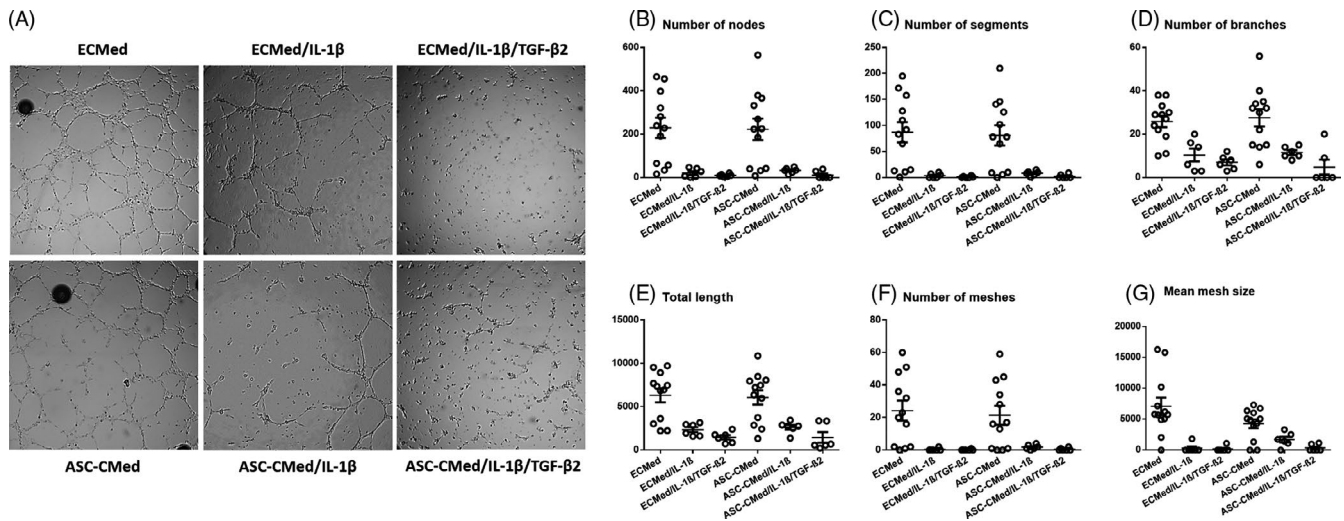


FIGURE 7 A, Sprouting assay (8 h) of HUVEC under stimulation with IL-1 β or co-stimulation with IL-1 β /TGF- β 2, both in ECMed and in ASC-CMed, for five days. Brightfield microscopy, augmentation 2.5X. Quantification of B, number of nodes, C, number of segments, D, number of branches, E, number of meshes, F, total length and G, mean mesh size. Values represent mean \pm SEM of three independent experiments in duplicate

HUVEC, while control treatment of HUVEC with ASC-CMed did not influence sprouting.

4 | DISCUSSION

The aim of our investigation was to assess the impact of factors secreted by ASC on EndMT induced by co-stimulation with IL-1 β and TGF- β 2. The main result is that ASC-CMed normalized or even promoted endothelial markers after EndMT induction, while constructive mesenchymal markers were suppressed. However, these ASC-secreted factors could not rescue the compromised endothelial functional phenotype because EC remained pro-inflammatory activated and had severely blunted sprouting capacity. Thus, the treatment of pro-inflammatory and pro-fibrotic-induced EndMT in vivo, such as during cardiac fibrosis, likely does not prevent endothelial dysfunction but might delay or suppress the mesenchymal transition itself, while more distant from a lesion ASC may still augment vascularization.

EndMT has been shown as an important process for the generation of myofibroblasts and, thus, fibrosis.³ The potential of ASC to inhibit EndMT may be one of the mechanisms involved in myocardial regeneration following cell therapies based on ASC.^{34-38,41} Literature supports that growth factors known to be secreted by ASC—such as FGF and VEGF^{53,54}—could block EndMT.⁵⁵⁻⁵⁷ Besides growth factors, the ASC secretome comprises microRNAs (often sequestered in exosomes), among which are miR-155, miR-31, and miR-21, all known regulators of EndMT.^{16,58,59} Another mechanism that may influence the expression of SM22 α is an epigenetic modification, for instance, the trimethylation of histone three (H3K27me3) by enhancer of zeste homolog 2 (EZH2)³⁰

Previously, mesenchymal cells derived from menstrual blood (MMC) were shown to ameliorate cardiac fibrosis via inhibition of

EndMT in myocardial infarction.⁶⁰ The authors showed that the total number of cells co-expressing CD31 and α SMA in the infarcted heart was reduced from 30% in the control group to 20% in the group treated with MMC. In our in vitro study, we also showed that the inhibition of EndMT occurred in a limited manner, corroborating the findings of the in vivo study, which showed the complete blockage of the EndMT process could not be achieved in vivo. The percentage of cells co-expressing endothelial and mesenchymal markers in the sham group, as a reference, was less than 4% (compared to the 20% in the group treated with MMC), but even with the moderate reduction evidenced in the treated group, modulation of cardiac damage could be demonstrated by the reduction in the infarcted area. The use of ASC, in turn, was demonstrated to inhibit epithelial-to-mesenchymal transition (EMT) and consequently renal fibrosis.^{61,62} Analogously to EndMT, EMT is a fibrotic process induced by TGF- β and mediated by key transcription factors such as Smad2/3, Snail and Twist.^{63,64} The effects demonstrated with the use of ASC in EMT are an important indicator that these cells would also play a role in EndMT; thus, our findings on endothelial cells are also in agreement with the findings described for epithelial cells.

The detailed underlying molecular mechanism of EndMT blockage was not dissected in the present study. We expected a decrease in *SNAI1*, *SNAI2* and *TWIST1* expression after use of ASC-CMed because these are transcription factors involved in TGF- β -induced EndMT.^{25,65} In contrast, we found that *SNAI2* was overexpressed when HUVEC co-stimulated with IL-1 β /TGF- β 2 were cultured in ASC-CMed, while no differences were found for *SNAI1* or *TWIST1*. Still, it was described in the literature that although EndMT is associated with an increased expression of *SNAI2*, the overexpression of *SNAI2* alone is not enough to promote EndMT, being also required the inhibition of the *SNAI2* inhibitor GSK-3 β .²³ The GSK-3 β , in turn, is inhibited by Smad2/3,⁶⁶ which is recruited by TGF- β .⁶⁷ Thus, in the hypothesis that ASC-CMed

would interrupt the canonical TGF- β pathway, Smad2/3 would be decreased and GSK-3 β would not be inhibited, consequently blocking the SNAI2. Still, besides the predominant TGF- β canonical pathway, the non-canonical pathway was also described as mediating EndMT.^{68,69} Other mechanisms involve the AKT signalling pathway, via the FOXO3 transcription factor,⁷⁰⁻⁷² and the MAPK/ERK pathway, via the ELK1 transcription factor.²⁸ Besides these pathways, the study of exosomes and miRNAs has emerged in the past few years, showing the presence of several entities involved in the EndMT process, such as mi21, mi146, let7^{12,72,73}

5 | CONCLUSION

The present study supports the anti-fibrotic effects of ASC-CMed through the modulation of the endothelial-mesenchymal transition process. We demonstrated that ASC-CMed reduces EndMT induced by co-stimulation with IL-1 β and TGF- β 2 as evidenced by the reduction in expression of mesenchymal markers. Still, further investigations are needed to elucidate the exact underlying mechanisms.

ACKNOWLEDGEMENTS

The authors would like to express their very great appreciation for the assistance provided by Henk Moorlag for the isolation and culture of human umbilical vein endothelial cells (HUVEC).


CONFLICT OF INTEREST

The authors declare no conflicts of interest.

AUTHOR CONTRIBUTION

TTAL has contributed to the conception and design of the work, data collection, data analysis and interpretation, drafting the article, critical revision of the article and final approval of the manuscript text. GRL has contributed to the conception and design of the work, data collection, data analysis and interpretation, drafting the article, critical revision of the article and final approval of the manuscript text. LFPM has contributed to the data analysis and interpretation, critical revision of the article and final approval of the manuscript text. MCH has contributed to the conception and design of the work, data analysis and interpretation, critical revision of the article and final approval of the manuscript text.

ORCID

Tácia Tavares Aquinas Liguori  <https://orcid.org/0000-0002-4150-3144>

Gabriel Romero Liguori  <https://orcid.org/0000-0002-8089-1477>

REFERENCES

- Bui AL, Horwich TB, Fonarow GC. Epidemiology and risk profile of heart failure. *Nat Rev Cardiol*. 2011;8(1):30-41.
- Howard CM, Baudino TA. Dynamic cell-cell and cell-ECM interactions in the heart. *J Mol Cell Cardiol*. 2014;70:19-26.
- Kong P, Christia P, Frangogiannis NG. The pathogenesis of cardiac fibrosis. *Cell Mol Life Sci*. 2014;71(4):549-574.
- Travers JG, Kamal FA, Robbins J, Yutzey KE, Blaxall BC. Cardiac Fibrosis: The Fibroblast Awakens. *Circ Res*. 2016;118(6):1021-1040.
- Krenning G, Zeisberg EM, Kalluri R. The origin of fibroblasts and mechanism of cardiac fibrosis. *J Cell Physiol*. 2010;225(3):631-637.
- Krenning G, Barauna VG, Krieger JE, Harmsen MC, Moonen J-R. Endothelial Plasticity: Shifting Phenotypes through Force Feedback. *Stem Cells Int*. 2016;2016:9762959.
- Souilhol C, Harmsen MC, Evans PC, Krenning G. Endothelial-mesenchymal transition in atherosclerosis. *Cardiovasc Res*. 2018;114(4):565-577.
- Aisagbonhi O, Rai M, Ryzhov S, Atria N, Feoktistov I, Hatzopoulos AK. Experimental myocardial infarction triggers canonical Wnt signaling and endothelial-to-mesenchymal transition. *Dis Model Mech*. 2011;4(4):469-483.
- Boyer AS, Ayerinkas II, Vincent EB, McKinney LA, Weeks DL, Runyan RB. TGFbeta2 and TGFbeta3 have separate and sequential activities during epithelial-mesenchymal cell transformation in the embryonic heart. *Dev Biol*. 1999;208(2):530-545.
- Moonen J-R, Lee ES, Schmidt M, et al. Endothelial-to-mesenchymal transition contributes to fibro-proliferative vascular disease and is modulated by fluid shear stress. *Cardiovasc Res*. 2015;108(3):377-386.
- Zeisberg EM, Tarnavski O, Zeisberg M, et al. Endothelial-to-mesenchymal transition contributes to cardiac fibrosis. *Nat Med*. 2007;13(8):952-961.
- Ghosh AK, Nagpal V, Covington JW, Michaels MA, Vaughan DE. Molecular basis of cardiac endothelial-to-mesenchymal transition (EndMT): differential expression of microRNAs during EndMT. *Cell Signal*. 2012;24(5):1031-1036.
- Kim J, Kim J, Lee SH, et al. Cytokine-Like 1 regulates cardiac fibrosis via modulation of TGF- β signaling. *PLoS ONE*. 2016;11(11):e0166480.
- Feng B, Cao Y, Chen S, Chu X, Chu Y, Chakrabarti S. miR-200b mediates endothelial-to-mesenchymal transition in diabetic cardiomyopathy. *Diabetes*. 2016;65(3):768-779.
- Tang R-N, Lv L-L, Zhang J-D, et al. Effects of angiotensin II receptor blocker on myocardial endothelial-to-mesenchymal transition in diabetic rats. *Int J Cardiol*. 2013;162(2):92-99.
- Kumarswamy R, Volkmann I, Jazbutyte V, Dangwal S, Park D-H, Thum T. Transforming growth factor- β -induced endothelial-to-mesenchymal transition is partly mediated by microRNA-21. *Arterioscler Thromb Vasc Biol*. 2012;32(2):361-369.
- Medici D. Endothelial-Mesenchymal Transition in Regenerative Medicine. *Stem Cells Int*. 2016;2016:1-7.
- Piera-Velazquez S, Mendoza FA, Jimenez SA. Endothelial to Mesenchymal Transition (EndoMT) in the Pathogenesis of Human Fibrotic Diseases. *J Clin Med Res*. 2016;5(4):45.
- Yoshimatsu Y, Watabe T. Roles of TGF- β signals in endothelial-mesenchymal transition during cardiac fibrosis. *Int J Inflamm*. 2011;2011:724080.
- Piera-Velazquez S, Li Z, Jimenez SA. Role of endothelial-mesenchymal transition (EndoMT) in the pathogenesis of fibrotic disorders. *Am J Pathol*. 2011;179(3):1074-1080.
- Gordon KJ, Blobel GC. Role of transforming growth factor- β superfamily signaling pathways in human disease. *Biochimica et Biophysica. Acta (BBA) - Mol Basis Dis*. 2008;1782(4):197-228.

22. Maring JA, van Meeteren LA, Goumans MJ, ten Dijke P. Interrogating TGF- β Function and Regulation in Endothelial Cells. *Methods Mol Biol*. 2016;193-203.
23. Medici D, Potenta S, Kalluri R. Transforming Growth Factor- β 2 promotes Snail-mediated endothelial-mesenchymal transition through convergence of Smad-dependent and Smad-independent signaling. *Biochem J*. 2011;437(3):515.
24. Li C, Dong F, Jia Y, et al. Notch signal regulates corneal endothelial-to-mesenchymal transition. *Am J Pathol*. 2013;183(3):786-795.
25. Kokudo T, Suzuki Y, Yoshimatsu Y, Yamazaki T, Watabe T, Miyazono K. Snail is required for TGF β -induced endothelial-mesenchymal transition of embryonic stem cell-derived endothelial cells. *J Cell Sci*. 2008;121(Pt 20):3317-3324.
26. Zeng L, Wang G, Ummarino D, et al. Histone deacetylase 3 unconventional splicing mediates endothelial-to-mesenchymal transition through transforming growth factor β 2. *J Biol Chem*. 2013;288(44):31853-31866.
27. Feng J, Zhang J, Jackson AO, et al. Apolipoprotein A1 Inhibits the TGF- β 1-induced endothelial-to-mesenchymal transition of human coronary artery endothelial cells. *Cardiology*. 2017;137(3):179-187.
28. Suzuki HI, Katsura A, Mihira H, Horie M, Saito A, Miyazono K. Regulation of TGF- β -mediated endothelial-mesenchymal transition by microRNA-27. *J Biochem*. 2017;161(5):417-420.
29. Maleszewska M, Moonen J-R, Huijckman N, van de Sluis B, Krenning G, Harmsen MC. IL-1 β and TGF β 2 synergistically induce endothelial to mesenchymal transition in an NF κ B-dependent manner. *Immunobiology*. 2013;218(4):443-454.
30. Maleszewska M, Gjaltema R, Krenning G, Harmsen MC. Enhancer of zeste homolog-2 (EZH2) methyltransferase regulates transgelin/smooth muscle-22 α expression in endothelial cells in response to interleukin-1 β and transforming growth factor- β 2. *Cell Signal*. 2015;27(8):1589-1596.
31. Lee ES, Boldo LS, Fernandez BO, Feelisch M, Harmsen MC. Suppression of TAK1 pathway by shear stress counteracts the inflammatory endothelial cell phenotype induced by oxidative stress and TGF- β 1. *Sci Rep*. 2017;7:42487.
32. Montorfano I, Becerra A, Cerro R, et al. Oxidative stress mediates the conversion of endothelial cells into myofibroblasts via a TGF- β 1 and TGF- β 2-dependent pathway. *Lab Invest*. 2014;94(10):1068-1082.
33. Richter K, Konzack A, Pihlajaniemi T, Heljasvaara R, Kietzmann T. Redox-fibrosis: Impact of TGF β 1 on ROS generators, mediators and functional consequences. *Redox Biol*. 2015;6:344-352.
34. Mazo M, Hernández S, Gavira JJ, et al. Treatment of Reperfused Ischemia With Adipose-Derived Stem Cells in a Preclinical Swine Model of Myocardial Infarction. *Cell Transplant*. 2012;21(12):2723-2733.
35. Yu LH, Kim MH, Park TH, et al. Improvement of cardiac function and remodeling by transplanting adipose tissue-derived stromal cells into a mouse model of acute myocardial infarction. *Int J Cardiol*. 2010;139(2):166-172.
36. Perin EC, Sanz-Ruiz R, Sánchez PL, et al. Adipose-derived regenerative cells in patients with ischemic cardiomyopathy: The PRECISE Trial. *Am Heart J*. 2014;168(1):88-95.e2.
37. Mazo M, Planat-Bénard V, Abizanda G, et al. Transplantation of adipose derived stromal cells is associated with functional improvement in a rat model of chronic myocardial infarction. *Eur J Heart Fail*. 2008;10(5):454-462.
38. Przybyt E, Harmsen MC. Mesenchymal Stem Cells: Promising for Myocardial Regeneration? *Curr Stem Cell Res Ther*. 2013;8(4):270-277.
39. ten Sande JN, Smit NW, Parvizi M, et al. Differential Mechanisms of Myocardial Conduction Slowing by Adipose Tissue-Derived Stromal Cells Derived from Different Species. *Stem Cells Transl Med*. 2017;6(1):22-30.
40. Tano N, Narita T, Kaneko M, et al. Epicardial placement of mesenchymal stromal cell-sheets for the treatment of ischemic cardiomyopathy; in vivo proof-of-concept study. *Mol Ther*. 2014;22(10):1864-1871.
41. Hamdi H, Boitard SE, Planat-Bénard V, et al. Efficacy of epicardially delivered adipose stroma cell sheets in dilated cardiomyopathy. *Cardiovasc Res*. 2013;99(4):640-647.
42. Araña M, Gavira JJ, Peña E, et al. Epicardial delivery of collagen patches with adipose-derived stem cells in rat and minipig models of chronic myocardial infarction. *Biomaterials*. 2014;35(1):143-151.
43. He J, Cai Y, Luo LM, Liu HB. Hypoxic adipose mesenchymal stem cells derived conditioned medium protects myocardial infarct in rat. *Eur Rev Med Pharmacol Sci*. 2015;19(22):4397-4406.
44. Jiang Y, Chang P, Pei YU, et al. Intramyocardial injection of hypoxia-preconditioned adipose-derived stromal cells treats acute myocardial infarction: an in vivo study in swine. *Cell Tissue Res*. 2014;358(2):417-432.
45. Spiekman M, Przybyt E, Plantinga JA, Gibbs S, van der Lei B, Harmsen MC. Adipose tissue-derived stromal cells inhibit TGF- β 1-induced differentiation of human dermal fibroblasts and keloid scar-derived fibroblasts in a paracrine fashion. *Plast Reconstr Surg*. 2014;134(4):699-712.
46. Zvonc S, Lefevre M, Kilroy G, et al. Secretome of primary cultures of human adipose-derived stem cells: modulation of serpins by adipogenesis. *Mol Cell Proteomics*. 2007;6(1):18-28.
47. Kapur SK, Katz AJ. Review of the adipose derived stem cell secretome. *Biochimie*. 2013;95(12):2222-2228.
48. Kalinina N, Kharlampieva D, Loguinova M, et al. Characterization of secretomes provides evidence for adipose-derived mesenchymal stromal cells subtypes. *Stem Cell Res Ther*. 2015;6:221.
49. Przybyt E, Krenning G, Brinker M, Harmsen MC. Adipose stromal cells primed with hypoxia and inflammation enhance cardiomyocyte proliferation rate in vitro through STAT3 and Erk1/2. *J Transl Med*. 2013;11:39.
50. Mert T, Kurt AH, Arslan M, Çelik A, Tugtag B, Akkurt A. Anti-inflammatory and Anti-nociceptive Actions of Systemically or Locally Treated Adipose-Derived Mesenchymal Stem Cells in Experimental Inflammatory Model. *Inflammation*. 2015;38(3):1302-1310.
51. Tuin A, Kluijtmans SG, Bouwstra JB, Harmsen MC, Van Luyn M. Recombinant gelatin microspheres: novel formulations for tissue repair? *Tissue Eng Part A*. 2010;16(6):1811-1821.
52. Parvizi M, Bolhuis-Versteeg L, Poot AA, Harmsen MC. Efficient generation of smooth muscle cells from adipose-derived stromal cells by 3D mechanical stimulation can substitute the use of growth factors in vascular tissue engineering. *Biotechnol J*. 2016;11(7):932-944.
53. An H-Y, Shin H-S, Choi J-S, Kim HJ, Lim J-Y, Kim Y-M. Adipose Mesenchymal Stem Cell Secretome Modulated in Hypoxia for Remodeling of Radiation-Induced Salivary Gland Damage. *PLoS ONE*. 2015;10(11):e0141862.
54. Lee CS, Burnsed OA, Raghuram V, Kalisvaart J, Boyan BD, Schwartz Z. Adipose stem cells can secrete angiogenic factors that inhibit hyaline cartilage regeneration. *Stem Cell Res Ther*. 2012;3(4):35.
55. Illigens BM-W, Casar Berazaluce A, Poutias D, Gasser R, DeNido PJ, Friehs I. Vascular endothelial growth factor prevents endothelial-to-mesenchymal transition in hypertrophy. *Ann Thorac Surg*. 2017;104(3):932-939.
56. Chen P-Y, Qin L, Barnes C, et al. FGF regulates TGF- β signaling and endothelial-to-mesenchymal transition via control of let-7 miRNA expression. *Cell Rep*. 2012;2(6):1684-1696.
57. Correia A, Moonen J-R, Brinker M, Krenning G. FGF2 inhibits endothelial-mesenchymal transition through microRNA-20a-mediated repression of canonical TGF- β signaling. *J Cell Sci*. 2016;129(3):569-579.

58. Bijkerk R, G. de Bruin R, van Solingen C, et al. MicroRNA-155 functions as a negative regulator of RhoA signaling in TGF- β -induced endothelial to mesenchymal transition. *Microna*. 2012;1(1):2-10.
59. Katsura A, Suzuki HI, Ueno T, et al. MicroRNA-31 is a positive modulator of endothelial-mesenchymal transition and associated secretory phenotype induced by TGF- β . *Genes Cells*. 2016;21(1):99-116.
60. Zhang Z, Wang J-A, Xu Y, et al. Menstrual blood derived mesenchymal cells ameliorate cardiac fibrosis via inhibition of endothelial to mesenchymal transition in myocardial infarction. *Int J Cardiol*. 2013;168(2):1711-1714.
61. Donizetti-Oliveira C, Semedo P, Burgos-Silva M, et al. Adipose tissue-derived stem cell treatment prevents renal disease progression. *Cell Transplant*. 2012;21(8):1727-1741.
62. Song Y, Peng C, Lv S, et al. Adipose-derived stem cells ameliorate renal interstitial fibrosis through inhibition of EMT and inflammatory response via TGF- β 1 signaling pathway. *Int Immunopharmacol*. 2017;44:115-122.
63. Lamouille S, Xu J, Derynck R. Molecular mechanisms of epithelial-mesenchymal transition. *Nat Rev Mol Cell Biol*. 2014;15(3):178-196.
64. Luna-Zurita L, Prados B, Grego-Bessa J, et al. Integration of a Notch-dependent mesenchymal gene program and Bmp2-driven cell invasiveness regulates murine cardiac valve formation. *J Clin Invest*. 2010;120(10):3493-3507.
65. Medici D, Potenta S, Kalluri R. Transforming growth factor- β 2 promotes Snail-mediated endothelial-mesenchymal transition through convergence of Smad-dependent and Smad-independent signaling. *Biochem J*. 2011;437(3):515-520.
66. Aragon E, Goerner N, Zaromytidou A-I, et al. A Smad action turnover switch operated by WW domain readers of a phosphoserine code. *Genes Dev*. 2011;25(12):1275-1288.
67. Zi Z, Chapnick DA, Liu X. Dynamics of TGF- β /Smad signaling. *FEBS Lett*. 2012;586(14):1921-1928.
68. Chang A, Fu YangXin, Garside V, et al. Notch initiates the endothelial-to-mesenchymal transition in the atrioventricular canal through autocrine activation of soluble guanylyl cyclase. *Dev Cell*. 2011;21(2):288-300.
69. Cho JG, Lee A, Chang W, Lee M-S, Kim J. Endothelial to Mesenchymal Transition Represents a Key Link in the Interaction between Inflammation and Endothelial Dysfunction. *Front Immunol*. 2018;9:294.
70. Zhang Z, Zhang T, Zhou Y, et al. Activated phosphatidylinositol 3-kinase/Akt inhibits the transition of endothelial progenitor cells to mesenchymal cells by regulating the forkhead box subgroup O-3a signaling. *Cell Physiol Biochem*. 2015;35(4):1643-1653.
71. Zhang J, Zhang Z, Zhang DY, Zhu J, Zhang T, Wang C. microRNA 126 inhibits the transition of endothelial progenitor cells to mesenchymal cells via the PIK3R2-PI3K/Akt signalling pathway. *PLoS ONE*. 2013;8(12):e83294.
72. Kumarswamy R, Volkmann I, Jazbutyte V, Dangwal S, Park D-H, Thum T. Transforming Growth Factor- β -Induced Endothelial-to-Mesenchymal Transition Is Partly Mediated by MicroRNA-21. *Arterioscler Thromb Vasc Biol*. 2012;32(2):361-369.
73. Baglio SR, Rooijers K, Koppers-Lalic D, et al. Human bone marrow- and adipose-mesenchymal stem cells secrete exosomes enriched in distinctive miRNA and tRNA species. *Stem Cell Res Ther*. 2015;6:127.

SUPPORTING INFORMATION

Additional supporting information may be found online in the Supporting Information section at the end of the article.

How to cite this article: Liguori TTA, Liguori GR, Pinho Moreira LF, Harmsen MC. Adipose tissue-derived stromal cells' conditioned medium modulates endothelial-mesenchymal transition induced by IL-1 β /TGF- β 2 but does not restore endothelial function. *Cell Prolif*. 2019;52:e12629. <https://doi.org/10.1111/cpr.12629>

CHAPTER 3

Bioactive decellularized cardiac extracellular matrix-based hydrogel as a sustained-release platform for human adipose tissue-derived stromal cell-secreted factors.

Tácia Tavares de Aquinas Liguori^{1,2}, Gabriel Romero Liguori^{1,2}, Joris A. van Dongen¹, Luiz Felipe Pinho Moreira², Martin C. Harmsen¹

1. Department of Pathology and Medical Biology, University of Groningen and University Medical Center Groningen, Groningen, Netherlands
2. Heart Institute (InCor), Hospital das Clinicas HCFMUSP, Faculdade de Medicina, Universidade de Sao Paulo, Sao Paulo, Brazil

Submitted

ABSTRACT

INTRODUCTION: The administration of trophic factors (TF) released by mesenchymal stromal cells (MSC) as therapy for cardiovascular diseases requires a delivery vehicle capable of binding and releasing the TF in a sustained manner. We hypothesized that hydrogels derived from the decellularized cardiac extracellular matrix (dECM) bind MSC secretome-derived TF and release these in a sustained fashion. **METHODS:** Pig-derived ventricular tissue was decellularized, milled to powder, digested, and assembled as a hydrogel upon warming at 37°C. The conditioned medium (CMed) of adipose tissue-derived stromal cells (ASC) was collected, concentrated, and incorporated into the hydrogel at 1x, 10x, and 100x the original concentration. The release of 11 ASC-secreted factors (angiopoietin-1, angiopoietin-2, FGF-1, HGF, PDGF-AA, VEGF-A, IL-1 β , IL-6, IL-8, CXCL8, and MMP-1) from hydrogels was immune assessed. Bioactivity was determined by endothelial cell proliferation, function, and assessment of endothelial mesenchymal transition. **RESULTS:** We showed that dECM hydrogels could be loaded with human ASC-secreted trophic factors, which are released in a sustained manner for several days subsequently. Different trophic factors had different release kinetics, which correlates with the initial concentration of CMed in the hydrogel. We observed that the more concentrated was the hydrogel, the more inflammation-related cytokines, and the less pro-regenerative trophic factors were released. Finally, we showed that the factors secreted by the hydrogel are biologically active as these influence cell behavior. **CONCLUSION:** The use of dECM hydrogels as a platform to bind and

release paracrine factors secreted by (mesenchymal) cells is a potential alternative in the context of cardiovascular regeneration.

Keywords: trophic factors, mesenchymal stromal cells (MSC), sustained-release, extracellular matrix, secretome, conditioned medium, hydrogels, endothelial cells

INTRODUCTION

The use of stem cells to treat heart failure has been under investigation for two decades. Besides constructive stem cells that differentiate directly to cardiomyocytes or endothelial cells, reconstruction of the damaged myocardium may prevent and reverse disease progression. Heart failure is both the result of a deteriorated pump function along with an exaggerated response of the connective tissue in the form of excessive extracellular matrix deposition (1–3). We argued that the derailed myocardial tissue requires to be re-educated. In normal physiology, tissue homeostasis is maintained by the tissue stroma, i.e., extracellular matrix, mesenchymal cells and vasculature. As it appears, cultured stromal cells from bone marrow (BM-MSC) or adipose tissue (ASC) are potent tissue remodelers via secretion of a plethora of paracrine factors that suppress apoptosis, promote the proliferation of parenchyma, modulate immune reactions and are pro-angiogenic (4–6). These mesenchymal stromal cells (MSC), including ASC, also remodel extracellular matrix through their secretion of, e.g. matrix metalloproteinases (MMP) and deposition of extracellular matrix (ECM) components. These MSC are widely used in cardiac cell-based therapies, albeit their mode of action has become

(partially) clear only in recent years. The ASC secretome comprises angiogenic factors, immunomodulatory factors, mitogenic factors and ECM-remodeling proteases, among others. That means MSC, by secreting trophic factors (TF), may augment repair of cardiac tissue damage and to reinstate homeostasis (7,8). These factors may directly normalize the function of already present cells or instruct surrounding cells to facilitate repairs. Two significant mechanisms that underlie cardiac fibrosis and thus heart failure and which are influenced by TF are endothelial mesenchymal transition (EndMT) and myofibroblast differentiation of cardiac fibroblasts (9,10).

Clinical cardiac stem cell therapy has proven of marginal benefit to treating myocardial infarction and cardiac fibrosis (11,12). The main reason is the poor retention of stem cells, irrespective of the route of administration. Thus, it is not only essential to warrant the retention of therapeutic cells in the cardiac tissue, but also to ensure that their secreted TF reach the affected cardiac target cells to direct tissue regeneration. Instead of administration of the TF-secreting MSCs, the administration of the TF themselves is an alternative that reduces possible donor- and disease-dependent variations in TF composition. The challenge, however, is to enable the sustained release of injected TF because usually these are rapidly drained from damaged tissue. To accomplish this task, it is necessary to use a delivery vehicle capable of binding the TF and releasing these in a sustained manner. Several synthetic hydrogels with different tunable characteristics have been proposed as injectable release vehicles to perform this task. In general, these platforms show a burst-release kinetic profile while they efficiently bind all factors in

the MSCs' secretome. Recently, our group demonstrated the use of natural hydrogels based on decellularized extracellular matrix (ECM) of adipose tissue as a release platform for secreted paracrine factors in the context of skin wound regeneration (13). The proteoglycans and glycosaminoglycans but also non-fibrillar proteins and matricellular proteins in the ECM, bind the TF secreted by MSC. In vivo, the ECM functions to store and on-demand release these factors physiologically.

In this study, we hypothesized that hydrogels derived from decellularized cardiac tissue bind MSC secretome-derived TF and release these in a sustained fashion. We investigated the feasibility of fabricating hydrogels derived from porcine myocardial ECM and evaluated the uptake and release of human ASC-derived paracrine factors by these hydrogels. Finally, we explored the influence of the TF released by the hydrogels on endothelial cell proliferation, function, and endothelial mesenchymal transition.

METHODS

An overview of the methods used in the present study is illustrated in Figure 1. The detailed information for each method is described below.

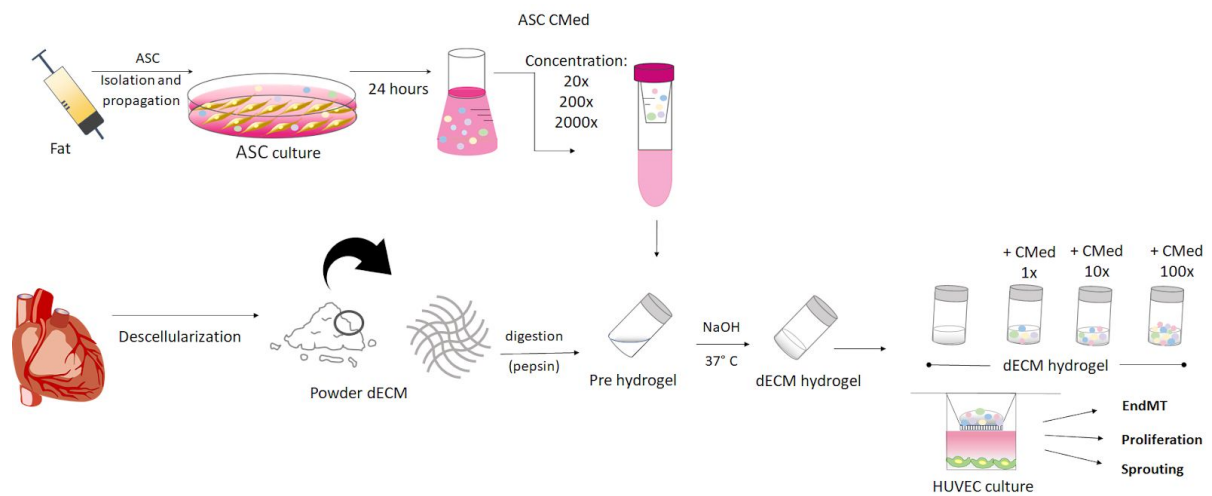


Figure 1 - Overview of the study design.

Extracellular Matrix Decellularization, Characterization and dECM Hydrogels Fabrication

Decellularization Protocol

Porcine hearts (16-week pigs) were acquired through a local slaughterhouse (Kroon Vlees, Groningen, Netherlands) and dissected to separate the left ventricle myocardial tissue. Tissue was washed in phosphate buffer saline (PBS) and triturated in a commercial blender until tissue fragments were smaller than 1 mm. Following the second wash in PBS, tissue was submitted to sonication for 1 minute, washed a third time, and incubated in 0.05% trypsin in PBS (Gibco, Thermo Fisher Scientific, Waltham, USA) and constant shaking at 37°C for 3 hours. After trypsin treatment, tissue was rewashed with PBS and frozen overnight or longer at -20°C. After thawing, tissue was incubated in demineralized water for 3 hours and then in

saturated (6M) NaCl for another 3 hours, both steps in constant shaking. Next, tissue was washed in 70% ethanol for 10 minutes and in water for another 10 minutes. After ethanol wash, tissue was collected, centrifuged at 3,000 xg for 3 minutes, discarded the supernatant followed by tissue resuspension and incubation with 1% sodium dodecyl sulfate (SDS) in water (Sigma-Aldrich, St Louis, USA) for 12 hours, washed three times with water, incubated with 1% Triton X-100 (Sigma-Aldrich, St Louis, USA) for 12 hours, washed three times with water, incubated with 1% sodium deoxycholate (Sigma-Aldrich, St Louis, USA) for 12 hours and, again, washed three times with water, all steps under constant shaking. After detergent treatment and washing, tissue was incubated for 24 hours with DNase solution (30 μ g/ml DNase (Worthington Biochemical Corporation, Lakewood, USA), 1.3 mM $MgSO_4$, 2 mM $CaCl_2$) at 37°C and constant shaking. After DNase treatment, tissue was washed overnight with 70% ethanol and stored at 4°C in 1% penicillin/streptomycin (#15140122, Gibco Invitrogen, Carlsbad, USA) in sterile PBS. In the following the final product is denoted as dECM (decellularized ECM)

DNA Quantification

Genomic DNA was isolated as previously described (13). Briefly, dried native and dECM samples (n=3) were weighed and separated as samples of 10 – 15 mg in a 1.5 mL Eppendorf tube. Each sample was digested at 55°C overnight in a solution containing 162 μ g/mL proteinase K, 10 mg/ml SDS, and 500 μ L SE-buffer (75 mM NaCl; 25 mM EDTA; pH 8.0). Following the enzymatic digestion, samples were added with 222 μ L of 6 M NaCl and 777 μ L of chloroform, thoroughly shaken on a

top-over-top rotator for one hour in room temperature (RT) and centrifuged at 2,000 xg at 20°C for 10 minutes. After centrifuging, two liquid layers were formed with a white layer in between. The upper layer of the supernatant was pipetted out of the original tube and transferred into a new clean one, leaving the protein pellet behind. In the new tube, a volume of ice-cold isopropanol was added to the transferred supernatant and gently mixed until white threads of DNA formed visible clumps. The tubes were then centrifuged at 12,000 xg at 4°C for 15 minutes, forming a pellet. The supernatant was carefully pipetted out, without disturbing the DNA pellet, and 500 μL of 70% ethanol was added to wash the pellet. The tubes were centrifuged again at 12,000 xg at 4°C for 5 minutes, the supernatant was pipetted out, and the pellet was left to air-dry at RT. Once the pellet was dissolved in 100 μL of TE-buffer (10 mM Tris; 0.1 mM EDTA; pH 8.0) at 55°C and quantified with NanoDrop spectrophotometry (Thermo Scientific, Hemel Hempstead, United Kingdom).

dECM Gelation

For dECM gelation, the decellularized extracellular matrix of left ventricle myocardial tissue in PBS was centrifuged at 12,000 xg at 4°C for 5 minutes. The supernatant was discarded the tissue pellet lyophilized and milled to a fine powder. Digestion was done on 20% w/v dECM powder in 0.01 M HCl with 2% w/v pepsin (#P6887; >3,200 IU; Sigma-Aldrich, St. Louis, USA) at RT under constant stirring for six hours. After digestion, the pH was neutralized by adding 1/10th volume 0.1 M NaOH and brought to 1x PBS by adding 1/10th volume 10x PBS. The resulting

solution could be stored in liquid form (pre-gel) at 4° C for months or converted into a hydrogel by warming to 37°C, which induced spontaneous gelation.

Grow factors from ASC-CMed Released by dECM Hydrogels

Conditioned Medium Collection, Concentration and Resuspension in dECM Hydrogel

Human ASC were isolated and characterized as described previously (9,14,15). Briefly, human abdominal fat was obtained by liposuction, washed with phosphate-buffered saline (PBS) and digested enzymatically with 0.1% collagenase A (#11088793001, Roche Diagnostic, Mannheim, Germany) in PBS with 1% bovine serum albumin (BSA; #A9647, Sigma-Aldrich, Boston, USA). The tissue was shaken constantly at 37°C for 2 hours. After this, the digested tissue was mixed with 1% PBS/BSA, filtered, centrifuged and the cell pellet was resuspended in Dulbecco's Modified Eagle's Medium (DMEM; #12-604F, Lonza, Basel, Switzerland) with 10% fetal bovine serum (FBS; #F0804, Sigma-Aldrich, Missouri, United States), 1% penicillin/streptomycin (#15140122, Gibco Invitrogen, Carlsbad, USA) and 1% L-glutamine (#17-605E, Lonza Bio Whittaker, Verviers, Belgium). Cells were cultured at 37°C in a humidified incubator with 5% CO₂. The medium was refreshed every two days. Cells were passed at a ratio of 1:3 after confluency had reached.

ASC conditioned medium (ASC-CMed) was obtained from confluent cultures of ASC between passages 3 and 6 from at least three different donors. Cells were cultured in DMEM, and the serum-free conditioned medium (5 ml/cm²) was

harvested after 48 hours, filtered through 0.22 μm filters. ASC-CMed was concentrated with the use of 3 kDa cutoff Amicon® Ultra Centrifugal filters (Sigma-Aldrich). ASC-CMed was concentrated 2,000-fold by repeating the concentrating procedure with previously concentrated samples. After concentration, ASC-CMed was diluted in DMEM to reach the following concentrations: 2,000x, 200x, and 20x. These ASC-CMed solutions were then added as 1/20th final volume to dECM pre-gel, resulting in pre-gels containing, respectively, 100x, 10x, and 1x ASC-CMed.

Trophic Factors Release from dECM Hydrogel

ASC-CMed-containing dECM pre-gels were fabricated as described above. In sequence, 500 μL of each pre-gel (1x ASC-CMed, 10x ASC-CMed, and 100x ASC-CMed) was added to 1.5 mL microtubes and placed in an incubator for 1h at 37°C to allow for self-assembly gelation. This yields 2% w/v dECM hydrogels. After gelation, 500 μL of serum-free DMEM, without any additional factors, was added to the dECM hydrogel, and the microtubes were kept closed inside a 37°C incubator. The supernatant was collected from the microtubes and refreshed at 1, 3, and 5 days, constituting, respectively, the first, second, and third waves of TF release. The collected supernatant was used to determine trophic factors release from dECM hydrogel over time.

The factor release profile of dECM hydrogel was determined by the concentration of eleven factors that are representative for tissue regeneration and

remodeling (angiopoietin-1, angiopoietin-2, fibroblast growth factor 1 (FGF-1), hepatocyte growth factor (HGF), platelet-derived growth factor-AA (PDGF-AA), vascular endothelial growth factor (VEGF-A), interleukin-1 β (IL-1 β), interleukin-6 (IL6), interleukin-8 (IL-8), monocyte chemotactic protein 1 (CXCL8/MCP-1/CCL2), and matrix metalloproteinase 1 (MMP-1)) in the medium collected from the dECM hydrogel. For this purpose, Magnetic Luminex Human Premixed Multi-Analyte Kit (R&D Systems) was used according to the manufacturer's protocol. Serum-free DMEM only and DMEM extracted from dECM hydrogels without ASC-CMed were used as negative controls, while the concentrated ASC-CMed was used as a positive control.

Endothelial Cells' Proliferation, Function, and Transdifferentiation under ASC-CMed Release by dECM Hydrogels

Cell Sources and Cell Culture

Human umbilical vein endothelial cells (HUVEC) were obtained from the endothelial cell culture facility of our institution and comprised pools of at least three donors, as previously described (10). Cells were seeded on gelatin-coated plates (1% gelatin solution in PBS) at a density of 35,000 cells/cm² and cultured until confluency in endothelial cell medium (ECMed) composed of RPMI-1640 basal medium (#BE04-558F, Lonza, Basel, Switzerland) with 10% heat-inactivated fetal bovine serum (FBS; #F0804, Sigma-Aldrich, Missouri, United States), 1% penicillin/streptomycin (#15140122, Gibco Invitrogen, Carlsbad, USA), 1%

L-glutamine (#17-605E, Lonza Bio Whittaker, Verviers, Belgium), 5 U/mL heparin (LEO Laboratories Limited, Ballerup, Denmark), and 50 g/mL bovine brain extract (BBE, in-house preparation). HUVEC between passages 3 and 6 were used for the experiments.

Endothelial Cells Proliferation

A transwell membrane insert ThinCert™ with 0.4 µm (#662640, Greiner Bio-One International, Kremsmünster, Austria) was used with hydrogel and/or the concentrated conditioned medium on top of 24 well tissue culture plates of HUVEC. After five days of culture with endothelial cell media with 10% FBS and ECGF, cells were fixed at room temperature with 2% paraformaldehyde (PFA) for 30 min and stained as described below (see Immunofluorescence section)

Endothelial Cell Function

ASC-CMed-containing dECM pre-gels were generated as described above. In sequence, 500 µL of each pre-gel (without ASC-CMed, 1x ASC-CMed, 10x ASC-CMed, and 100x ASC-CMed) was added to 1.5 mL microtubes and placed in an incubator for 1 h at 37°C to allow for self-assembly gelation. After gelation, 500 µL of ECMed, without any additional factors, was added to the dECM hydrogel, and the microtubes were kept closed inside a 37°C incubator for 24 hours. After this time, the

500 μL of ECMed were pipetted out from the microtubes and stored for use in the endothelial sprouting assay.

HUVEC were cultured with ECMed in 75 cm^2 culture flasks. After reaching confluency, cells were detached from the flasks, counted, and, for each group, 15,000 cells were resuspended in 50 μL of the ECMed collected from the microtubes as described above. Pure ECMed was used as a positive control. Subsequently, cells were seeded in wells of a μ -Slide Angiogenesis Plate (Ibidi GmbH, Martinsried, Germany) previously coated and incubated at 37°C with 10 μL of Matrigel® (#356231, BD Biosciences, San Jose, USA) for 2 hours. The sprouting was allowed to proceed for 4 hours. Every condition was done in triplicate, and the experiment was performed three times independently. Formation sprouting networks was imaged with a DM2000 LED inverted microscope (Leica, Wetzlar, Germany) using 2.5x magnification and analyzed using ImageJ Fiji with Angiogenesis Analyzer plugin. The number of branches was determined.

Endothelial Cell Mesenchymal Transition (EndMT)

Confluent HUVEC were divided into 10 groups with different induction/dECM hydrogel combinations, as described in Table 1, and cultured for five days. Human recombinant interleukin 1 β (IL-1 β ; #200-01B, PeproTech, New Jersey, USA) and human transforming growth factor-beta 2 (TGF- β 2; #100-35B, PeproTech, New Jersey, USA) both at 10 ng/ml , were used to induce EndMT.

| Table 1. Experimental groups | | | |
|--|--------------|-----------------|------------------|
| Group | EndMT | Hydrogel | Secretome |
| Control | - | - | - |
| Control + Induction | + | - | - |
| Hydrogel | - | + | - |
| Hydrogel + Induction | + | + | - |
| Hydrogel with 1x ASC-CMed | - | + | 1x |
| Hydrogel with 1x ASC-CMed + Induction | + | + | 1x |
| Hydrogel with 10x ASC-CMed | - | + | 10x |
| Hydrogel with 10x ASC-CMed + Induction | + | + | 10x |
| Hydrogel with 100x ASC-CMed | - | + | 100x |
| Hydrogel with 100x ASC-CMed + Induction | + | + | 100x |
| EndMT: Induction of endothelial mesenchymal transition | | | |

ASC-CMed-containing dECM pre-gels were generated as described above. In sequence, 500 μ L of pre-gel was added to the inner part of ThinCert™ Cell Culture Inserts 24 Well (Greiner Bio-One) and placed in an incubator for 1 h at 37 °C to allow

for gelation. Wells of 24-well plates seeded with HUVEC were allocated within the experimental groups described above. The ThinCert™ Cell Culture Inserts containing dECM hydrogels were then placed above the HUVEC culture according to their experimental groups. The culture medium was refreshed every two days, while dECM hydrogel was not changed during the experiment. After five days of culture with endothelial cell media with 10% FBS and ECGF, cells were fixed at room temperature with 2% paraformaldehyde (PFA) for 30 min and stained as described below (see Immunofluorescence section)

Immunofluorescence

After the appropriate period for each experiment, the cells were fixed at room temperature with 2% paraformaldehyde (PFA) in PBS for 30 min. Cells were permeabilized with 1% Triton-X100 in PBS at RT for 15 min and blocked with 5% donkey serum in PBS and 1% BSA at room temperature for 15 min. Subsequently, cells were incubated with primary antibodies diluted in 5% donkey serum in PBS at RT for 2 hours.

For cell proliferation, rabbit anti-Ki67 (1:400; #ab15580, Abcam, Cambridge, UK) polyclonal antibody was used. To visualize EndMT, rabbit anti-SM22 α (1:400; #ab14106, Abcam, Cambridge, UK) and mouse anti-human VE-Cadherin (1:200, #AF1002, R&D Systems, Minnesota, United States) were used as mesenchymal and endothelial markers, respectively. Controls were incubated with 5% donkey serum in PBS instead of the primary antibody.

Next, the cells were washed with 0.05% Tween-20 in PBS and incubated with secondary antibodies in 5% donkey serum in PBS with 4',6-diamidino-2-phenylindole (DAPI; 1:5000; #D9542-5MG, Sigma-Aldrich, Missouri, United States) at room temperature for 1 hour. For the transdifferentiation experiment, cells were also incubated with Alexa Fluor® 488 phalloidin (1:400; #A12379, Life Technologies, Carlsbad, United States). The following secondary antibodies were used: donkey anti-rabbit IgG (H+L) Alexa Fluor® 594 (1:400; #A-21207, Life Technologies, Carlsbad, United States) and donkey anti-mouse IgG (H+L) Alexa Fluor® 594 (1:400; #ab150108, Abcam, Cambridge, UK). Finally, cells were washed 3 times with PBS and the plates were imaged with Evos FL System (Thermo Fisher Scientific, Waltham, United States) using Texas Red (TXR), DAPI and Green Fluorescent Protein (GFP) channels with 20x magnification.

Statistical Analysis

All data were obtained from at least three independent experiments performed in duplicate or triplicate. Data are presented as mean \pm standard error of the mean (SEM). Graphs and statistical analyses were done using GraphPad Prism (Version 6.01; GraphPad Software, Inc., La Jolla, United States). Differences among multiple groups were analyzed by Kruskal–Wallis with Dunn's multiple comparison test for the two groups of interested in each scenario.

RESULTS

Effective decellularization

The presence of remaining DNA in the decellularized ECM was assessed by genomic DNA quantification. The dry myocardial tissue before decellularization contained $3,617 \pm 342.1$ ng/mg versus 14.3 ± 3.6 ng/mg after the process (t-student test, $p < 0.0001$). Genomic DNA quantification showed around 99% of reduction in DNA content, with decellularized ECM presenting less than 50 ng/mg of DNA per dry weight, the standard value for successful decellularization (16).

dECM hydrogels can release trophic factors in a sustained manner

The trophic factor release profile of dECM hydrogel was determined by the measurement of eleven different factors in the medium collected from the dECM hydrogel after 3 consecutive waves of release, i.e. a 1st of 24 hours and a 2nd and 3rd wave of 48 hours, using the Magnetic Luminex Human Premixed Multi-Analyte Kit. Empty control gels did not release detectable amounts of factors (not shown). The release of CXCL8 from dECM hydrogels loaded with 100x concentrated ASC-Cmed was above the maximal detection level, while the release of IL-1 β from dECM hydrogels loaded with 1x concentrated ASC-CMed was below the detection limit.

Although the increase in ASC-CMed concentration in the hydrogels was exponential (tenfold), this pattern was not observed in the release behavior of

individuals by the hydrogels. In general, the hydrogels loaded with 1x and 10x concentrated CMed showed a similar release pattern, with low trophic factor concentration and a relatively constant trophic factor release speed. The 100x concentrated hydrogels, on the other hand, showed a strong release in the first wave, that leveled off in subsequent waves (Figures 2A and 2B).

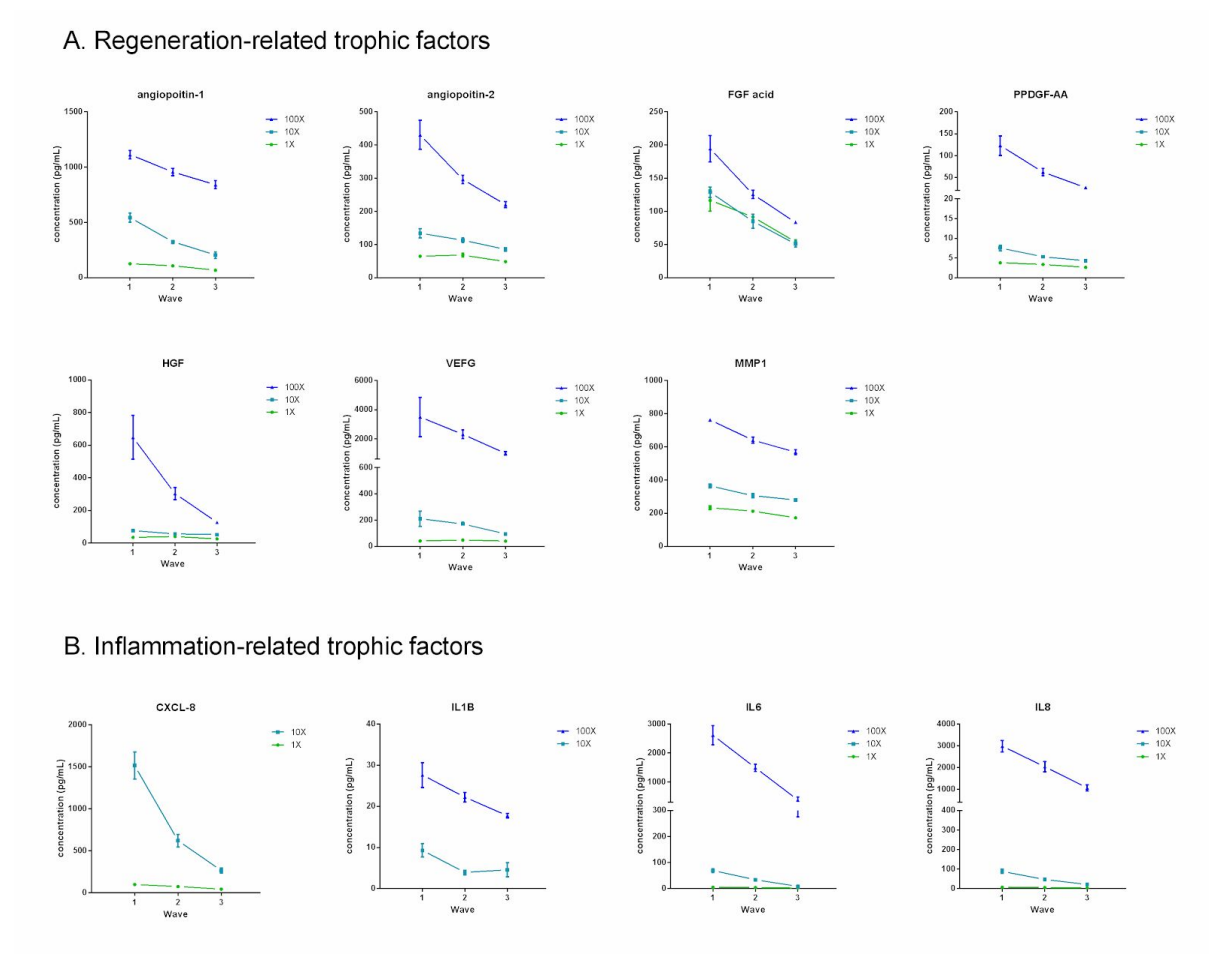


Figure 2 - 2A - Regeneration-related trophic factors release pattern after the 1st, 2nd, and 3rd waves of release. 2B - Inflammation-related trophic factors release pattern after the 1st, 2nd, and 3rd waves of release. CXCL-8 was above the detection limit in 100x concentrated CMed, and IL-1 β was below the detection limit in 1x concentrated CMed (n=4 independent experiments).

VEGF-A amount was the most released, reaching 6,805 pg/mL by hydrogels loaded with 100x concentrated CMed after the three waves. Following VEGF-A were IL-8 (6,068 pg/mL), IL-6 (4,478 pg/mL), and angiopoietin-1 (2,908 pg/mL). The IL-1 β releasing pattern could not be determined for the hydrogels loaded with 1x CMed. When the CMed was concentrated 100x, the release was low, with only 68 pg/mL after the three waves. The other factors showing low release include PDGF-AA (212 pg/mL), FGF-1 (403 pg/mL), and angiopoietin-2 (946 pg/mL). HGF and MMP-1 showed intermediate release, showing a release after three waves of, respectively, 1,078 pg/mL and 1,969 pg/mL for the hydrogel loaded with 100x concentrated CMed.

Release of regeneration-related trophic factors

Among the eleven trophic factors investigated in this study, seven potentially augment to tissue regeneration: angiopoietin-1, angiopoietin-2, FGF-1, PDGF-AA, HGF, VEGFA, and MMP-1.

The release curve of angiopoietin-1 and angiopoietin-2 showed the same pattern, although the concentration reached by angiopoietin-1 was higher in all time points compared with angiopoietin-2. During the first 24 h (1st wave), 100x CMed hydrogels released a mean concentration of 1,111 pg/mL of angiopoietin-1, followed by 542 pg/ml and 125 pg/ml for 10x and 1x CMed hydrogels. On the 3rd wave, the mean concentration of this TF was still considerable in all groups, representing at least around 50% of the concentration found in the 1st wave (first 24h). For

angiopoietin-2, in turn, the mean concentration reached in the 1st wave was 430.3 pg/mL, 133 pg/mL, and 64 pg/mL, respectively, for the hydrogels loaded with 100x, 10x and 1x CMed. After the 3rd wave, a similar behavior to angiopoietin-1 was observed, with a mean concentration of about 50% of the concentration of the 1st wave's release.

FGF-1 and PDGF-AA showed the lowest release among all the regeneration-related trophic factors investigated in the present study. While for FGF-1 the mean concentrations during the 1st release wave (first 24h) were 194 pg/mL, 128 pg/mL and 116 pg/mL, respectively for the hydrogels loaded with 100x, 10x and 1x CMed, for PDGF-AA it was 123 pg/mL, 7.5 pg/mL and 3.8 pg/mL. The release kinetics differed between TFs, and there was disparity on concentrations between the most and least concentrated hydrogels, so for FGF-1, hydrogels containing 1x and 100x concentrated CMed did not differ on the released TF amount, while for PDGF-AA, these two concentrations led to a different final load of released TF.

The release of HGF reached a mean concentration in the 1st wave of 647 pg/mL for the 100x CMed, which decreased fivefold to 127 pg/mL in the next wave. The same did not happen with the 1x and 10x concentrated CMed, which reached lower maximum concentrations of 35 pg/ml and 75 pg/ml in 24 hours, reaching 52 pg/ml and 25 pg/ml after the 3rd wave (five days). VEGF, in turn, showed a more controlled release, with a maximum TF concentration of 3,490 pg/mL for the 100x concentrated CMed at 1st wave, representing the most abundant of all analyzed

regeneration-related trophic factors. Even after five days of the experiment, VEGFA concentration remained high, with a mean value of 1,003 pg/mL. On the other hand, the 10x and 1x concentrated CMed showed low TF concentrations, 209 pg/mL, and 40 pg/mL, respectively, after the 1st wave.

Finally, MMP1 showed a sustained release along with the experiment. At 1st wave (first 24h), the 100x CMed group reached a mean concentration of 761 pg/mL, which remained stable at 568 pg/mL at the end of the experiment. The same was true for 10x and 1x concentrated CMed, which reached, respectively, 364 pg/mL and 232 pg/mL at 24 hours and kept the concentration at 279 pg/mL and 172 pg/mL, respectively, by the end of the experiment. Thus, MMP-1 showed a smaller difference between CMed concentrations and the most sustained release curves.

Release of inflammation-related trophic factors

Among the eleven trophic factors investigated in this study, four of them were related to inflammation: CXCL8, IL-1 β , IL-6, and IL-8.

The concentration of released inflammation-related trophic factors was, in general, higher than that observed for pro-regenerative trophic factors. CXCL8 was, by far, the most released factor. Its concentration was so high that, in the 100x CMed, it surpassed the upper limit of the assay (7,820 pg/mL). Even for the 10x concentrated CMed, the released concentration at 1st wave was high, 1,514 pg/mL, and quickly dropped after that, reaching 263 pg/mL on the 3rd wave. The 1x

concentrated CMed, however, showed lower initial concentrations, 97 pg/mL in the 1st wave, but a stable release, reaching 43 pg/mL on the fifth day. In contrast to CXCL8, however, was the behavior of IL-1 β , for which the minimal concentration was below the lower limit of the assay (2 pg/mL). Even at 100x concentrated CMed, the cytokine reached no more than 27 pg/mL, remaining relatively stable at 18pg/mL on the 3rd wave. IL-6 and IL-8 showed similar release kinetics, with both cytokines reaching concentrations close to 3,000 pg/mL during the 1st wave for the 100x concentrated CMed (2,613 pg/mL for IL-6 and 2,978 pg/mL for IL-8), but lower than 100 pg/mL for the 10x and 1x concentrated CMed.

Trophic factor relative concentration varies according to the level of concentration of the CMed

The relative concentration, i.e. the proportion of each released trophic factor, for all the three release waves, in the analyzed medium varied according to the level of concentration of the CMed (Figure 3). While in the hydrogels loaded with 1x concentrated CMed the most prevalent released trophic factors were MMP-1 (616 pg/mL), angiopoietin-1 (300 pg/mL), and FGF-1 (261 pg/mL), for the 10x concentrated CMed they were CXCL8 (2,397 pg/mL), angiopoietin-1 (1,071 pg/mL), and MMP1 (948 pg/mL). Finally, for the 100x concentrated CMed, the three most prevalent TF were CXCL8 (>7,820 pg/mL), VEGFA (6,804 pg/mL), and IL-8 (6,068 pg/mL). In general, the more concentrated was the medium, more inflammation-related cytokines and less pro-regenerative trophic factors were present.

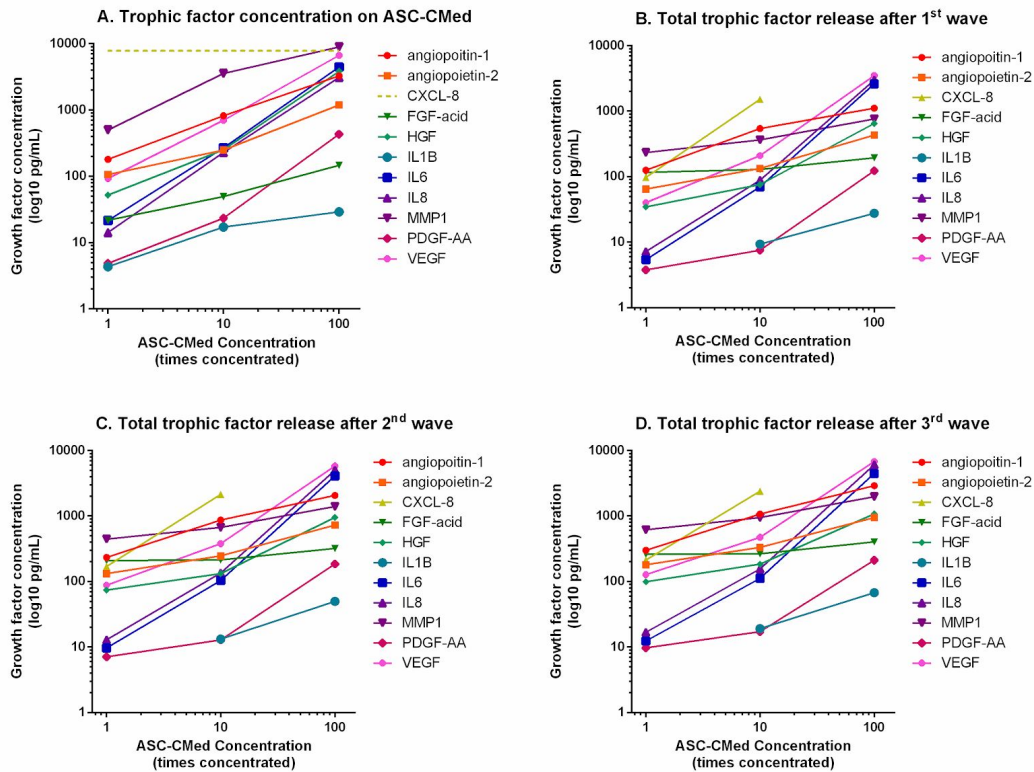


Figure 3 - A. Trophic factor concentration in the collected ASC-CMed at different concentrations (1x, 10x, and 100x). CXCL-8 was above the detection limit in the ASC-CMed for all concentrations (the dotted line represents the upper assay limit for CXCL-8). B. Total trophic factor release from the hydrogel loaded with different ASC-CMed concentrations (1x, 10x, and 100x) after the 1st release wave. CXCL-8 was above the detection limit for 100x concentration hydrogel, and IL-1 β was below the detection limit for 1x concentrated hydrogel. (n=4 independent experiments). C. Total trophic factor release from the hydrogel loaded with different ASC-CMed concentrations (1x, 10x, and 100x) after the 2nd release wave. CXCL-8 was above the detection limit for 100x concentration hydrogel, and IL-1 β was below the detection limit for 1x concentrated hydrogel. (n=4 independent experiments). D. Total trophic factor release from the hydrogel loaded with different ASC-CMed concentrations (1x, 10x, and 100x) after the 3rd release wave. CXCL-8 was above the detection limit for 100x concentration hydrogel, and IL-1 β was below the detection limit for 1x concentrated hydrogel. (n=4 independent experiments).

Influence of the trophic factors released from dECM hydrogels on cell proliferation, endothelial function, and transdifferentiation

The proliferation capacity, endothelial function, and transdifferentiation of HUVEC were assessed after culturing these cells with the trophic factors released by the dECM hydrogel loaded with ASC conditioned medium.

Neither hydrogel alone nor the hydrogel loaded with trophic factors, irrespective of CMed concentration (1x, 10x, and 100x) influenced HUVEC proliferation (Figure 4). For all the experimental groups, about 60% of the endothelial cells proliferated, with no significant differences among them (Kruskal-Wallis, $p=0.128$).

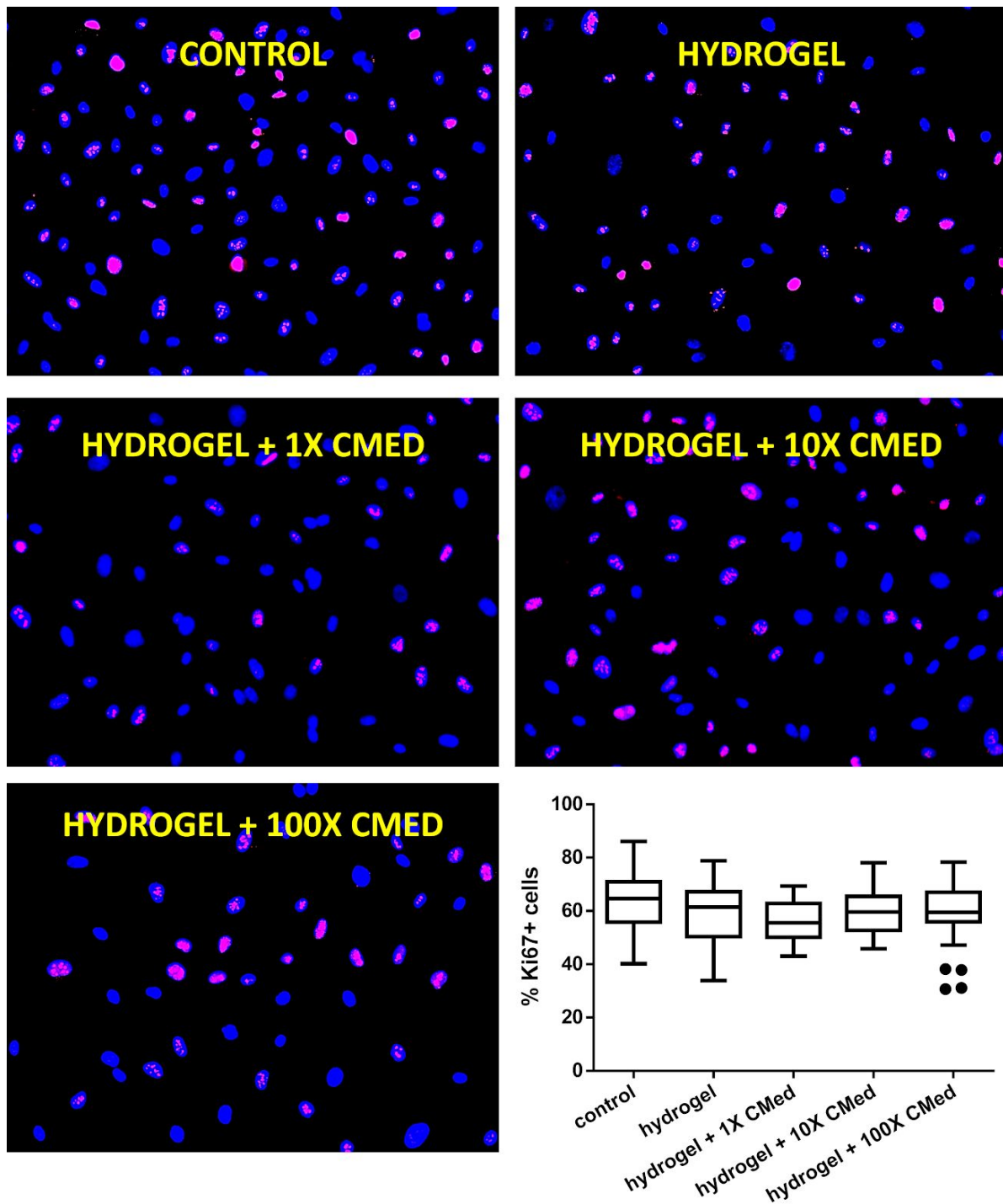


Figure 4 - Endothelial cell proliferation after 5 days of co-culture with trophic factors-loaded dECM hydrogel. (n=3 experiments in duplicate).

In contrast to proliferation, endothelial cell sprouting changed markedly upon the application of dECM hydrogels loaded with ASC secretome (Figure 5). Factors

released from hydrogels loaded with 1x and 10x CMed inhibited in vitro endothelial sprouting as observed by a decreased number of branches compared to controls (Kruskal-Wallis, $p=0.0003$; 1x CMed vs. control, $p=0.0009$; 10x CMed vs. control, $p=0.0005$). In contrast, the release of factors from cardiac dECM hydrogels loaded with 100x Cmed did not affect endothelial sprouting. Similarly, bare dECM hydrogel did not affect sprouting.

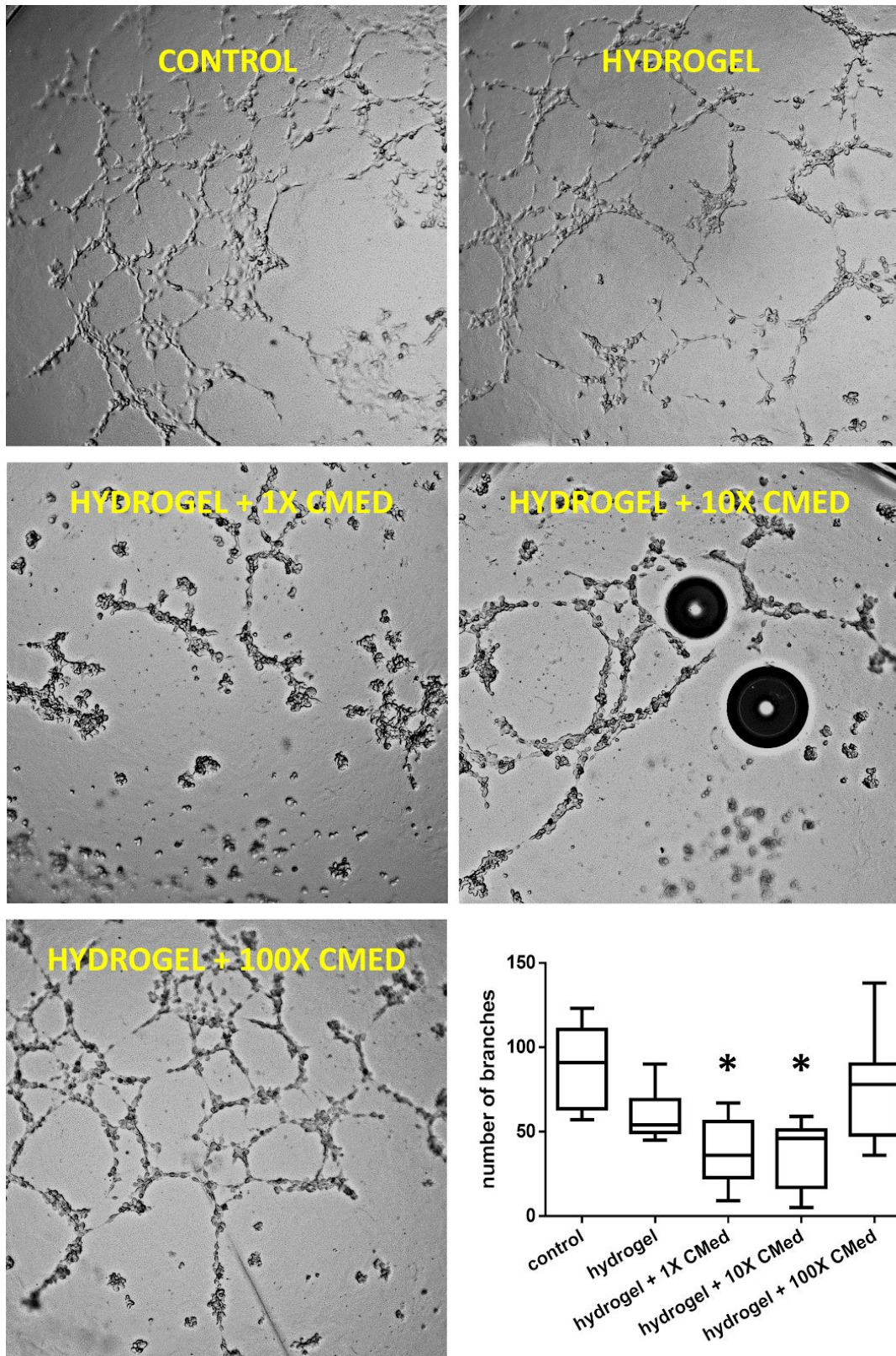


Figure 5 - Endothelial cells sprouting after 4 hours under the influence of trophic factors released from dECM hydrogels for 24 hours. * $p < 0.001$ (n=3 independent experiments in triplicate).

Finally, we assessed the influence of dECM-released CMed factors on TGF- β -induced endothelial mesenchymal transition (EndMT). Controls, i.e., HUVEC without induction, did not show signs of EndMT because mesenchymal marker expression was undetectable (Fig. 6). Co-incubation of HUVECs with dECM hydrogels in transwells did not induce EndMT, nor did the CMed factors released from these hydrogels (irrespective of their concentration factor). Under these conditions, the endothelial phenotype was maintained as determined by the expression of the endothelial marker VE-Cadherin (Fig. 6). Induction of EndMT caused the cytoplasmic expression of SM22 α (Fig. 6) in controls and HUVECs exposed to bare dECM hydrogels in transwells. Although there was a trend towards a decreased expression of mesenchymal markers in the experimental groups loaded with 10x CMed, these did not differ from controls (Kruskal-Wallis $p=0.284$; 10x CMed vs. control, $p=0.1220$). Concerning VE-Cadherin expression, EndMT induction reduced VE-Cadherin expression on the endothelial cell membrane. This loss was not rescued by the trophic factors released from the hydrogel (Kruskal-Wallis $p=0.653$).

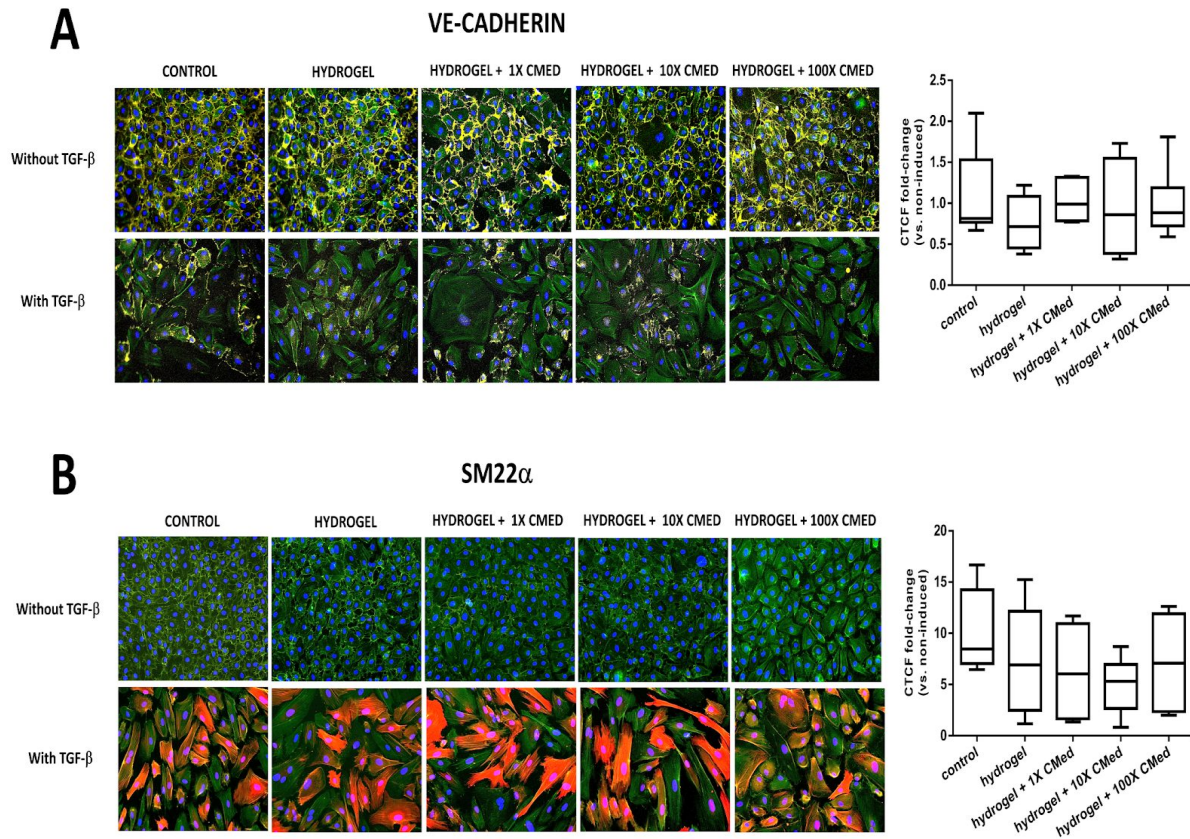


Figure 6 - Influence of trophic factors released from dECM hydrogels on endothelial cells transdifferentiation. A. VECadherin in yellow and phalloidin in green; B. SM22 α in red and phalloidin in green. (n=3 independent experiments in duplicates).

DISCUSSION

In the present study, we investigated the use of porcine left ventricle-derived decellularized extracellular matrix hydrogels to release trophic factors secreted by cultured human adipose tissue-derived stromal cells. We developed a method to produce this trophic factor-loaded hydrogel system and assessed the release pattern of 11 different trophic factors related to tissue regeneration and assessed their biological activity on endothelial cells. Firstly, we showed that porcine dECM

hydrogels could be loaded with human ASC-secreted trophic factors, which are released in a sustained manner for several days subsequently. Secondly, we demonstrated that these trophic factors had different release kinetics, which correlates with the initial concentration of CMed in the hydrogel. We observed that the more concentrated was the hydrogel, the more inflammation-related cytokines, and the less pro-regenerative trophic factors were present. Finally, we showed that the factors secreted by the hydrogel are biologically active as these influence cell behavior, particularly concerning endothelial cell function.

The differential release of the 11 trophic factors herein investigated points to the possibility that each TF has a different binding saturation threshold. This finding directly affects the outcomes from CMed-based therapies based on the release of TF by hydrogel, particularly dECM hydrogels. We showed that in low concentrations, i.e., hydrogels loaded with 1x CMed, the most prevalent TF released were MMP-1, angiopoietin-1, and FGF-1, all pro-regenerative factors. At this level of CMed concentration, however, the concentration of these factors is also low, probably not enough to produce beneficial results. On hydrogels loaded with 10x CMed, the TF release profile starts to alter towards a more inflammatory-related set of factors, so that, at this concentration, the most prevalent TF is CXCL8, already in a considerable concentration (2397 pg/mL). In fibrotic disease, pro-inflammatory chemokines such as CXCL8, orchestrate endothelial cell proliferation and apoptosis resulting in reduced cell repair capacity (17–21) and contributing to EndMT (22–24). At 100x concentrated hydrogels, the concentration of CXCL8 surpassed the upper limit of the assay (7820 pg/mL), and the two factors that had higher concentrations

and were under the upper limit detection of the test were VEGF and IL8. At this concentration, VEGF seems to be the responsible factor for restoring the endothelial cell function, which was lost in hydrogels loaded with 1x and 10x CMed.

The release of trophic factors has been previously shown to be modulated by several factors, such as GF-scaffold binding, hydrogel material and, in the case of dECM hydrogels, the ECM donor and the presence of diseased matrix, e.g. matrix from diabetic patients (13,25,26). Certainly, one of the main aspects involved in TF release by dECM hydrogels is the binding of such TF to the glycosaminoglycans (GAG). These are large, negatively charged polysaccharides that bind both the cells, the other ECM proteins, and the TF. It has been previously shown that even the same trophic factor, in two different isoforms, show variable behavior when binding to GAG (27). Another factor that can contribute to the release behavior of TF is the presence of matrix metalloproteinases (MMP), which cleaves not only ECM proteins but also the binding of these proteins to others (28). In our study, we investigated only MMP1 (an interstitial collagenase), but probably other MMPs are also present in the CMed and possibly also expressed in high concentrations, as MMP1. Thus, the release of the different trophic factors could be affected by the presence and concentration of MMP.

The use of dECM hydrogels as a platform to bind and release paracrine factors secreted by (mesenchymal) cells is a potential alternative to the use of synthetic hydrogels in the context of cardiovascular regeneration. Recently, our group proposed the use of adipose tissue dECM hydrogels as a release platform to

deliver secreted paracrine factors for wound healing applications (13). To the best of our knowledge, this work is the first to demonstrate the use of myocardial dECM hydrogels loaded with trophic factors derived from mesenchymal cells as a potential approach to cardiac regeneration. The fine-tuning of the manufacturing methods and the appropriate balance between CMed concentration and the release of the right TF remains to be investigated. Herein, however, we demonstrated the feasibility of the method and the differences which can be found when the mesenchymal cells secretome is concentrated on a logarithmic scale. Future studies should focus on how hydrogels from different tissues differ regarding the release of trophic factors - in different concentrations - but also on the *in vivo* behavior of these hydrogels and the outcomes achieved by dECM hydrogels-based therapies.

REFERENCES

1. Bui AL, Horwich TB, Fonarow GC. Epidemiology and risk profile of heart failure. *Nat Rev Cardiol*. 2010;8(1):30–41.
2. Benjamin EJ, Blaha MJ, Chiuve SE, Cushman M, Das SR, Deo R, et al. Heart Disease and Stroke Statistics-2017 Update: A Report From the American Heart Association. *Circulation*. 2017 Mar 7;135(10):e146–603.
3. Masarone D, Kaski JP, Pacileo G, Elliott PM, Bossone E, Day SM, et al. Epidemiology and Clinical Aspects of Genetic Cardiomyopathies. *Heart Fail Clin*. 2018 Apr;14(2):119–28.
4. Spees JL, Lee RH, Gregory CA. Mechanisms of mesenchymal stem/stromal cell function [Internet]. Vol. 7, *Stem Cell Research & Therapy*. 2016. Available from: <http://dx.doi.org/10.1186/s13287-016-0363-7>
5. Liang X, Ding Y, Zhang Y, Tse H-F, Lian Q. Paracrine mechanisms of mesenchymal stem cell-based therapy: current status and perspectives. *Cell Transplant*. 2014;23(9):1045–59.
6. Zhou Y, Yamamoto Y, Xiao Z, Ochiya T. The Immunomodulatory Functions of Mesenchymal Stromal/Stem Cells Mediated via Paracrine Activity. *J Clin Med Res* [Internet]. 2019 Jul 12;8(7). Available from:

<http://dx.doi.org/10.3390/jcm8071025>

7. Kapur SK, Katz AJ. Review of the adipose derived stem cell secretome. *Biochimie*. 2013 Dec;95(12):2222–8.
8. Rehman J, Traktuev D, Li J, Merfeld-Clauss S, Temm-Grove CJ, Bovenkerk JE, et al. Secretion of angiogenic and antiapoptotic factors by human adipose stromal cells. *Circulation*. 2004 Mar 16;109(10):1292–8.
9. Liguori TTA, Liguori GR, Moreira LFP, Harmsen MC. Fibroblast growth factor-2, but not the adipose tissue-derived stromal cells secretome, inhibits TGF- β 1-induced differentiation of human cardiac fibroblasts into myofibroblasts [Internet]. Vol. 8, *Scientific Reports*. 2018. Available from: <http://dx.doi.org/10.1038/s41598-018-34747-3>
10. Liguori TTA, Liguori GR, Moreira LFP, Harmsen MC. Adipose tissue-derived stromal cells' conditioned medium modulates endothelial-mesenchymal transition induced by IL-1 β /TGF- β 2 but does not restore endothelial function. *Cell Prolif*. 2019 Aug 29;e12629.
11. Banovic M, Pusnik-Vrckovnik M, Nakou E, Vardas P. Myocardial regeneration therapy in heart failure: Current status and future therapeutic implications in clinical practice. *Int J Cardiol*. 2018 Jun 1;260:124–30.
12. Costantino S, Paneni F. Stem cell therapy in heart failure: Is the best yet to come? *Int J Cardiol*. 2018 Jun 1;260:135–6.
13. van Dongen JA, Getova V, Brouwer LA, Liguori GR, Sharma P, Stevens HP, et al. Adipose tissue-derived extracellular matrix hydrogels as a release platform for secreted paracrine factors [Internet]. *Journal of Tissue Engineering and Regenerative Medicine*. 2019. Available from: <http://dx.doi.org/10.1002/term.2843>
14. Tuin A, Kluijtmans SG, Bouwstra JB, Harmsen MC, Van Luyn MJA. Recombinant gelatin microspheres: novel formulations for tissue repair? *Tissue Eng Part A*. 2010 Jun;16(6):1811–21.
15. Parvizi M, Bolhuis-Versteeg LAM, Poot AA, Harmsen MC. Efficient generation of smooth muscle cells from adipose-derived stromal cells by 3D mechanical stimulation can substitute the use of growth factors in vascular tissue engineering. *Biotechnol J*. 2016 Jul;11(7):932–44.
16. Crapo PM, Gilbert TW, Badylak SF. An overview of tissue and whole organ decellularization processes. *Biomaterials*. 2011 Apr;32(12):3233–43.
17. Liu D, Zhang X-L, Yan C-H, Li Y, Tian X-X, Zhu N, et al. MicroRNA-495 regulates the proliferation and apoptosis of human umbilical vein endothelial cells by targeting chemokine CCL2. *Thromb Res*. 2015 Jan;135(1):146–54.
18. Feng B, Chen S, Gordon AD, Chakrabarti S. miR-146a mediates inflammatory

- changes and fibrosis in the heart in diabetes. *J Mol Cell Cardiol.* 2017 Apr;105:70–6.
19. Ding Y-F, Peng Y-R, Shen H, Shu L, Wei Y-J. Gualou Xiebai decoction inhibits cardiac dysfunction and inflammation in cardiac fibrosis rats. *BMC Complement Altern Med.* 2016 Feb 4;16:49.
 20. Wang X-T, Gong Y, Zhou B, Yang J-J, Cheng Y, Zhao J-G, et al. Ursolic acid ameliorates oxidative stress, inflammation and fibrosis in diabetic cardiomyopathy rats. *Biomed Pharmacother.* 2018 Jan;97:1461–7.
 21. Fang L, Ellims AH, Beale AL, Taylor AJ, Murphy A, Dart AM. Systemic inflammation is associated with myocardial fibrosis, diastolic dysfunction, and cardiac hypertrophy in patients with hypertrophic cardiomyopathy. *Am J Transl Res.* 2017 Nov 15;9(11):5063–73.
 22. Chao J, Wang X, Zhang Y, Zhu T, Zhang W, Zhou Z, et al. Role of MCP1 in the Endothelial-Mesenchymal Transition Induced by Silica. *Cell Physiol Biochem.* 2016 Nov 21;40(1-2):309–25.
 23. Kim J, Kim J, Lee SH, Kepreotis SV, Yoo J, Chun J-S, et al. Cytokine-Like 1 Regulates Cardiac Fibrosis via Modulation of TGF- β Signaling. *PLoS One.* 2016 Nov 11;11(11):e0166480.
 24. Soldano S, Paolino S, Pizzorni C, Trombetta AC, Montagna P, Brizzolara R, et al. Dual endothelin receptor antagonists contrast the effects induced by endothelin-1 on cultured human microvascular endothelial cells. *Clin Exp Rheumatol.* 2017 May;35(3):484–93.
 25. Cai L, Dewi RE, Goldstone AB, Cohen JE, Steele AN, Woo YJ, et al. Regulating Stem Cell Secretome Using Injectable Hydrogels with In Situ Network Formation. *Adv Healthc Mater.* 2016 Nov;5(21):2758–64.
 26. Robert AW, Azevedo Gomes F, Rode MP, Marques da Silva M, Veleirinho MB da R, Maraschin M, et al. The skin regeneration potential of a pro-angiogenic secretome from human skin-derived multipotent stromal cells. *J Tissue Eng.* 2019 Jan;10:2041731419833391.
 27. García-Olivas R, Hoebeke J, Castel S, Reina M, Fager G, Lustig F, et al. Differential binding of platelet-derived growth factor isoforms to glycosaminoglycans. *Histochem Cell Biol.* 2003 Nov;120(5):371–82.
 28. Thompson S, Martínez-Burgo B, Sepuru KM, Rajarathnam K, Kirby JA, Sheerin NS, et al. Regulation of Chemokine Function: The Roles of GAG-Binding and Post-Translational Nitration. *Int J Mol Sci [Internet].* 2017 Aug 3;18(8). Available from: <http://dx.doi.org/10.3390/ijms18081692>

CHAPTER 4

Intrapericardial injection of hydrogels derived from decellularized cardiac extracellular matrix loaded with mesenchymal stromal cells and their secretome: a novel therapeutic approach to treat cytostatics-induced dilated cardiomyopathy.

Tacia Tavares Aquinas Liguori^{1,2}, Gabriel Romero Liguori^{1,2}, Viktor Sinkunas¹, Cristiano de Jesus Correia¹, Raphael dos Santos Coutinho e Silva¹, Fernando Luiz Zanoni¹, Vera Demarchi Aiello¹, Martin C. Harmsen², Luiz Felipe Pinho Moreira¹

1. Heart Institute (InCor), Hospital das Clinicas HCFMUSP, Faculdade de Medicina, Universidade de Sao Paulo, Sao Paulo, Brazil

2. Department of Pathology and Medical Biology, University of Groningen and University Medical Center Groningen, Groningen, Netherlands

To be submitted

ABSTRACT

INTRODUCTION: Intramyocardial injection (IM) of hydrogels containing stem cells, their secretome, or both, may hold promise to treat dilated cardiomyopathy (DCM). This therapy, however, may lead to adverse outcomes, such as arrhythmias, related to the trauma of the IM injection, and poor conductivity of the biomaterial. Additionally, DCM is a multichambered disease, which demands a treatment setup that reaches the entire heart. Thus, the optimal route of administration for cardiac cell therapy in DCM remains a challenge. We hypothesized that the intrapericardial injection of hydrogels derived from the cardiac decellularized extracellular matrix (dECM) loaded with adipose tissue-derived stromal cells (ASC) and their secretome (conditioned medium, CMed) dampen or reverse the progression of DCM.

METHODS: DCM was induced in Wistar, male rats through ten weekly intraperitoneal injections of doxorubicin (cumulative dose: 18mg/kg). In week five, the animals were divided into intrapericardial treatments (2ml/kg): 1) saline, 2) dECM hydrogel, and 3) dECM hydrogel loaded with ASC and their CMed. ASC concentration was 20 million per mL while 100x concentrated CMed in the hydrogel was used. Non-treated, healthy rats were used as controls. Interstitial myocardial fibrosis was determined by Sirius Red staining, and pressure-volume loops determined hemodynamic parameters. **RESULTS:** Interstitial myocardial fibrosis was reduced in ASC/CMed-treated animals compared to saline controls ($p=0.0139$). Ejection fraction and cardiac work efficiency were improved in the ASC/CMed-treated rats compared to saline ($p=0.0151$ and $p=0.0655$, respectively). Treatment with sole dECM hydrogel did not reduce interstitial fibrosis nor improve hemodynamic parameters. **CONCLUSIONS:** The intrapericardial injection of dECM

hydrogels loaded with ASC and their secretome warrant a novel therapeutic possibility by improving ventricular hemodynamics and reducing cardiac remodeling in doxorubicin-induced DCM.

INTRODUCTION

Background

Doxorubicin is a chemotherapeutic, cytostatic drug of the anthracycline family, which also causes a progressive and dose-dependent dilated cardiomyopathy (DCM) through several mechanisms. These include changes in ATP production by the myocytes and topoisomerases as well as inhibition of the expression of sarcoplasmic reticulum calcium-ATPase, increased fibrosis, an increase of oxidative stress, and apoptosis. All these changes cause a loss of contractility and compromise ventricular function, leading to remodeling and, finally, heart failure (1–3). According to the cumulative dosage, 3-26% of patients may experience heart failure with a 50% survival rate of 3.5 years (4–9).

The use of stem cells to treat cardiovascular diseases has become one of the pillars of cardiovascular regenerative medicine. This includes the treatment of cardiomyopathies, mainly ischemic cardiomyopathy (10). Cell therapy-based treatments have concentrated efforts to efficiently deliver and retain stem cells (11), e.g., embedded in degradable biomaterials (12,13) to reverse or inhibit the disease

progression, in order to improve cardiac function. The outcomes of this type of therapeutic intervention are variable and also underlying mechanisms are not entirely understood and it still does not constitute an admittedly successful clinical application (14,15). Still, regenerative medicine has made many advances and has progressed over the years concerning cardiac regeneration, particularly for ischemic cardiomyopathy (16). Two main approaches have been used in this regard, which are the injection of stem cells into the myocardium and the use of pericardial patches seeded with cells that could assist the restoration of cardiac function (17). Although much has been studied, none of these alternatives progressed enough to fulfill all the criteria necessary for its clinical use (18).

An alternative approach, the intrapericardial injection of cells, to treat cardiac degeneration was first proposed in 2009 (19). This approach, however, has never received the same attention as the intramyocardial injection of cells. Previously, this route had been used for gene (20) and chemotherapy drug (21) delivery, more recently is also described as an alternative for antibiotics delivery (22). The use of intrapericardial injection for cell therapy has been limited to a handful of studies; all of them focused on the treatment of myocardial infarction (19,23–25). We believe, however, that this route is much more interesting for dilated, multi-chambered, cardiomyopathies than for the ischemic, localized disease, considering the injection of cells into the pericardial space allows reaching the whole heart.

Objectives

Herein, we propose a new approach - merging both principles of stem cells injection and the use of pericardial patches - to address the current limitations existing in these two methods. We evaluated the use of intrapericardial injection of decellularized extracellular matrix hydrogels loaded with adipose tissue-derived stromal cells and their secretome to treat doxorubicin-induced heart failure secondary to dilated cardiomyopathy. We hypothesized that this approach could dampen or reverse the progression of DCM induced by doxorubicin.

METHODS

ETHICAL STATEMENT

Animals were handled according to the Brazilian College of Animal Experimentation (COBEA) (26–28) for a humanized and ethical use of laboratory animals. This project was approved by the internal Ethical Committee for the Use of Animals (CEUA) (1011/2018).

Study design

Dilated cardiomyopathy was induced by a ten-week protocol applying doxorubicin, a cytostatic drug (Figure 1).

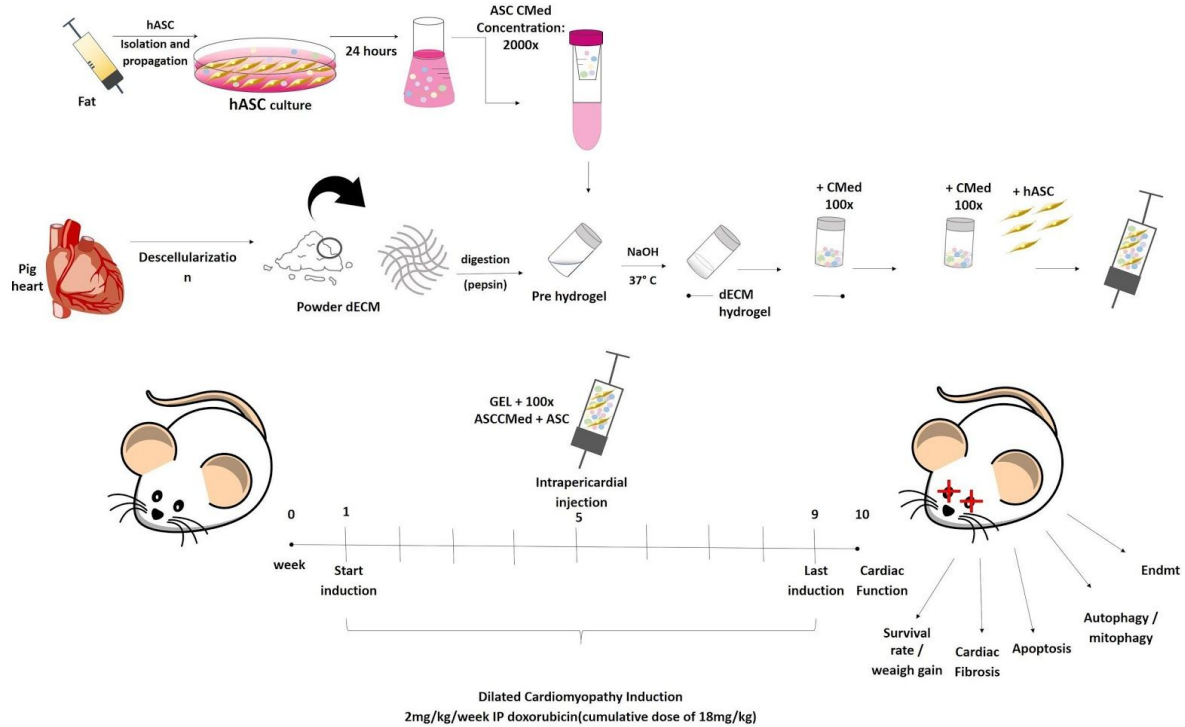


Figure 1. Study design.

Randomization

In the 5th week after the first doxorubicin injection, rats were randomly distributed into four groups (Table 1) using a list randomizer online tool (29). Two different surgeons performed the surgeries. For each animal, the responsible surgeon was also defined by using the above-mentioned list randomizer online tool. An assistant, who was not blinded to the rat group inclusion, was responsible for preparing the syringes containing either of the four combinations of treatment.

| Table 1. Experimental Groups | | | | | |
|-------------------------------------|---|------------|-------------|--------------------|----------------------|
| Group | Description | IPI | Doxo | dECM HG | ASC/ CMed |
| Naive | Healthy animals | - | - | - | - |
| Saline | Doxorubicin-induced dilated cardiomyopathy treated with intrapericardial saline injection | + | + | - | - |
| Gel | Doxorubicin-induced dilated cardiomyopathy treated with intrapericardial injection of the decellularized extracellular matrix-based hydrogel | + | + | + | - |
| ASC/CMed | Doxorubicin-induced dilated cardiomyopathy treated with intrapericardial injection of the decellularized extracellular matrix-based hydrogel loaded with adipose tissue-derived stromal cells and their secretome | + | + | + | + |

IPI: intrapericardial injection; Doxo: doxorubicin induction; dECM HG: decellularized extracellular matrix-based hydrogel; ASC: adipose tissue-derived stromal cells; CMed: conditioned medium

Cell Sources, Cell Culture, and Conditioned Medium

Human ASC were isolated as described previously (30–32), with minor modifications. Briefly, human abdominal fat was obtained by liposuction, washed with phosphate-buffered saline (PBS) and digested enzymatically with 0.1% collagenase A (#11088793001, Roche Diagnostic, Mannheim, Germany) in Dulbecco's Modified Eagle's Medium (DMEM; #12-604F, Lonza, Basel, Switzerland) with 1% bovine serum albumin (BSA; #A9647, Sigma-Aldrich, Boston, USA). The tissue was shaken constantly at 23°C (room temperature) for 18h. After this, the digested tissue was mixed with 1% PBS/BSA, filtered, centrifuged and the cell pellet was resuspended in DMEM with 10% fetal bovine serum (FBS; #F0804, Sigma-Aldrich, Missouri, United States), 1% penicillin/streptomycin (#15140122, Gibco Invitrogen, Carlsbad, USA) and 1% L-glutamine (#17-605E, Lonza Bio Whittaker, Verviers, Belgium). Cells were cultured at 37°C in a humidified incubator with 5% CO₂. The medium was refreshed every two days. Cells were passed at a ratio of 1:3 after they reached confluency.

ASC conditioned medium (ASC-CMed) was obtained from confluent cultures of ASC between passages 2 and 4 from at least three different donors. For ASC-CMed, cells were cultured for 18 hours in serum-free DMEM. After this, they were allowed to recover in DMEM with serum for 24 hours before following a new passage. Cells were kept at 37°C with a minimum relative humidity of 95% and an atmosphere of 5% CO₂ in the air. The harvested conditioned medium was filtered in a 0.22µm filter and stored at -20°C until use.

Extracellular Matrix Decellularization and Hydrogel Fabrication

Decellularization Protocol

Decellularization was performed as previously described, with minor modifications. Briefly, porcine hearts were purchased from a local slaughterhouse (Porco Feliz, Sao Paulo, Brazil) and dissected as to separate the left myocardial tissue. The tissue was washed in phosphate buffer saline (PBS) and triturated in a commercial blender until no pieces larger than 1mm could be discriminated. Following the second wash in PBS, tissue was incubated in 0.05% trypsin at 37°C for 3 hours and constant shaking. After trypsin treatment, tissue was rewashed with PBS and frozen overnight at -20°C. After thawing, tissue was incubated in demineralized water (H₂O) for 3 hours and then in saturated sodium chloride solution (NaCl, 6M) for another 3 hours, both steps in constant shaking. Following the osmotic shock, tissues were washed in ethanol 70% for 10 minutes and in H₂O for another 10 minutes. After washed, tissues were incubated with 1% sodium dodecyl sulfate (SDS) for 12 hours, washed three times with H₂O, incubated with 1% Triton X-100 for 12 hours, washed three times with H₂O, incubated with 1% deoxycholate for 12 hours and, again, washed three times with H₂O, all steps under constant shaking. After detergent treatment, tissues were incubated for 24 hours with DNase solution (30ug/ml DNase, 1.3mM MgSO₄, 2mM CaCl₂) at 37°C and constant shaking. After DNase treatment, tissues were washed three times with H₂O and stored at 4°C in 1% penicillin/streptomycin in sterile PBS.

Hydrogel Fabrication

For dECM gelation, the decellularized extracellular matrix was lyophilized and milled to a fine powder. The resulting dECM powder (20 mg/ml) was digested with 2 mg/ml pepsin (3,200IU/mg; Sigma-Aldrich) in 0.01 HCl with 2mg/mL of pepsin for six hours at RT and constant stirring. After digestion, the pH was neutralized with 1/10th volume 0.1 M NaOH and the electrolytes equilibrated by adding 1/10th volume of 10x PBS). Finally, 1/10th volume with 10x DMEM was added. The resulting solution could then be stored in liquid form (pre-gel) or transformed into hydrogel by warming to 37°C.

For hydrogels containing ASC and their secretome, before each experiment, the CMed obtained from ASC was concentrated 2,000-fold using 3kDa Amicon® Ultra Centrifugal 15 mL filters (UFC900324, Merck, Darmstadt, Germany) by repeating the concentrating procedure with previously concentrated samples. After concentration, CMed was added as 1/20th of the final volume in dECM pre-gel, resulting in pre-gels containing 100-fold concentrated CMed. ASC, at passages 2 to 5, were seeded inside the pre-gel at a concentration of 20 million cells/mL.

ANIMAL CARE AND MONITORING

Rats underwent cardiomyopathy induction by the weekly intraperitoneal (IP) administration of 2 mg/kg doxorubicin (Rubidox 50mg, Laboratório Bergamo, Taboão

da Serra, Brazil) in 0.9% NaCl, reaching a cumulative dosage of 18 mg/kg by the end of the 9th injection. Intraperitoneal injection of doxorubicin was performed under isoflurane anesthesia (2% isoflurane in 50% O₂) (Grupo Cristália, São Paulo, Brazil), with a custom-made mask.

In the 5th week of the protocol, rats were submitted to the therapeutic intervention, being allocated in one of the four experimental groups. For all but the naive group, rats were submitted to the intrapericardial injection (IPC) of either saline, dECM hydrogel, or dECM hydrogel with ASC and their secretome.

In order to execute the procedure, rats were sedated with 5% isoflurane inside a closed transparent acrylic chamber, and endotracheal intubation was performed with a 16G polyethylene catheter. Following intubation, anesthesia was maintained with isoflurane (2% isoflurane in 50% O₂). After anesthesia, but before the beginning of the surgery, rats were submitted to an analgesics/antibiotics protocol, as described in Table 2. Still, before the procedure, 20µL of blood were taken from the tail vein to perform hemogram and leukogram exams.

| Table 2. Analgesics/antibiotics protocol | |
|--|--------------------|
| Drug | Dosage, via |
| Tramadol hydrochloride | 10 mg/kg, IP |
| Dipirona | 200 mg/kg, SC |
| Meloxicam | 0.2 mg/kg, SC |
| Pentabiotics | 24,000 mg/kg, IM |
| IP: intraperitoneal; SC: subcutaneous; IM: intramuscular | |

After intubation and anesthetic maintenance, animals were positioned in the right lateral decubitus, on constant heating at 37°C, and submitted to trichotomy of the left hemithorax. Antisepsis was done with iodopovidone (Riodeine, Rioquímica, Sao Paulo, Brazil) and an incision was performed, first, on the skin, and then, on the intercostal musculature of the fourth left intercostal space. The left lung was secluded with a gauze embedded in saline solution, and the pericardium was exposed. With delicate tweezers, the pericardium was carefully pulled. With a flexible piercing catheter, 2mL of hydrogel (or saline) per kilo of rat weight was injected into the intrapericardial space (Supplementary Material, Video S1). In sequence, the catheter was slowly withdrawn and the integrity of the pericardium was evaluated. To finalize the procedure, the intercostal muscles and skin were sutured, the wound

area was cleaned and local anesthesia was applied to the skin (lidocaine 2% - Xylestesin 2%, Cristalia, Sao Paulo, Brazil). Tramadol and dipyron were repeated after 24h.

Five weeks after the intervention (IPC injection) and one week after the last doxorubicin injection, rats were anesthetized as described above, placed in dorsal decubitus position and the ventral cervical region was trichotomized, and skin disinfectant was performed with iodopovidone (Riodeine, Rioquímica, Sao Paulo, Brazil). The right carotid artery was isolated, and a 2F pressure-volume acquisition catheter (SPR-838; ADInstruments, Colorado Springs, USA) was inserted retrograde to the left ventricle (LV) and connected to the data acquisition system (MPVS -Ultra Single Segment Foundation System for Rats; ADInstruments, Colorado Springs, USA) for continuous recording of pressure and volume curves in the LV (Ugurlucan et al., 2008). At the end of the experiment, blood samples were collected from the carotid artery, as well as ascitic fluid, in order to perform biochemical analysis.

Following the procedure, animals were kept anesthetized, submitted to cardiac arrest in diastole induced by perfusion of a solution containing 0.9% NaCl and 14 mEq/L KCl, and exsanguinated by puncture of the abdominal aorta. Blood samples were centrifuged for 20 minutes at RT at 8,000xg, and aliquots of 500µL of the supernatant were stored at -80°C until used. The heart was collected for *post mortem* analysis, and the animal remains were sent to incineration.

HOUSING AND HUSBANDRY

Male Wistar rats (*Rattus norvegicus domestica*), specific-pathogen-free (SPF) aged nine weeks with 405.5g (382.3-430.0) of weight, were used as an animal model for dilated cardiomyopathy and as controls. Rats were kept at $23\pm 2^{\circ}\text{C}$, with a light and dark period of 12h, without restrictions on water and food intake. They were fed with a pellet diet (Nuvilab CR-1[®], Quimtia, Colombo, Brazil) composed of 63% of carbohydrates, 26% protein and 11% of lipids. During the ten weeks, they were maintained into cages filled with wood sawdust. Each cage contained three rats, except for the week after the surgery (5th week), when rats were maintained in separate cages for healing.

Sample size

Sample size calculation was performed using the software G*Power: Statistical Power Analyses for Windows (Version 3.1.9.4) (33,34). Setup considered the F tests family, using ANOVA fixed effects, omnibus, one-way statistical test as reference. The following values were considered for the test: effect size f , 0.65; alpha error, 0.05; power, 0.80; the number of groups, 4. This resulted in a total sample size of 32 animals, with an actual power of 0.831. Rats were operated on five distinct days. For all the five occasions, the number of animals, the group allocation, and the responsible surgeon were randomized and defined using a list randomizer online tool (29).

Inclusion and Exclusion Criteria

Animal samples were excluded from analysis when they could not be retrieved at any time point or were damaged.

Blinding

All the outcome analyses were done on blinded samples.

Experimental readouts

The primary experimental outcome of the present study was heart function, as defined by the pressure overload curve. Secondary outcomes included: weight, hematologic parameters, ascites volume, cardiac morphometry, interstitial fibrosis, apoptosis, mitophagy, and autophagy.

In vivo analysis

Heart function

The characterization of blood pressure, systolic, and diastolic function was performed under anesthesia by the micro-conductor catheter technique immediately before the euthanasia, as previously described (35). Briefly, cardiac function was

measured primarily by the ejection fraction, cardiac work efficiency, and preload recruitable stroke work (PRSW, mmHg). Other hemodynamic parameters such as stroke work, stroke volume, end-systolic pressure, end-systolic volume, end-diastolic pressure, end-diastolic volume, $dP/dt(\max)$, $dP/dt(\min)$, heart rate, and Tau were evaluated as well. For cardiac stimulation, 5mg/kg/min of dobutamine were continuously infused for 10 minutes and the data were acquired during the last 5 minutes. Then, the dosage was increased to 10mg/kg/min for 10 minutes and the data were acquired during the last 5 minutes. After this, the euthanasia was performed under anesthesia isoflurane anesthesia by exsanguination followed by the infusion of a solution 19% potassium chloride in 0,9% NaCl solution, with diastolic arrest.

Weight

The weight in grams of each rat was measured once a week for ten weeks, every week before the induction rats were weighed, and the ascites volume was discarded from the initial one.

Ascites Volume

Every week, after being weighed, rats received anesthesia in a custom-made mask with 2% isoflurane in 50% O₂ (Grupo Cristália, São Paulo, Brazil). A catheter 24G was introduced 1cm distal of umbilical scar, in the alba line, through the skin to

reach the abdominal cavity. All the liquid was removed and measured. Then, the induction was performed.

Hematologic parameters

The blood was collected on three time points: 1) after the first induction, 2) on the 5th week, before the surgery, and 3) on the 10th week before the euthanasia. Briefly, 20 μ L of blood were taken from the tail vein to perform hemogram and leukogram exams (lymphocyte-to-platelet ratio and neutrophil-to-lymphocyte ratio).

Post mortem analysis

The collected hearts were sectioned into three parts. The first section, performed at the midpoint of the distance between the apex and the coronary sulcus of the heart, at the height of the papillary muscles, produced samples that were fixed in formaldehyde solution for cardiac morphometric analysis. The second, immediately below the first, was embedded and frozen in an optimal cutting temperature (OCT) compound for cryosection.

Morphometric analysis and cardiac fibrosis

Heart samples were fixed in 10% formaldehyde solution for 48 hours. After conventional histological processing, 5 μ m cross-sections of the ventricles were

prepared and stained with hematoxylin-eosin (HE) or Picrosirius red for quantitative assessment of cardiac morphology and tissue fibrosis, respectively. Movat's pentachrome staining was performed for a qualitative illustration of the myocardial tissue.

Image Tool software, developed by the Department of Dental Diagnostics Science of the University of Texas Health Science Center, San Antonio, USA(36,37), was used to perform measurements of cardiac structures. The following measures were carried out: 1) thickness of the left ventricle wall; 2) thickness of the right ventricle wall; 3) thickness of the interventricular septum; 4) area of the left ventricular cavity; and 5) area of the right ventricular cavity. For quantification of interstitial cardiac fibrosis, collagen deposition was analyzed as previously described(38), with minor modifications. Briefly, collagen area fraction was quantified employing identification by color using the ImageJ software.

Immunohistochemistry assay for apoptosis, mitophagy, and autophagy

Apoptosis, mitophagy, and autophagy were evaluated by immunohistochemistry analysis of the cardiac tissue. Apoptosis was determined using B-cell lymphoma 2 (BCL2) and cleaved caspase-3. Mitophagy and autophagy were analyzed by PTEN-induced kinase 1 (PINK1) and Unc-51 Like Autophagy Activating Kinase 1 (ULK1), respectively.

Paraffin-embedded sections (5 µm), immobilized on silanized slides were deparaffinized (20 minutes in xylol 100% and 10min in each one of the following reagents: ethanol 100%, ethanol 96%, ethanol 70%, and demi water). Subsequently, antigen retrieval was performed according to the antibody. For BCL2 and cleaved caspase-3, 0.1M citrate buffer solution, pH 9.0, was used. For PINK1, we used 0.1M Tris-HCl buffer solution, pH 8.5. A 0.1M citrate buffer solution, pH 6, was used to incubate ULK1. For immunostaining, samples were incubated with the primary antibodies at 4°C overnight. The following antibodies were used: mouse anti-BCL2 (1:200, #sc-7382, Santa Cruz Biotechnology, Texas, United States), rabbit anti-caspase 3 (1:200, #9661, Cell Signalling, Massachusetts, United States), rabbit anti-PINK1 (1:200, ab23707, Abcam, Cambridge, UK) and Rabbit anti-pULK1 (1:200, ab203207, Abcam, Cambridge, UK). In sequence, the slides were washed with 0,05% Triton X-100 in PBS, and endogenous peroxidases were blocked using 3% H₂O₂ in Tris-buffered saline (TBS) for 10 min. Samples were then washed in TBS and incubated with a secondary antibody in TBS with 1% BSA and 5% rat serum for 30 min. The following secondary antibodies were used: goat anti-rabbit (1:100, #p0260, Dako, Denmark) and rabbit anti-mouse (1:100, #p0448, Dako, Denmark). Next, the samples were incubated for 15 min in 3-amino-9-ethyl carbazole (AEC) and stained with hematoxylin for 10 min. Finally, the slides were washed in TBS and scanned by the NanoZoomer slide scanner (Hamamatsu Photonics, Hamamatsu City, Japan).

Statistical Analysis

Data were treated as non-parametric and are presented as median and interquartile range. Graphs and statistical analyses were performed using GraphPad Prism (Version 6.01; GraphPad Software, Inc., La Jolla, United States). Differences among multiple groups were analyzed by Kruskal-Wallis with Dunn's multiple comparison test for the two groups of interest in each scenario.

RESULTS

Health status week-over-week

Health status was characterized by weight gain, ascites volume, neutrophil-to-lymphocyte, and platelet-to-lymphocyte ratios. Weight was measured every week, and the weight gain calculated per week (Figure 2A). Briefly, all treated groups started the treatment with a positive gain of weight, which persisted until the fifth week. There was no statistically significant difference in weight gain among the groups. Ascites volume, in turn, was also evaluated week-over-week (Figure 1B). In general, there was no ascitic fluid until the sixth week of induction, from which it started to increase for all groups. The volume of ascites, however, varied importantly over the weeks and also between and within the groups. There were weeks in which substantial differences could be noted among the groups, as the seventh week, but also weeks in which all groups showed the same median volume of ascites, as the tenth week. Within the groups, the variance was also substantial, as demonstrated in the graph. Neutrophil-to-lymphocyte (Figure 1C) and platelet-to-lymphocyte (Figure 1D) ratios were determined because they have been shown to predict the severity

and prognosis of heart failure (39). In our sample, none of the two ratios evidenced statistically significant differences among the groups. Unfortunately, only 11 animals could be used to calculate these ratios because they were plotted only for animals who survived until the last week of the experiment; among these animals, 12 presented missing data due to technical issues with the analyzer machine. The full data regarding hematological parameters, including red blood cells, white blood cells and platelet counting, are summarized in the Supplementary Material (Table S1).

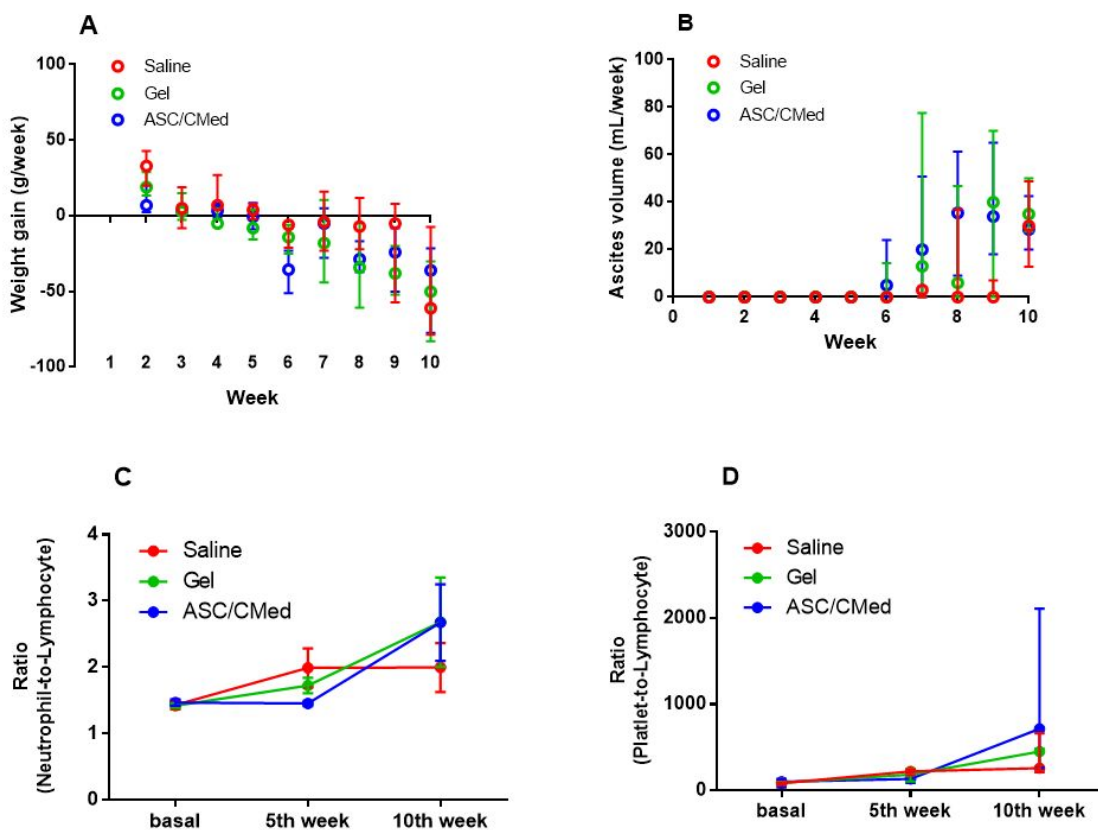


Figure 2. Health status. A) Weight gain week-over-week. B) Ascites volume week-over-week. C) Neutrophil-to-lymphocyte ratio. Numbers analysed: saline, n=4; gel, n=3; ASC/CMed, n=4. D) Platelet-to-lymphocyte ratio. Numbers analysed: saline, n=4; gel, n=3; ASC/CMed, n=4.

By the end of the tenth week, one (14.3%) rat had died in the saline group, three (33.3%) died in the gel group, and five (50%) died in the ASC/CMed group. All deaths were distributed in the final two weeks, and there was no statistically significant difference in mortality among the groups (Log-Rank test, $p=0.3910$)

ASC/CMed-loaded dECM hydrogel rescues cardiac function

When the cardiac function was evaluated at the basal state, naive rats demonstrated higher ejection fraction and cardiac work efficiency when compared to rats, which had been induced and treated with saline solution (Figure 3A-B). No differences were found regarding rats treated with hydrogel or hydrogel loaded with ASC/CMed. When dobutamine was infused at five $\mu\text{g}/\text{kg}/\text{min}$, however, simulating the recruitment of heart during exercise, both naive and ASC/CMed groups showed a statistically significant difference for both parameters (ejection fraction and cardiac work efficiency) when compared to rats treated with saline solution (Figure 3A-B). This difference persisted and became even more evident under stimulation with $10\mu\text{g}/\text{kg}/\text{min}$ (Figure 2A-B).

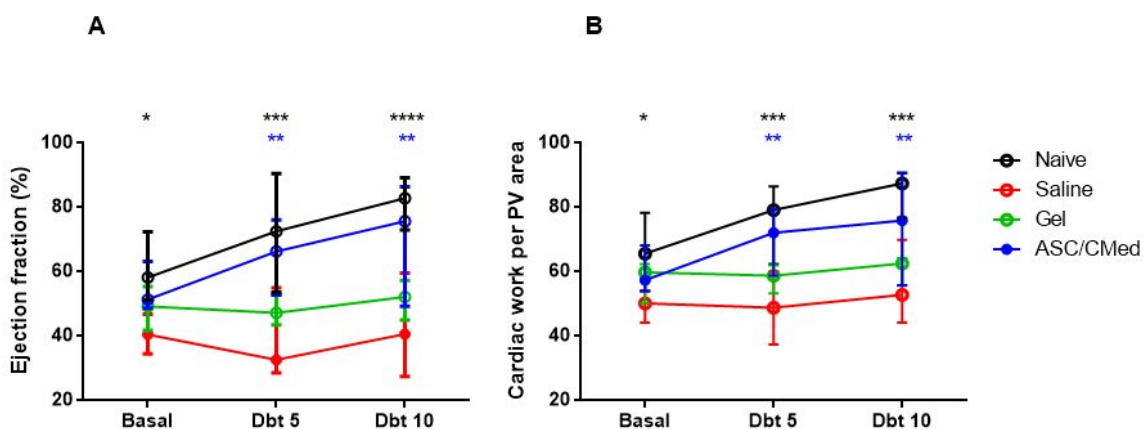


Figure 3. Cardiac function. A) Ejection fraction; B) Cardiac work efficiency. Asterisks represent the p-value of Dunnett's multiple comparisons test vs. saline group: *p<0.05; **p<0.01; *p=0.001; ****p<0.0001. Black asterisks represent naive group and blue asterisks represent ASC/CMed group. Numbers analysed: naive, n=6; saline, n=6; gel, n=5; ASC/CMed, n=5.**

Corroborating with the cardiac function results, myocardial contractility measured by preload recruitable stroke work (PRSW) was improved in the animals treated with ASC/CMed-loaded hydrogels compared to saline (Figure 4; Kruskal-Wallis, p=0.0069; Dunn's multiple comparisons test, p=0.0022).

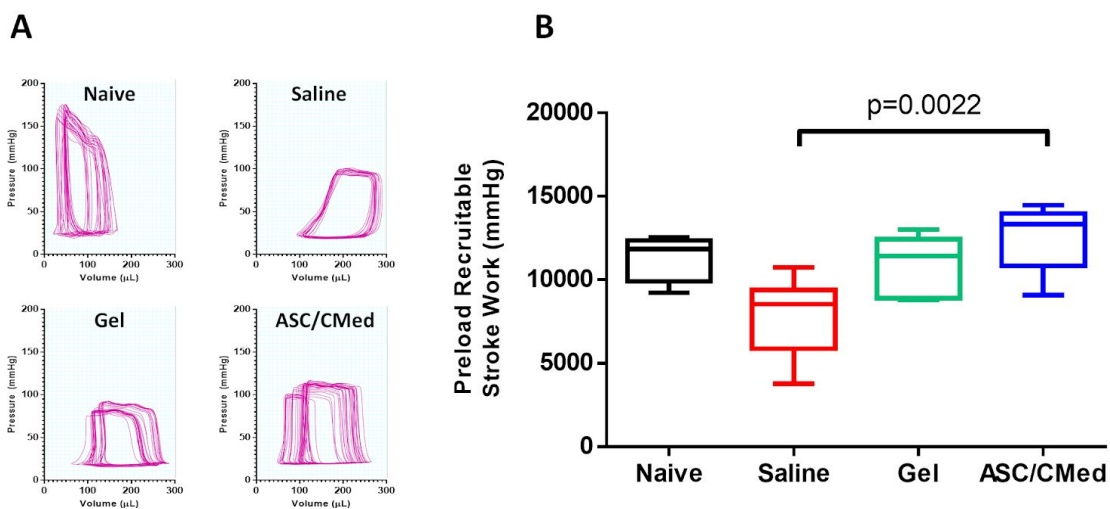


Figure 4. Preload maneuver. A) Representative pressure-volume loop in response to preload maneuver. B) Preload recruitable stroke work (PRSW). P-value for Dunnett's multiple comparisons test vs. saline group. Numbers analysed: naive, n=6; saline, n=6; gel, n=5; ASC/CMed, n=5.

Other parameters, such as heart rate (Kruskal-Wallis, p<0.0001; Dunnett's multiple comparisons test p=0.0004) and Tau (Kruskal-Wallis, p=0.0064; Dunnett's

multiple comparisons test $p=0.0473$) were different when comparing the saline and naive groups, but no differences were found between animals treated with ASC/CMed-loaded hydrogels and those with saline. The complete summary of hemodynamics parameters is listed in Table 3.

| Table 3. Left Ventricle Hemodynamic parameters | | | | | | |
|---|--------|---------------------------|--------------------------|---------------------------|---------------------------|-----------------|
| | | Naive | Saline | Gel | ASC/CMed | p-value* |
| Stroke work (mmHg* μ L) | Basal | 9,700 (8,640-12,425) | 10,578 (7,649-13,225) | 12,300 (9,714-13,700) | 11,700 (10,800-12,300) | 0.2052 |
| | Dbt 5 | 19,250 (13,075-21,300) | 12,100 (6,599-12,675) | 13,000 (10,40-15,400) | 12,200 (11,200-13,000) | |
| | Dbt 10 | 20,150 (15,125-22,775) | 12,150 (7,267-12,500) | 13,900 (10,000-14,500) | 12,300 (11,900-13,200) | |
| Stroke volume (μ L) | Basal | 132 (117-147) | 120 (94-132) | 143 (136 -149) | 138 (128-175) | 0.3820 |
| | Dbt 5 | 157 (136-201) | 113 (76-136) | 162 (127-173) | 154 (146-179) | |
| | Dbt 10 | 179 (130-220) | 118 (81-144) | 165(132-169) | 168 (155-186) | |
| End-systolic pressure (mmHg) | Basal | 104 (89-120) | 131 (108-137) | 121 (113-122) | 111 (104-119) | 0.7684 |
| | Dbt 5 | 122 (105-153) | 123 (105-134) | 108 (98-117) | 109(980-121) | |
| | Dbt 10 | 107(96-139) | 116 (97-129) | 112 (102-112) | 96 (91-115) | |

| | | | | | | |
|---------------------------------------|--------|---------------------------|----------------------------|----------------------------|---------------------------|--------|
| End-systolic volume (μL) | Basal | 152 (88-180) | 196 (137-243) | 161 (149-213) | 166 (155-187) | 0.1019 |
| | Dbt 5 | 99 (56-146) | 187 (141-254) | 206 (173-226) | 120 (105-135) | |
| | Dbt 10 | 68 (32-102) | 168 (119-210) | 177 (157-205) | 152 (49-156) | |
| dP/dt(max) (mmHg/s) | Basal | 6,331 (5,547-6,704) | 6,525 (4,959-7,292) | 6,216 (5,288-6,826) | 4,821 (4,775-5,777) | 0.0130 |
| | Dbt 5 | 9,601 (9,227-9,881) | 6,679 (5,628-8,377) | 5,642 (5,085-6,999) | 5,506 (4,951-6,089) | |
| | Dbt 10 | 9,948 (8,767-11,175) | 6,615 (6,137-8,062) | 6,252 (5,193-6,900) | 5,440 (5,365-5,900) | |
| End-diastolic pressure (mmHg) | Basal | 8.17 (6.07-9.74) | 8.12(6.50-9.54) | 8.21(6.48-10.25) | 6.57(3.91-7.41) | 0.0851 |
| | Dbt 5 | 3.05 (2.03-4.13) | 6.94 (6.09-8.03) | 7.90(7.25-10.8) | 6.27 (6.13-16.1) | |
| | Dbt 10 | 1.12 (-0.73-2.60) | 6.45 (5.49-7.11) | 7.55 (5.86-7.91) | 6.45 (5.16-15.1) | |
| End-diastolic volume (mL) | Basal | 252 (175-296) | 302 (220-365) | 290 (260-358) | 281 (276-327) | 0.8477 |
| | Dbt 5 | 247 (191-290) | 285 (225-341) | 324 (248-390) | 258 (236-338) | |
| | Dbt 10 | 252 (154-254) | 273 (192-328) | 299 (224-363) | 257 (177-342) | |
| dP/dt(min) (mmHg/s) | Basal | -5,774 (-6,129--4,722) | -5,139 (-6,548.--3,903) | -5,294 (-5,816.--4,077) | -2,226 (-2,429--2,222) | 0.0023 |
| | Dbt 5 | -7,463 (-8,649--6,941) | -5,428.5 (-6,761--4376) | -3,962 (-5,696--3,947) | -3,068 (-3,435--2,673) | |
| | Dbt 10 | -6,901 | -5,118 | -5,330 | -3,119 | |

| | | | | | | |
|--|--------|------------------|------------------|------------------|------------------|--------|
| | | (-9,185--6,04 | (-6,146--4,533) | (-5,434--3,629 | (-3,737--3,074) | |
| Heart rate (bpm) | Basal | 361 (338-368) | 274 (240-320) | 232 (221-267) | 256 (256-259) | 0.0001 |
| | Dbt 5 | 421 (409-434) | 276 (245-333) | 250 (227-285) | 285 (265-295) | |
| | Dbt 10 | 446 (439-453) | 279 (248-338) | 275(240-293) | 290 (274.1-304) | |
| Tau (ms) | Basal | 9.68 (8.79-10.3) | 13.9 (11.1-16.8) | 13.6(13.0-15.8) | 14.8 (13.0-14.8) | 0.0064 |
| | Dbt 5 | 6.57 (6.14-6.88) | 11.9(10.4-14.4) | 15.2 (11.6-16.6) | 16.9 (10.9-17.2) | |
| | Dbt 10 | 5.93 (5.75-6.63) | 11.8 (10.7-12) | 12 (10.75-13.47) | 19.1 (12.2-20.8) | |
| <p>*P-value for Kruskal-Wallis analysis; Dbt 5 - data acquired on 5 µg/kg/min infusion of dobutamine; Dbt 10 - data acquired on 10 µg/kg/min infusion of dobutamine. Numbers analysed: naive, n=6; saline, n=6; gel, n=5; ASC/CMed, n=5.</p> | | | | | | |

ASC/CMed-loaded dECM hydrogel abrogates cardiac interstitial fibrosis

The cardiac interstitial fibrosis, shown in Figure 5, was increased in animals of the saline group, compared to their naive peers (Kruskal-Wallis, $p=0.0002$; Dunn's multiple comparisons test, $p=0.0007$). Treatment with the hydrogel alone did not influence fibrosis, but it did in rats treated with ASC/CMed-loaded hydrogels (Kruskal-Wallis, $p=0.0002$; Dunn's multiple comparisons test, $p=0.017$).

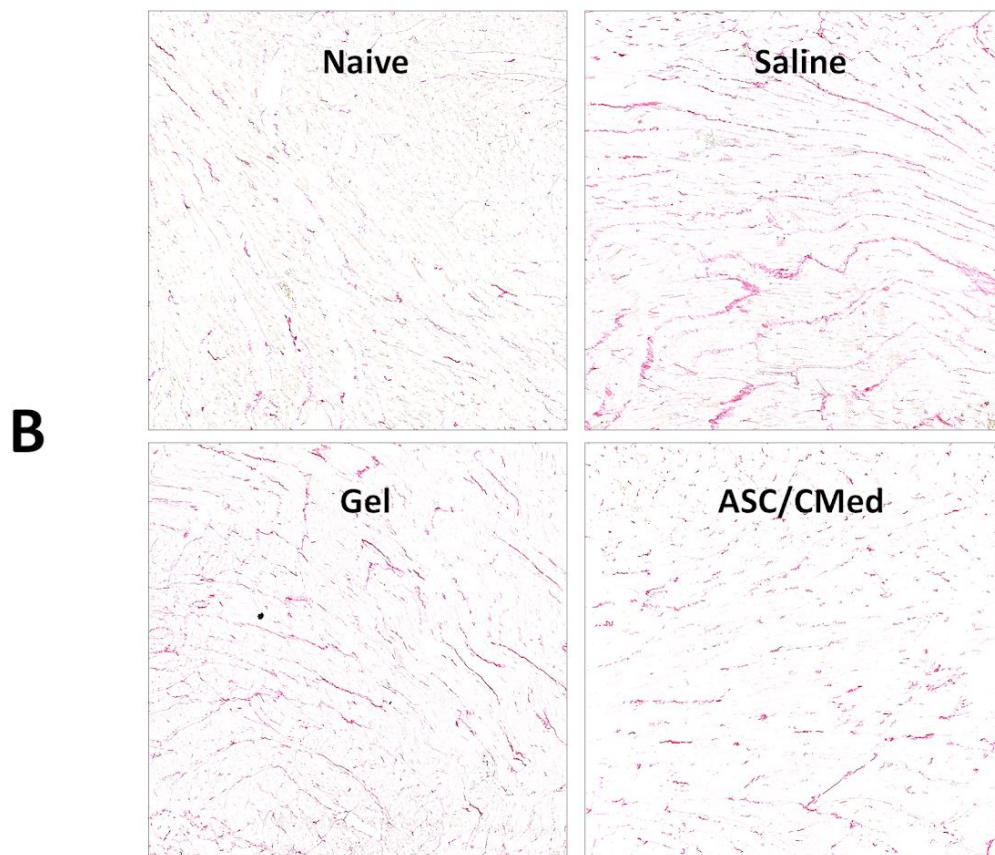
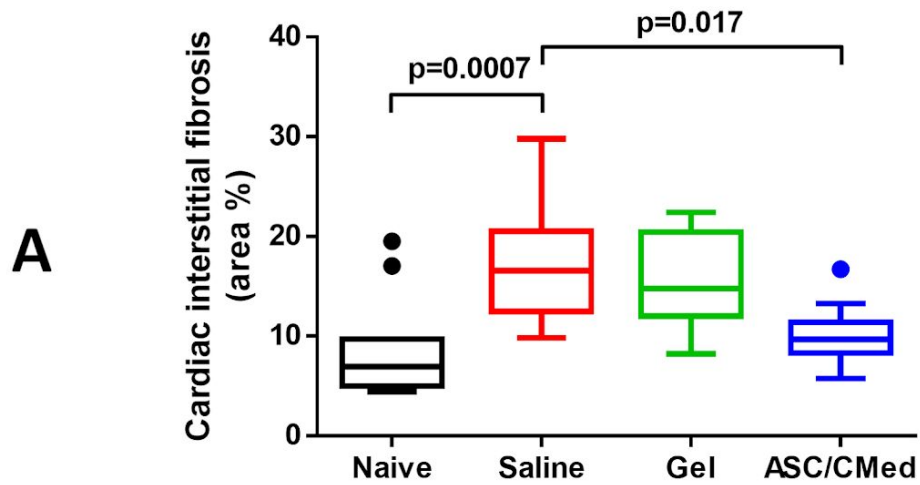


Figure 5. Cardiac interstitial fibrosis. A) Quantification of collagen area fraction (%). Numbers analysed: naive, n=6; saline, n=6; gel, n=5; ASC/CMed, n=6. P-value for Dunnett's multiple comparisons test vs. saline group. **B) Representative images of Picrosirius red staining.**

ASC/CMed-loaded dECM hydrogel prevents cardiac remodeling

Cardiac remodeling was evaluated according to the morphometric analysis of the left ventricular chamber. Animals that had induced cardiomyopathy and were treated with saline solution had an increased left ventricular chamber area by the end of the 10-weeks (Kruskal-Wallis, $p=0.0178$; Dunn's multiple comparisons test, $p=0.0262$) (Figure 6). Treatment with hydrogel only did not influence cardiac remodeling, but treatment with ASC/CMed-loaded hydrogel, virtually normalized chamber size as compared to the naive control, demonstrating the treatment prevented cardiac remodeling compared to the saline group (Kruskal-Wallis, $p=0.0178$; Dunn's multiple comparisons test, $p=0.03$).

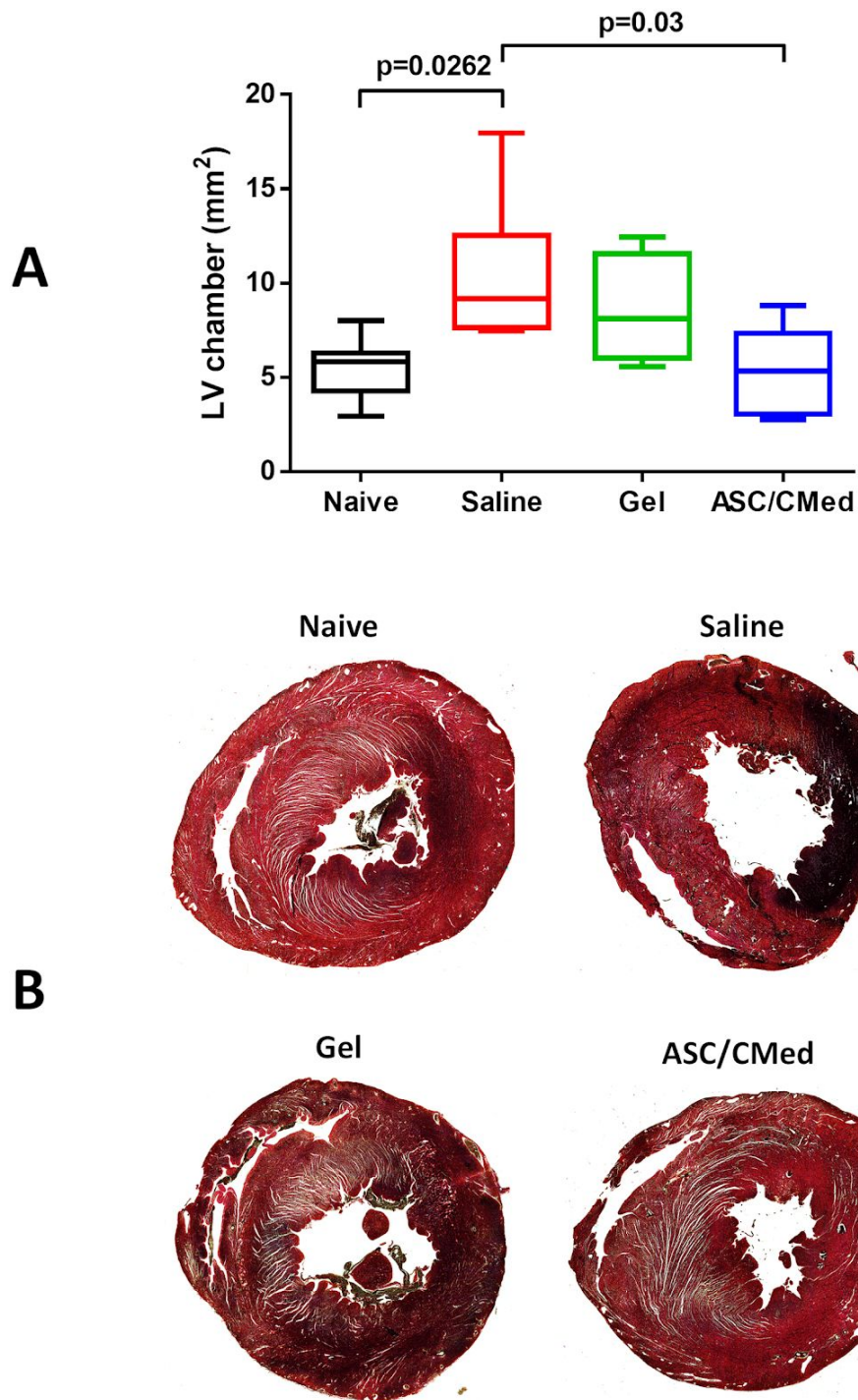


Figure 6. Cardiac remodeling. A) Area of the left ventricle chamber. P-value for Dunnett's multiple comparisons test vs. saline group. Numbers analysed: naive, n=6; saline, n=6; gel, n=5; ASC/CMed, n=6. B) Representative images of the cross-sectioned hearts stained with Movat's stain.

ASC/CMed-loaded dECM hydrogel does not affect myocardial apoptosis, mitophagy, and autophagy

The expression of the apoptosis marker, cleaved caspase-3, was low in all groups (Figure 7). Hydrogel only-injected rats had increased caspase-3 (Kruskal-Wallis, $p=0.028$; Dunn's multiple comparisons test, $p=0.04$). Rats treated ASC/Cmed-loaded hydrogels had a low expression of caspase-3 similarly as their naïve controls. This was corroborated by increased expression of the anti-apoptotic marker BCL2 in rats treated with ASC/Cmed-loaded hydrogels as compared to naïve controls. This did not reach significance due to the variation in the control group. Saline and hydrogel only-treated rats showed low BCL2 expression.

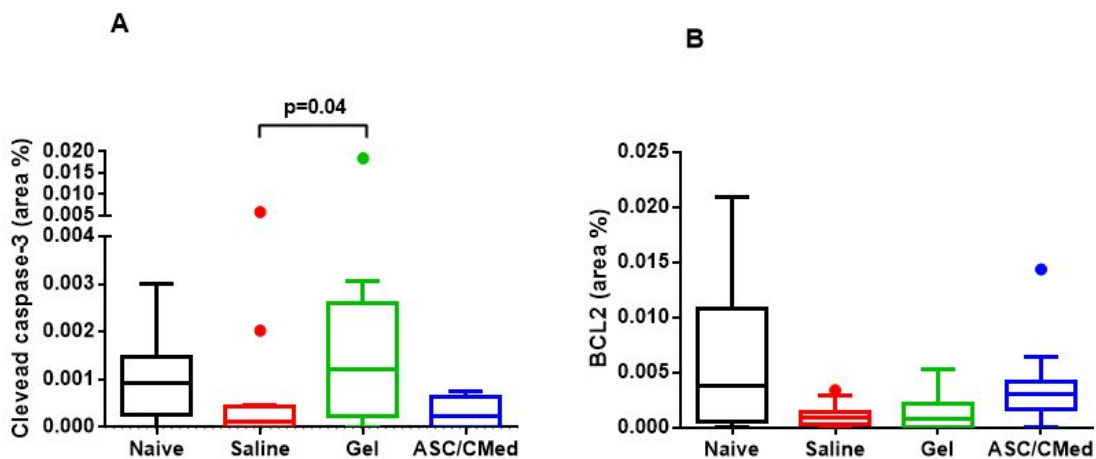


Figure 7. Apoptosis. A) Quantification of cleaved caspase-3 expression (area %). Numbers analysed: naive, n=6; saline, n=6; gel, n=5; ASC/CMed, n=6. B) Quantification of BCL2 expression (area %). Numbers analysed: naive, n=6; saline, n=6; gel, n=5; ASC/CMed, n=6. P-value for Dunnett's multiple comparisons test vs. saline group.

Mitophagy and autophagy markers, PINK1 and ULK1, respectively, did not evidence any influence from the ASC/CM treatment (Figure 8). Mitophagy was curiously increased in naive animals, compared to the saline group (Kruskal-Wallis, $p=0.046$; Dunn's multiple comparisons test, $p=0.036$). Autophagy, in turn, was increased in animals treated with hydrogel injection only, compared to the saline group (Kruskal-Wallis, $p=0.036$; Dunn's multiple comparisons test, $p=0.012$), but not in the other groups.

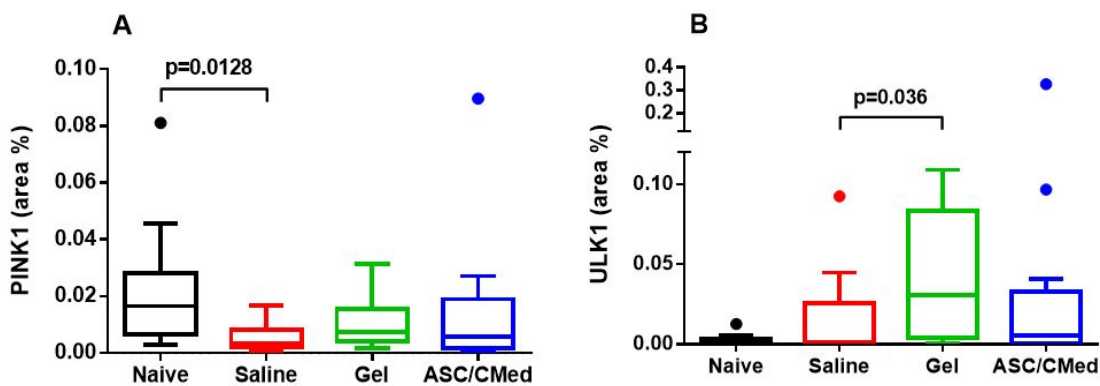


Figure 8. Mitophagy and autophagy. A) Quantification mitophagy by the expression of PINK1 marker (area %). Numbers analysed: naive, n=6; saline, n=6; gel, n=5; ASC/CMed, n=6. B) Quantification autophagy by the expression of ULK1 marker (area %). Numbers analysed: naive, n=6; saline, n=6; gel, n=5; ASC/CMed, n=6. P-value for Dunnett's multiple comparisons test vs. saline group.

Rare macrophages were found in the myocardium of a few animals. In the naive group, 17% (1/6) of the animals presented at least one focus of macrophage invasion in the myocardial tissue, while in the saline-treated animals, this percentage

was 20% (1/5). For both the groups treated with dECM hydrogel solely or dECM hydrogel loaded with ASC/ASC-CMed, the percentage of hearts presenting macrophages was 40% (2/5). Still, these differences were not statistically significant (Chi-square test, $p=0.7442$). For all the groups, even when present, macrophage density was negligible. In the pericardial tissue, however, macrophage invasion was more pronounced and differed substantially between the groups with and without the hydrogel (Figure 9). While in the naïve and saline groups the percentage of hearts presenting macrophage invasion in the pericardium was 0% (0/6) and 20% (1/5), respectively, in the groups treated with hydrogel solely and hydrogel loaded with ASC/ASC-CMed, this percentage was 60% (3/5) and 80% (4/5), respectively (Chi-square test, $p=0.0277$). There was a higher amount of ED1-expressing cells in the hydrogel containing ASC and trophic factors compared to the hydrogel alone. Interestingly, in the group injected with the hydrogel solely, other non-ED1-expressing cells migrated and could be found in the injected material.

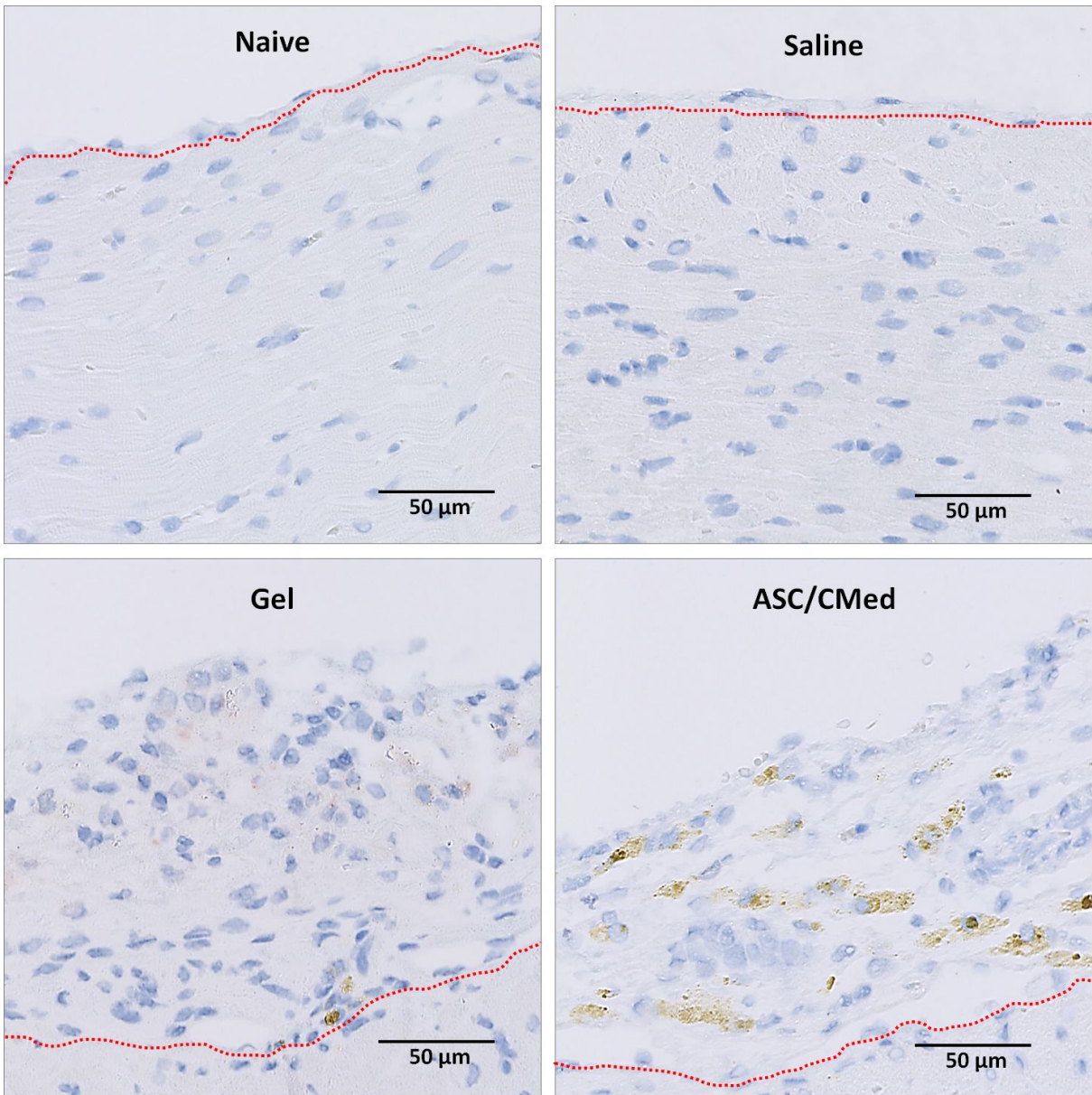


Figure 9. Representative images of the pericardial region of hearts stained with ED1 (macrophage) marker. Macrophages are shown in light brown. The red dotted line represents the transition between the myocardial and pericardial layers.

DISCUSSION

In the present study, we demonstrate that the intrapericardial injection of decellularized extracellular matrix-based hydrogels loaded with adipose tissue-derived stromal cells and their secretome is a feasible and successful approach to intervene in ongoing doxorubicin-induced dilated cardiomyopathy. Our primary readout was cardiac function, which was close to normal after treatment with the ASC/CMed-loaded hydrogels. This was likely the result of blocking ongoing fibrotic challenges of the heart with doxorubicin and the reversal of early fibrotic damage done after five weeks of doxorubicin treatment. The hydrogel itself, which served as a vehicle to deliver ASC and its secretome, did not affect doxorubicin-induced HF. To the best of our knowledge, our study is the first to describe the use of intrapericardial injection as a route for cell therapy in dilated cardiomyopathy.

Additionally, we described the use of extracellular matrix-based hydrogels as a platform to support the delivery of stromal cells and their secretome. These hydrogels are known for binding growth factors (40) and provide cells with all a microenvironment mimetic to the native extracellular matrix, offering biochemical and biomechanical clues capable of directing cell fate. Recently, such a hydrogel has been demonstrated to be safe to use in human patients, although it was applied intramyocardial and without cells or growth factors (41).

Although the treatment with dECM hydrogels loaded with ASC/CMed was capable of preventing cardiac dysfunction, interstitial cardiac fibrosis, and cardiac remodeling, it acted only locally, not preventing the systemic adverse effects of doxorubicin. Consequently, it was not capable of ameliorating the general health status of the animals (weight loss, ascites production, and hematological parameters), nor improve survival. These findings are in accordance with previous studies (42–44). A high dosage of doxorubicin, as used in the current study, does not affect the heart solely, but also all the other organs. Besides cardiomyopathy, doxorubicin is also known for causing chronic kidney disease and hepatotoxicity (45–48). Indeed, when animals were euthanized, the macroscopic evaluation of the abdominal organs showed kidneys and livers importantly affected, with signs of significant fibrosis. Thus, the general health status of these animals did not depend only on the status of the cardiac tissue, but of the whole organism. We believe, therefore, those animal deaths were derived from multiple organ failure, and not from a failing heart. Still, our mortality rates, even in the presence of a complex surgical procedure in the middle of the induction protocol, were lower than those reported in the literature (42,49,50).

There is no consensus in the literature, however, among the doxorubicin-based protocols for the induction of heart failure, regarding the dosage, intervention moment and the type and amount of cells used to treat the disease (51). Cumulative doxorubicin dosage, which varies from 5mg/kg to 40mg/kg depending on the protocol, can be administered as a single injection or divided in three, six, or even nine separate applications. Stem cells, conditioned medium, cardiospheres or

exosomes injection have been applied at different moments in diverse protocols (before, during, and after induction). The number of cells administered in order to treat the disease varied from 2×10^5 cells/mL to 5×10^7 cells/mL with most of the studies describing a concentration of $1-2 \times 10^6$ cells/mL. In the present study, we used 2×10^7 cells/mL, meaning it was one of the studies with the highest cell density in the literature. The type of cell used for cell therapy also varied among the studies, although the most prevalent was bone marrow mesenchymal stromal cells. All these variations make it difficult to compare the findings between the studies and also with our study. Still, in all studies, some degree of improvement in cardiac function, compared to control animals, was reported (52–71). Most studies also reported a decrease in myocardial fibrosis, although three studies reported increased fibrosis, even in the presence of an improved cardiac function (51,54,71). In the present study, we reported both the avoidance of cardiac dysfunction and interstitial fibrosis, but also the prevention of cardiac remodeling.

We demonstrated that death-related mechanisms such as apoptosis, mitophagy, and autophagy were not grossly affected by ASC/CMed-loaded hydrogels at the 10th week of treatment. At this time point, the death-related readouts showed virtually no difference, which does not preclude the influence of our intervention at an earlier stage. Such death-related mechanisms do not have a clearly defined time to be accessed (72). Possibly they are more evident in the early development of the cardiac disease. In order to investigate apoptosis, autophagy, and mitophagy, the main mechanisms described for the doxorubicin-induced DCM (73), we analyzed the markers cleaved caspase-3, BCL2, PINK1, and ULK1.

Cleaved caspase-3 is a marker for apoptosis which can be upregulated during the progression of severe heart failure (35,74)(70)(75). In the present study, cleaved caspase-3 was similarly expressed by naive animals and animals with induced cardiomyopathy and saline treatment, suggesting apoptosis was not occurring at critical levels anymore. BCL2, in turn, which is an anti-apoptotic marker commonly used to clarify the modulation of apoptosis mechanisms, also did not present important differences among the groups of the present study. The literature is not consistent regarding the findings involving BCL2, with manuscripts describing both increase (76–78) and decrease (74,79,80) of the marker in subjects suffering from dilated cardiomyopathy.

Mitophagy and autophagy also could not be identified as the key mechanisms involved in the disease and the consequent prevention of the same. We evaluated mitophagy with the PINK1, a kinase responsible for regulating the energy production by the mitochondria in healthy and diseased hearts through mitophagy, representing a protective mechanism to the tissue (81,82) (83). Animal models and patient studies of ischemic heart disease showed downregulation in the protein expression of PINK1 on chronic stimulated non-treated animals and patients (84–86). The opposite, however, was described for dilated cardiomyopathy animal models (87). In our study, PINK1 expression was reduced in animals with induced dilated cardiomyopathy and treated with saline solution, when compared with naive animals, contradicting the findings described in the literature for this type of cardiomyopathy and coinciding with the findings described for ischemic heart disease. Still, none of the proposed treatments, neither the hydrogel solely nor the ASC/CMed-loaded hydrogels, could

reverse the downregulation of PINK1. Autophagy was investigated with ULK1 and here, again, we could not find differences between naive animals and animals with induced cardiomyopathy treated with saline solution, suggesting that this process is not occurring at a critical level at this point.

Another important mechanism involved in cardiac regeneration is immunomodulation (88). CD68⁺ (ED1) cells are a heterogeneous population composed of both CCR2⁻ subtype macrophages, which is involved in cardiac regeneration, and CCR2⁺ subtype macrophages, which are involved in inflammation and fibrosis (89–91). A small amount of CCR2⁺ macrophages is known to be associated with the increase of ventricular function in patients and mice (90,91). Intramyocardial injection of stem cells in a rat model of ischemia-reperfusion injury is described to induce a local influx of CCR2⁺ macrophages, which is lately responsible for the improvement of cardiac function (92). Although the present work demonstrated that the ASC/CMed group led to a considerable influx of CD68⁺ towards the injected hydrogel, we could only find a negligible amount of macrophages in the myocardial tissue. If the macrophages were, by any means, linked to the improvement in cardiac function, this effect should be attributed to paracrine mechanisms from those present in the pericardial tissue.

Irrespective of which mechanisms were involved in the improvement of heart morphological and hemodynamic parameters, herein, we demonstrated a new alternative for cardiovascular cell therapy, which demonstrates substantial advantages in comparison to the conventional intramyocardial approach. Differently

from the techniques which apply stem/stromal cells by myocardial injection, accompanied or not by a hydrogel vehicle, our approach does not lead to myocardial injury, inflammation, and arrhythmias (93). We also did not see any signs of pericarditis or cardiac tamponade, which could be expected for this intervention. Another advantage of our approach is the possibility to efficiently deliver and retain stromal cells acting on the degenerated organ. In the conventional myocardial injection technique, cells tend to migrate out of the injured tissue, reducing the efficacy of the treatment and requiring new interventions (10,94). Our approach was capable of keeping cells surrounding the heart for five weeks, but this time could be even longer if the animals were not euthanized at this time point. Moreover, the pericardial route is particularly interesting for dilated, multi-chambered, cardiomyopathies considering the injection of cells into the pericardial space allows reaching the whole heart. Besides that, once the technique could be applied in humans using minimally invasive approaches, if new interventions were necessary, they would be feasible and much less traumatic than the intramyocardial injections.

CONCLUSION

The intrapericardial injection of decellularized extracellular matrix-based hydrogels loaded with adipose tissue-derived stromal cells and their secretome warrant a feasible and successful novel approach to treat dilated cardiomyopathy in doxorubicin-induced animal models. This therapeutic alternative was capable of preventing cardiac dysfunction, interstitial cardiac fibrosis, cardiac remodeling.

PROTOCOL REGISTRATION AND DATA ACCESS

A complete protocol, including the research question, animal experiment plan, as well as the analysis plan, was prepared before the study and is available, together with the data from the study, under request.

FUNDING AND CONFLICTS OF INTEREST

This study was partly financed by the Coordenação de Aperfeiçoamento de Pessoal de Nível Superior – Brasil (CAPES) – Finance Code 001 and National Council for Scientific and Technological Development (CNPQ).

The authors declare no conflict of interest.

ACKNOWLEDGMENTS

The authors would like to express their very high appreciation for the assistance provided by Linda Brouwer for performing ED1 immunohistochemistry staining and microphotography.

REFERENCES

1. Bui AL, Horwich TB, Fonarow GC. Epidemiology and risk profile of heart failure. *Nat Rev Cardiol.* 2010;8(1):30–41.
2. Benjamin EJ, Blaha MJ, Chiuve SE, Cushman M, Das SR, Deo R, et al. Heart

Disease and Stroke Statistics-2017 Update: A Report From the American Heart Association. *Circulation*. 2017 Mar 7;135(10):e146–603.

3. Masarone D, Kaski JP, Pacileo G, Elliott PM, Bossone E, Day SM, et al. Epidemiology and Clinical Aspects of Genetic Cardiomyopathies. *Heart Fail Clin*. 2018 Apr;14(2):119–28.
4. Houser SR, Margulies KB, Murphy AM, Spinale FG, Francis GS, Prabhu SD, et al. Animal models of heart failure: a scientific statement from the American Heart Association. *Circ Res*. 2012 Jun 22;111(1):131–50.
5. Riehle C, Bauersachs J. Small animal models of heart failure. *Cardiovasc Res*. 2019 Nov 1;115(13):1838–49.
6. Yeh ETH, Tong AT, Lenihan DJ, Yusuf SW, Swafford J, Champion C, et al. Cardiovascular complications of cancer therapy: diagnosis, pathogenesis, and management. *Circulation*. 2004 Jun 29;109(25):3122–31.
7. Yeh ETH, Bickford CL. Cardiovascular complications of cancer therapy: incidence, pathogenesis, diagnosis, and management. *J Am Coll Cardiol*. 2009 Jun 16;53(24):2231–47.
8. Felker GM, Thompson RE, Hare JM, Hruban RH, Clemetson DE, Howard DL, et al. Underlying causes and long-term survival in patients with initially unexplained cardiomyopathy. *N Engl J Med*. 2000 Apr 13;342(15):1077–84.
9. Farhad H, Staziaki PV, Addison D, Coelho-Filho OR, Shah RV, Mitchell RN, et al. Characterization of the Changes in Cardiac Structure and Function in Mice Treated With Anthracyclines Using Serial Cardiac Magnetic Resonance Imaging. *Circ Cardiovasc Imaging* [Internet]. 2016 Dec;9(12). Available from: <http://dx.doi.org/10.1161/CIRCIMAGING.115.003584>
10. Tompkins BA, Balkan W, Winkler J, Gyöngyösi M, Goliash G, Fernández-Avilés F, et al. Preclinical Studies of Stem Cell Therapy for Heart Disease. *Circ Res*. 2018 Mar 30;122(7):1006–20.
11. Tompkins BA, Balkan W, Winkler J, Gyöngyösi M, Goliash G, Fernández-Avilés F, et al. Preclinical Studies of Stem Cell Therapy for Heart Disease. *Circ Res*. 2018 Mar 30;122(7):1006–20.
12. Saludas L, Pascual-Gil S, Prósper F, Garbayo E, Blanco-Prieto M. Hydrogel based approaches for cardiac tissue engineering. *Int J Pharm*. 2017 May 25;523(2):454–75.
13. O'Neill HS, Gallagher LB, O'Sullivan J, Whyte W, Curley C, Dolan E, et al. Biomaterial-Enhanced Cell and Drug Delivery: Lessons Learned in the Cardiac Field and Future Perspectives. *Adv Mater*. 2016 Jul;28(27):5648–61.
14. Banovic M, Pusnik-Vrckovnik M, Nakou E, Vardas P. Myocardial regeneration therapy in heart failure: Current status and future therapeutic implications in

- clinical practice. *Int J Cardiol.* 2018 Jun 1;260:124–30.
15. Costantino S, Paneni F. Stem cell therapy in heart failure: Is the best yet to come? *Int J Cardiol.* 2018 Jun 1;260:135–6.
 16. Poglajen G, Zemljič G, Frljak S, Cerar A, Andročec V, Sever M, et al. Stem Cell Therapy in Patients with Chronic Nonischemic Heart Failure. *Stem Cells Int.* 2018 Jan 18;2018:6487812.
 17. Wang Z, Lee SJ, Cheng H-J, Yoo JJ, Atala A. 3D bioprinted functional and contractile cardiac tissue constructs. *Acta Biomater.* 2018 Apr 1;70:48–56.
 18. Sarig U, Machluf M. Engineering cell platforms for myocardial regeneration. *Expert Opin Biol Ther.* 2011 Aug;11(8):1055–77.
 19. Branco É, Fioretto ET, Cabral R, Palmera CAS, Gregores GB, Stopiglia AJ, et al. Homing miocárdico após infusão intrapericárdica de Células Mononucleares de Medula Óssea. *Arq Bras Cardiol.* 2009 Sep;93(3):e50–3.
 20. Fromes Y, Salmon A, Wang X, Collin H, Rouche A, Hagège A, et al. Gene delivery to the myocardium by intrapericardial injection. *Gene Ther.* 1999 Apr;6(4):683–8.
 21. Kunitoh H, Tamura T, Shibata T, Imai M, Nishiwaki Y, Nishio M, et al. A randomised trial of intrapericardial bleomycin for malignant pericardial effusion with lung cancer (JCOG9811). *Br J Cancer.* 2009 Feb 10;100(3):464–9.
 22. Aijaz T, Kattoor A, Behnamfar O, Shami S, Sawaqed R, Doukky R, et al. UNCOMMON APPROACH TO UNUSUAL CASE OF PURULENT PERICARDITIS. *J Am Coll Cardiol.* 2019 Mar;73(9):2271.
 23. Blázquez R, Sánchez-Margallo FM, Crisóstomo V, Báez C, Maestre J, García-Lindo M, et al. Intrapericardial administration of mesenchymal stem cells in a large animal model: a bio-distribution analysis. *PLoS One.* 2015 Mar 27;10(3):e0122377.
 24. Blázquez R, Sánchez-Margallo FM, Crisóstomo V, Báez C, Maestre J, Álvarez V, et al. Intrapericardial Delivery of Cardiosphere-Derived Cells: An Immunological Study in a Clinically Relevant Large Animal Model. *PLoS One.* 2016 Feb 11;11(2):e0149001.
 25. Zhang J, Wu Z, Fan Z, Qin Z, Wang Y, Chen J, et al. Pericardial application as a new route for implanting stem-cell cardiospheres to treat myocardial infarction. *J Physiol.* 2018 Jun;596(11):2037–54.
 26. Marques RG, Morales MM, Petroianu A. Brazilian law for scientific use of animals. *Acta Cir Bras.* 2009 Jan;24(1):69–74.
 27. Goldenberg S. Ethical aspects when using animals in research. *Braz Oral Res* [Internet]. 2005 Mar;19(1). Available from: http://www.scielo.br/scielo.php?script=sci_arttext&pid=S1806-83242005000100

001&lng=en&tlng=en

28. de A e Tréz T. Refining animal experiments: the first Brazilian regulation on animal experimentation. *Altern Lab Anim.* 2010 Jun;38(3):239–44.
29. Haahr M. RANDOM.ORG - List Randomizer [Internet]. [cited 2019 Oct 21]. Available from: www.random.org/lists/
30. Liguori TTA, Liguori GR, Moreira LFP, Harmsen MC. Adipose tissue-derived stromal cells' conditioned medium modulates endothelial-mesenchymal transition induced by IL-1 β /TGF- β 2 but does not restore endothelial function. *Cell Prolif.* 2019 Aug 29;e12629.
31. Liguori TTA, Liguori GR, Moreira LFP, Harmsen MC. Fibroblast growth factor-2, but not the adipose tissue-derived stromal cells secretome, inhibits TGF- β 1-induced differentiation of human cardiac fibroblasts into myofibroblasts. *Sci Rep.* 2018 Nov 9;8(1):16633.
32. Liguori GR, Zhou Q, Liguori TTA, Barros GG, Kühn PT, Moreira LFP, et al. Directional Topography Influences Adipose Mesenchymal Stromal Cell Plasticity: Prospects for Tissue Engineering and Fibrosis. *Stem Cells Int.* 2019 May 5;2019:5387850.
33. Faul F, Erdfelder E, Lang A-G, Buchner A. G*Power 3: a flexible statistical power analysis program for the social, behavioral, and biomedical sciences. *Behav Res Methods.* 2007 May;39(2):175–91.
34. Faul F, Erdfelder E, Buchner A, Lang A-G. Statistical power analyses using G*Power 3.1: tests for correlation and regression analyses. *Behav Res Methods.* 2009 Nov;41(4):1149–60.
35. Coutinho e Silva R dos S, Zanoni FL, Simas R, Fernandes Martins da Silva MH, Junior RA, de Jesus Correia C, et al. Effect of bilateral sympathectomy in a rat model of dilated cardiomyopathy induced by doxorubicin. *J Thorac Cardiovasc Surg* [Internet]. 2019 Sep; Available from: <https://linkinghub.elsevier.com/retrieve/pii/S002252231932015X>
36. Dove SB, McDavid WD, Welander U, Tronje G, Wilcox CD. Design and implementation of an image management and communications system (IMACS) for dentomaxillofacial radiology. *Dentomaxillofac Radiol.* 1992 Nov;21(4):216–21.
37. ImageTool. Get the software safe and easy [Internet]. *Software Informer.* [cited 2020 Apr 15]. Available from: <https://imagetool.software.informer.com/3.0/>
38. Liguori GR, Jatene MB, Ho SY, Aiello VD. Morphological variability of the arterial valve in common arterial trunk and the concept of normality. *Heart.* 2017 Jun;103(11):848–55.
39. Ye G-L, Chen Q, Chen X, Liu Y-Y, Yin T-T, Meng Q-H, et al. The prognostic role

- of platelet-to-lymphocyte ratio in patients with acute heart failure: A cohort study. *Sci Rep*. 2019 Jul 23;9(1):10639.
40. van Dongen JA, Getova V, Brouwer LA, Liguori GR, Sharma PK, Stevens HP, et al. Adipose tissue-derived extracellular matrix hydrogels as a release platform for secreted paracrine factors. *J Tissue Eng Regen Med*. 2019 Jun;13(6):973–85.
 41. Traverse JH, Henry TD, Dib N, Patel AN, Pepine C, Schaer GL, et al. First-in-Man Study of a Cardiac Extracellular Matrix Hydrogel in Early and Late Myocardial Infarction Patients [Internet]. Vol. 4, *JACC: Basic to Translational Science*. 2019. p. 659–69. Available from: <http://dx.doi.org/10.1016/j.jacbts.2019.07.012>
 42. O'Connell JL, Romano MMD, Campos Pulici EC, Carvalho EEV, de Souza FR, Tanaka DM, et al. Short-term and long-term models of doxorubicin-induced cardiomyopathy in rats: A comparison of functional and histopathological changes. *Exp Toxicol Pathol*. 2017 Apr 4;69(4):213–9.
 43. Anjos Ferreira AL, Russell RM, Rocha N, Placido Ladeira MS, Favero Salvadori DM, Oliveira Nascimento MCM, et al. Effect of lycopene on doxorubicin-induced cardiotoxicity: an echocardiographic, histological and morphometrical assessment. *Basic Clin Pharmacol Toxicol*. 2007 Jul;101(1):16–24.
 44. Siveski-Iliskovic N, Kaul N, Singal PK. Probucol promotes endogenous antioxidants and provides protection against adriamycin-induced cardiomyopathy in rats. *Circulation*. 1994 Jun;89(6):2829–35.
 45. Octavia Y, Tocchetti CG, Gabrielson KL, Janssens S, Crijns HJ, Moens AL. Doxorubicin-induced cardiomyopathy: from molecular mechanisms to therapeutic strategies. *J Mol Cell Cardiol*. 2012 Jun;52(6):1213–25.
 46. Mansouri E, Jangaran A, Ashtari A. Protective effect of pravastatin on doxorubicin-induced hepatotoxicity. *Bratisl Lek Listy*. 2017;118(5):273–7.
 47. Ding Z-H, Xu L-M, Wang S-Z, Kou J-Q, Xu Y-L, Chen C-X, et al. Ameliorating Adriamycin-Induced Chronic Kidney Disease in Rats by Orally Administrated Cardiotoxin from *Naja naja atra* Venom. *Evid Based Complement Alternat Med*. 2014 Apr 30;2014:621756.
 48. Jačević V, Dragojević-Simić V, Tatomirović Ž, Dobrić S, Bokonjić D, Kovačević A, et al. The Efficacy of Amifostine against Multiple-Dose Doxorubicin-Induced Toxicity in Rats. *Int J Mol Sci* [Internet]. 2018 Aug 12;19(8). Available from: <http://dx.doi.org/10.3390/ijms19082370>
 49. Schwarz E. A small animal model of non-ischemic cardiomyopathy and its evaluation by transthoracic echocardiography. *Cardiovasc Res*. 1998 Jul 1;39(1):216–23.
 50. Gava FN, Zacché E, Ortiz EMG, Champion T, Bandarra MB, Vasconcelos RO,

- et al. Doxorubicin induced dilated cardiomyopathy in a rabbit model: an update. *Res Vet Sci*. 2013 Feb;94(1):115–21.
51. Abushouk AI, Salem AMA, Saad A, Afifi AM, Afify AY, Afify H, et al. Mesenchymal Stem Cell Therapy for Doxorubicin-Induced Cardiomyopathy: Potential Mechanisms, Governing Factors, and Implications of the Heart Stem Cell Debate. *Front Pharmacol*. 2019 Jun 14;10:635.
 52. Yu Q, Li Q, Na R, Li X, Liu B, Meng L, et al. Impact of repeated intravenous bone marrow mesenchymal stem cells infusion on myocardial collagen network remodeling in a rat model of doxorubicin-induced dilated cardiomyopathy. *Mol Cell Biochem*. 2014 Feb;387(1-2):279–85.
 53. Abd Allah SH, Hussein S, Hasan MM, Deraz RHA, Hussein WF, Sabik LME. Functional and Structural Assessment of the Effect of Human Umbilical Cord Blood Mesenchymal Stem Cells in Doxorubicin-Induced Cardiotoxicity. *J Cell Biochem*. 2017 Oct;118(10):3119–29.
 54. A Soliman N, Abd-Allah SH, Hussein S, Alaa Eldeen M. Factors enhancing the migration and the homing of mesenchymal stem cells in experimentally induced cardiotoxicity in rats. *IUBMB Life*. 2017 Mar;69(3):162–9.
 55. Garbade J, Dhein S, Lipinski C, Aupperle H, Arsalan M, Borger MA, et al. Bone marrow-derived stem cells attenuate impaired contractility and enhance capillary density in a rabbit model of Doxorubicin-induced failing hearts. *J Card Surg*. 2009 Sep;24(5):591–9.
 56. Li L, Xia Y. Study of adipose tissue-derived mesenchymal stem cells transplantation for rats with dilated cardiomyopathy. *Ann Thorac Cardiovasc Surg*. 2014 Feb 4;20(5):398–406.
 57. Mao C, Hou X, Wang B, Chi J, Jiang Y, Zhang C, et al. Intramuscular injection of human umbilical cord-derived mesenchymal stem cells improves cardiac function in dilated cardiomyopathy rats. *Stem Cell Res Ther*. 2017 Jan 28;8(1):18.
 58. Singla DK, Ahmed A, Singla R, Yan B. Embryonic stem cells improve cardiac function in Doxorubicin-induced cardiomyopathy mediated through multiple mechanisms. *Cell Transplant*. 2012 Mar 22;21(9):1919–30.
 59. Aupperle H, Garbade J, Schubert A, Barten M, Dhein S, Schoon H-A, et al. Effects of autologous stem cells on immunohistochemical patterns and gene expression of metalloproteinases and their tissue inhibitors in doxorubicin cardiomyopathy in a rabbit model. *Vet Pathol*. 2007 Jul;44(4):494–503.
 60. Dhein S, Garbade J, Rouabah D, Abraham G, Ungemach F-R, Schneider K, et al. Effects of autologous bone marrow stem cell transplantation on beta-adrenoceptor density and electrical activation pattern in a rabbit model of non-ischemic heart failure. *J Cardiothorac Surg*. 2006 Jun 26;1:17.

61. Vandergriff AC, de Andrade JBM, Tang J, Hensley MT, Piedrahita JA, Caranasos TG, et al. Intravenous Cardiac Stem Cell-Derived Exosomes Ameliorate Cardiac Dysfunction in Doxorubicin Induced Dilated Cardiomyopathy. *Stem Cells Int.* 2015 Aug 17;2015:960926.
62. Abe J, Yamada Y, Takeda A, Harashima H. Cardiac progenitor cells activated by mitochondrial delivery of resveratrol enhance the survival of a doxorubicin-induced cardiomyopathy mouse model via the mitochondrial activation of a damaged myocardium. *J Control Release.* 2018 Jan 10;269:177–88.
63. Ammar HI, Sequiera GL, Nashed MB, Ammar RI, Gabr HM, Elsayed HE, et al. Comparison of adipose tissue- and bone marrow- derived mesenchymal stem cells for alleviating doxorubicin-induced cardiac dysfunction in diabetic rats. *Stem Cell Res Ther.* 2015 Aug 22;6:148.
64. Deng B, Wang JX, Hu XX, Duan P, Wang L, Li Y, et al. Nkx2.5 enhances the efficacy of mesenchymal stem cells transplantation in treatment heart failure in rats. *Life Sci.* 2017 Aug 1;182:65–72.
65. Hensley MT, de Andrade J, Keene B, Meurs K, Tang J, Wang Z, et al. Cardiac regenerative potential of cardiosphere-derived cells from adult dog hearts. *J Cell Mol Med.* 2015 Aug;19(8):1805–13.
66. Aminzadeh MA, Tseliou E, Sun B, Cheng K, Malliaras K, Makkar RR, et al. Therapeutic efficacy of cardiosphere-derived cells in a transgenic mouse model of non-ischaemic dilated cardiomyopathy. *Eur Heart J.* 2015 Mar 21;36(12):751–62.
67. Guo J, Zhang H, Xiao J, Wu J, Ye Y, Li Z, et al. Monocyte chemotactic protein-1 promotes the myocardial homing of mesenchymal stem cells in dilated cardiomyopathy. *Int J Mol Sci.* 2013 Apr 15;14(4):8164–78.
68. Li T-S, Mikamo A, Takahashi M, Suzuki R, Ueda K, Ikeda Y, et al. Comparison of cell therapy and cytokine therapy for functional repair in ischemic and nonischemic heart failure. *Cell Transplant.* 2007;16(4):365–74.
69. Sun Y, Chi D, Tan M, Kang K, Zhang M, Jin X, et al. Cadaveric cardiosphere-derived cells can maintain regenerative capacity and improve the heart function of cardiomyopathy. *Cell Cycle.* 2016 May 2;15(9):1248–56.
70. Singla DK. Akt-mTOR Pathway Inhibits Apoptosis and Fibrosis in Doxorubicin-Induced Cardiotoxicity Following Embryonic Stem Cell Transplantation. *Cell Transplant.* 2015;24(6):1031–42.
71. Bhuvanlakshmi G, Arfuso F, Kumar AP, Dharmarajan A, Warriar S. Epigenetic reprogramming converts human Wharton's jelly mesenchymal stem cells into functional cardiomyocytes by differential regulation of Wnt mediators. *Stem Cell Res Ther.* 2017 Aug 14;8(1):185.

72. Marín-García J. Cell death in the pathogenesis and progression of heart failure. *Heart Fail Rev.* 2016 Mar;21(2):117–21.
73. Nebigil CG, Désaubry L. Updates in Anthracycline-Mediated Cardiotoxicity. *Front Pharmacol.* 2018 Nov 12;9:1262.
74. Guo R, Hua Y, Ren J, Bornfeldt KE, Nair S. Cardiomyocyte-specific disruption of Cathepsin K protects against doxorubicin-induced cardiotoxicity. *Cell Death Dis.* 2018 Jun 7;9(6):692.
75. Ueno M, Kakinuma Y, Yuhki K-I, Murakoshi N, Iemitsu M, Miyauchi T, et al. Doxorubicin induces apoptosis by activation of caspase-3 in cultured cardiomyocytes in vitro and rat cardiac ventricles in vivo. *J Pharmacol Sci.* 2006 Jun;101(2):151–8.
76. Latif N, Khan MA, Birks E, O'Farrell A, Westbrook J, Dunn MJ, et al. Upregulation of the Bcl-2 family of proteins in end stage heart failure. *J Am Coll Cardiol.* 2000 Jun;35(7):1769–77.
77. Zhao J, Yin M, Deng H, Jin FQ, Xu S, Lu Y, et al. Cardiac Gab1 deletion leads to dilated cardiomyopathy associated with mitochondrial damage and cardiomyocyte apoptosis. *Cell Death Differ.* 2016 Apr;23(4):695–706.
78. Wang Y, Li M, Xu L, Liu J, Wang D, Li Q, et al. Expression of Bcl-2 and microRNAs in cardiac tissues of patients with dilated cardiomyopathy. *Mol Med Rep.* 2017 Jan;15(1):359–65.
79. Lu P-P, Ma J, Liang X-P, Guo C-X, Yang Y-K, Yang K-Q, et al. Xinfuli improves cardiac function, histopathological changes and attenuate cardiomyocyte apoptosis in rats with doxorubicin-induced cardiotoxicity. *J Geriatr Cardiol.* 2016 Dec;13(12):968–72.
80. Hong YM, Lee H, Cho M-S, Kim KC. Apoptosis and remodeling in adriamycin-induced cardiomyopathy rat model. *Korean J Pediatr.* 2017 Nov;60(11):365–72.
81. Zhou B, Tian R. Mitochondrial dysfunction in pathophysiology of heart failure. *J Clin Invest.* 2018 Aug 31;128(9):3716–26.
82. Shires SE, Gustafsson ÅB. Regulating Renewable Energy: Connecting AMPK α 2 to PINK1/Parkin-Mediated Mitophagy in the Heart. *Circ Res.* 2018 Mar 2;122(5):649–51.
83. Nah J, Miyamoto S, Sadoshima J. Mitophagy as a Protective Mechanism against Myocardial Stress. *Compr Physiol.* 2017 Sep 12;7(4):1407–24.
84. Yu Z, Chen R, Li M, Yu Y, Liang Y, Han F, et al. Mitochondrial calcium uniporter inhibition provides cardioprotection in pressure overload-induced heart failure through autophagy enhancement. *Int J Cardiol.* 2018 Nov 15;271:161–8.
85. Wang B, Nie J, Wu L, Hu Y, Wen Z, Dong L, et al. AMPK α 2 Protects Against the

Development of Heart Failure by Enhancing Mitophagy via PINK1 Phosphorylation. *Circ Res*. 2018 Mar 2;122(5):712–29.

86. Siddall HK, Yellon DM, Ong S-B, Mukherjee UA, Burke N, Hall AR, et al. Loss of PINK1 increases the heart's vulnerability to ischemia-reperfusion injury. *PLoS One*. 2013 Apr 29;8(4):e62400.
87. Marques-Aleixo I, Santos-Alves E, Torrella JR, Oliveira PJ, Magalhães J, Ascensão A. Exercise and Doxorubicin Treatment Modulate Cardiac Mitochondrial Quality Control Signaling. *Cardiovasc Toxicol*. 2018 Feb;18(1):43–55.
88. de Couto G. Macrophages in cardiac repair: Environmental cues and therapeutic strategies. *Exp Mol Med*. 2019 Dec 19;51(12):1–10.
89. Aurora AB, Porrello ER, Tan W, Mahmoud AI, Hill JA, Bassel-Duby R, et al. Macrophages are required for neonatal heart regeneration. *J Clin Invest*. 2014 Mar;124(3):1382–92.
90. Bajpai G, Schneider C, Wong N, Bredemeyer A, Hulsmans M, Nahrendorf M, et al. The human heart contains distinct macrophage subsets with divergent origins and functions. *Nat Med*. 2018 Jun 11;24(8):1234–45.
91. Lavine KJ, Epelman S, Uchida K, Weber KJ, Nichols CG, Schilling JD, et al. Distinct macrophage lineages contribute to disparate patterns of cardiac recovery and remodeling in the neonatal and adult heart. *Proc Natl Acad Sci U S A*. 2014 Nov 11;111(45):16029–34.
92. Vagnozzi RJ, Maillet M, Sargent MA, Khalil H, Johansen AKZ, Schwanekamp JA, et al. An acute immune response underlies the benefit of cardiac stem cell therapy. *Nature*. 2020 Jan;577(7790):405–9.
93. Almeida SO, Skelton RJ, Adigopula S, Ardehali R. Arrhythmia in stem cell transplantation. *Card Electrophysiol Clin*. 2015 Jun;7(2):357–70.
94. van den Akker F, Feyen DAM, van den Hoogen P, van Laake LW, van Eeuwijk ECM, Hoefler I, et al. Intramyocardial stem cell injection: go(ne) with the flow. *Eur Heart J*. 2017 Jan 14;38(3):184–6.

SUPPLEMENTARY MATERIAL

| Table S1. Hematological parameters | | | | | |
|---|-----------------|------------------------|----------------------------|-----------------------------|-----------------|
| | | Basal | 5th week | 10th week | p-value* |
| WBC (x10⁹) | saline | 10.9 (9.225-14.45) | 10.9 (5.50-14.33) | 6.60 (5.22-7.15) | - |
| | gel | 7.20 (5.90-13.30) | 12.30 (7.30-12.60) | 8.70 (7.30-10.50) | 0.9351 |
| | ASC/CMed | 10.50 (5.925-14.40) | 11.75 (7.35-16.15) | 2.55 (1.375-6.65) | 0.7024 |
| Lymph (x10⁹) | saline | 7.60 (6.70-9.775) | 4.90 (3.675-6.35) | 3.7 (2.025-5.075) | - |
| | gel | 5.20 (4.20-9.00) | 7.100 (3.80-8.30) | 2.70 (2.10-7.80) | 0.9986 |
| | ASC/CMed | 7.20 (7.00-10.30) | 5.60 (5.20-10.80) | 0.80 (0.400-2.200) | 0.9986 |
| RBC (x10¹²/L) | saline | 6.135 (6.078-6.598) | 8.225 (5.895-8.625) | 5.72 (3.788-7.510) | - |
| | gel | 4.73 (3.663-6.743) | 7.25 (6.583-8.510) | 4.85 (2.978-7.045) | 0.6396 |
| | ASC/CMed | 7.27 (5.87-8.34) | 8.095 (6.808-9.353) | 4.225 (3.525-6.620) | 0.8328 |
| HGB (g/L) | saline | 122 (121.3-122.8) | 150 (111.30-165.50) | 115 (75.25-141.3) | - |
| | gel | 92.0 | 133 (123.80-162.5) | 92 (56.50-133.5) | 0.4830 |

| | | | | | |
|------------------------------------|-----------------|------------------------|------------------------|------------------------|--------|
| | | (68.00-130.30) | | | |
| | ASC/CMed | 136 (103.50-151.5) | 151 (132.50-164) | 87 (78.00-122.5) | 0.9820 |
| HCT (%) | saline | 35.55 (34.55-35.88) | 43.25 (31.88-46.53) | 31.65 (21.08-38.85) | - |
| | gel | 26.60 (20.05-37.28) | 37.15 (35.25-45.28) | 28.45 (15.85-38.73) | 0.5298 |
| | ASC/CMed | 37.80 (29.30-43.15) | 43.60 (37.95-47.05) | 23.70 (21.20-33.05) | 0.9473 |
| PLT (x10⁹/L) | saline | 636 (603-671.3) | 1,059 (831.8-1201) | 1,091 (886.8-1242) | - |
| | gel | 448 (340.8-615.0) | 1112 (880.5-1295) | 1219 (993.3-15.84) | 0.9818 |
| | ASC/CMed | 511 (340.5- 801.5) | 898 (885-1076) | 1487 (293-1943) | 0.9818 |

*Two-way ANOVA with Holm-Sidak's multiple comparisons test vs. saline; WBC, white blood count; Lymph, lymphocyte; RBC, red blood count; HGB, hemoglobin; HCT, hematocrit; PLT, platelet.

CRITICAL ANALYSIS AND FUTURE PERSPECTIVES

This doctoral thesis aimed to develop a new therapeutic approach to treat dilated cardiomyopathy (DCM). By performing *in vitro* experiments, we could study mechanisms playing an important role in fibrosis. Then, we demonstrated *in vitro* the use of a decellularized extracellular matrix-based hydrogel as a platform to deliver trophic factors. Finally, we demonstrated the use of this platform to deliver adipose tissue-derived stromal cells (ASC) and their secretome as a therapeutic approach to treat dilated cardiomyopathy in a rat model.

Our three *in vitro* studies focused on the mechanisms underlying fibrosis, namely the transdifferentiation of cardiac fibroblasts to myofibroblasts and the endothelial-mesenchymal transition (EndMT). While the transdifferentiation of fibroblasts is the primary source of fibrosis in the injured heart, EndMT also plays an essential role in the process, being responsible for around 25% of the extracellular matrix deposition. For this reason, both mechanisms have been studied as potential targets to treat cardiovascular disease (1,2).

In our first study, ***Fibroblast growth factor-2, but not the adipose tissue-derived stromal cells secretome, inhibits TGF- β 1-induced differentiation of human cardiac fibroblasts into myofibroblasts*** (published in Scientific Reports), we hypothesized that considering fibroblast growth factor-2 (FGF-2) is a

growth factor secreted by ASC and capable of antagonizing TGF- β 1 signaling, the secretome of such cells would abrogate the cardiac fibroblast transdifferentiation. Our experiments demonstrated that, although FGF-2 could block TGF- β 1-induced transdifferentiation, the same was not true for ASC conditioned medium (ASC-CMed). Thus, the ASC secretome could not ameliorate the progression of fibroblast transdifferentiation *in vitro*.

Our second work, ***Adipose tissue-derived stromal cells' conditioned medium modulates endothelial-mesenchymal transition induced by IL-1 β /TGF- β 2 but does not restore endothelial function*** (published in Cell Proliferation), we turn our eyes to the second mechanism, the EndMT. We tested the hypothesis that ASC-CMed could modulate EndMT and prevents the formation of adverse myofibroblasts. This time, we could demonstrate that ASC-CMed reduces IL-1 β /TGF- β 2-induced EndMT, as observed by mesenchymal markers. These results were encouraging, even considering endothelial cells could not completely recover their function.

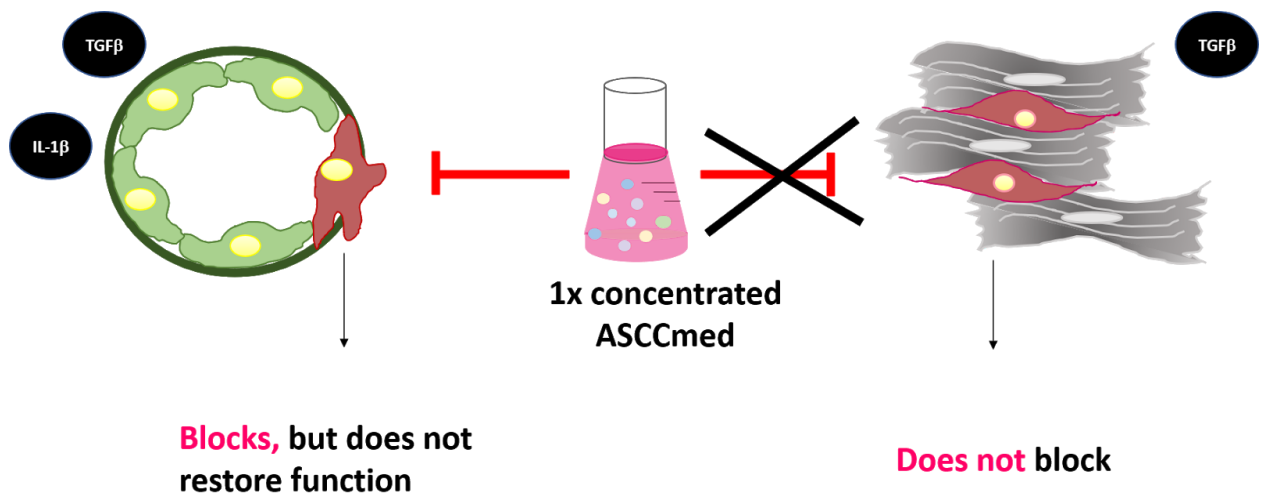


Figure 1. Schematic overview of the findings from the first two studies. ASC-CMed could block the EndMT process, but not the cardiac fibroblast transdifferentiation to myofibroblast.

The findings of our previous studies suggested that ASC-CMed indeed could exert a beneficial effect targeting at least of the mechanisms involved in cardiac fibrosis, EndMT, but that the concentration and methods of delivery should still be optimized to proceed. This brings us to our third study; ***Bioactive decellularized cardiac extracellular matrix-based hydrogel as a sustained-release platform for human adipose tissue-derived stromal cell-secreted factors*** (submitted). Considering that the administration of trophic factors (TF) secreted by ASC requires a delivery vehicle capable of binding and releasing these factors in a sustained manner, we hypothesized the use of hydrogels derived from the decellularized cardiac extracellular matrix (dECM) as such platform. Additionally, we tested the use of different concentrations (1X, 10X, and 100X) of ASC-CMed regarding the dynamics of TF release and the potential effect on EndMT. We showed that dECM hydrogels could be loaded with human ASC-secreted trophic factors, which are

released in a sustained manner for several days subsequently. Different trophic factors had different release kinetics, which correlates with the initial concentration of CMed in the hydrogel. We observed that the more concentrated was the hydrogel, the more inflammation-related cytokines, and the less pro-regenerative trophic factors were released. Finally, we showed that the factors secreted by the hydrogel were biologically active, as these influenced cell behavior, but could not block the EndMT process.

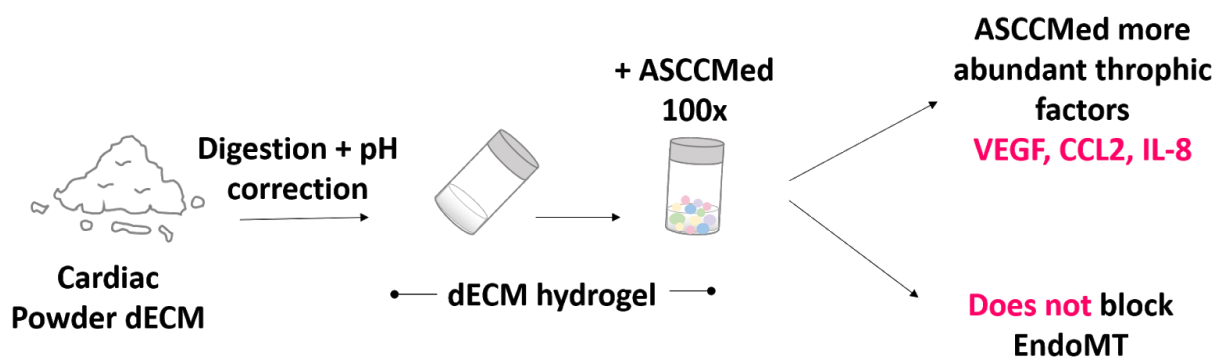


Figure 2. Schematic overview of the findings from the third study.

Aiming to investigate the findings mentioned above in a physiologically relevant model, we performed our fourth and last study, ***Intrapericardial injection of hydrogels derived from decellularized cardiac extracellular matrix loaded with mesenchymal stromal cells and their secretome: a novel therapeutic approach to treat cytostatics-induced dilated cardiomyopathy***. In our *in vivo* experiment, a rat model was used to investigate the intrapericardial injection of the previously studied platform, i.e., dECM hydrogels, this time containing both ASC and their concentrated secretome, as a therapeutic approach to dilated cardiomyopathy.

Differently from the conventional cell therapy approach, which injects stem cells directly into the myocardial tissue, we proposed to fill the intrapericardial space with the dECM hydrogel containing cells and their secretome. This new approach was proposed for two main reasons; first, it has been shown that intramyocardial injections can lead to serious adverse effects, with tissue inflammation and arrhythmias (3), besides being subjected to cell migration away from the tissue (4); second, we believe the pericardial route is particularly interesting for dilated, multi-chambered, cardiomyopathies considering the injection of cells into the pericardial space allows reaching the whole heart. Our results demonstrated that interstitial myocardial fibrosis was reduced in ASC/CMed-treated animals compared to saline controls. Ejection fraction, contractility and cardiac work efficiency were also improved in these animals. Treatment with sole dECM hydrogel did not reduce interstitial fibrosis nor improve hemodynamic parameters. We concluded that the intrapericardial injection of dECM hydrogels loaded with ASC and their secretome warrants a novel therapeutic possibility by improving ventricular hemodynamics and reducing cardiac remodeling in DCM.

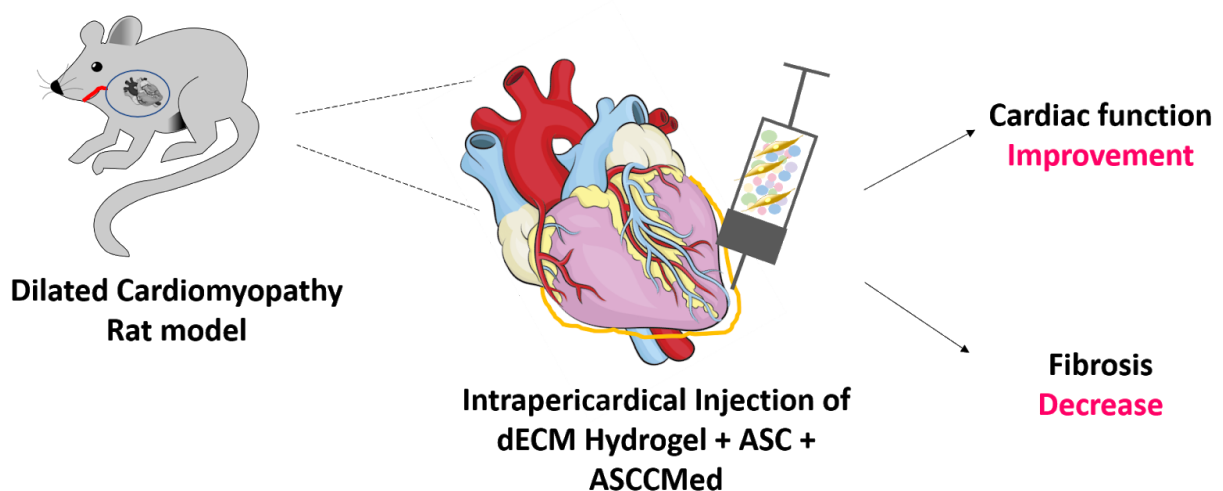


Figure 3. Schematic overview of the findings from the fourth study.

One of the most critical limitations of the present thesis is the fact that our *in vivo* experiments somehow contradict our *in vitro* findings. We demonstrated that ASC-CMed treatment could abrogate the interstitial fibrosis developed during DCM. However, the same could not be entirely supported by our experiments on the transdifferentiation of cardiac fibroblasts to myofibroblasts and the EndMT. The first mechanism showed not to be affected by our treatment, while the second could be blocked with direct exposure to ASC-CMed, but not when using the dECM hydrogel platform. *In vivo*, however, the effect of the injection of dECM hydrogels loaded with ASC and their secretome was beneficial. One can elaborate a few hypotheses on the reasons for that. Among them, it is of highest relevance: 1) the interaction with the immune system; 2) the role of ASC themselves, rather than their secretome; 3) other mechanisms not addressed by our *in vitro* work.

Concerning the first topic, the interaction with the immune system, recent studies have shown that the enhancement in cardiac function derived from a cell therapy is importantly related to the activation of immune cells, such as macrophages, which play a role in modifying ECM composition and cardiac cells activity. This process, rather than the action of stem cells themselves, results in cardiac repair (5,6). We did find macrophages in our heart samples after five weeks of ASC transplantation, but only a negligible number of them were found in the myocardial tissue. They were, however, found in a considerable amount in the pericardial tissue, inside the remaining hydrogel, for both the groups with and without cells, although more pronounced in the former. This finding may bring some

questioning on whether the macrophages themselves secrete factors that act in a paracrine manner in the cardiac tissue.

The second hypothesis that ASC themselves, rather than their secretome, play a role in cardiac regeneration, has a foundation on previous studies, which described intercellular communication as an essential effector of cell therapy beneficial effects (7). Mesenchymal stem cells, for instance, form microtubes towards cardiomyocytes (8), which is related to reduced mortality of cardiac myoblasts cultured cells (9), secretion of anti-fibrotic factors - that vary according to the distance between stem cells and native cardiac cells (10) - as well as cardiomyogenic differentiation (11,12). Besides cell-to-cell contact, it is still unclear how the transplanted cells interact with the native extracellular matrix. In our study, however, we did not find evidence, yet, that ASC had direct contact with the cardiomyocytes or even the cardiac fibroblasts and endothelial cells. During preliminary experiments, we could not find ASC inside the myocardial tissue, but further experiments are currently being performed to clarify this aspect.

Finally, regarding the mechanisms addressed during our *in vitro* studies and those present in an *in vivo* animal model, a few aspects must be highlighted. First, fibroblast transdifferentiation and EndMT, the two processes investigated *in vitro* are, indeed, related to cardiac fibrosis. It is crucial, however, to remember that uncountable other processes, ruled by several other pathways rather than the TGF β signaling, are ongoing in such a complex disease as the doxorubicin-induced dilated cardiomyopathy. Some of these mechanisms, including apoptosis, mitophagy, and

autophagy, we did address in our *in vivo* study, although not in our *in vitro* studies. Still, these mechanisms did not show any particular result, *in vivo*, suggesting they were being affected by our cell therapy approach. We must be argumentative, however, regarding the timing in which these analyses were performed. We investigated the markers caspase-3, BLC2, PINK1, and ULK1, all at the 10th week after the beginning of doxorubicin induction and 5th week after cell transplantation. Thus, it might be that they were, possibly, affected at some point between the 5th and 10th weeks. Besides the mechanisms mentioned above, doxorubicin is known to cause cardiomyopathy by several other paths, including renin-angiotensin system activation; mitochondrial dysfunction; increase of myocardial endoplasmic reticulum stress; oxidative stress by stimulation of Toll-like receptors 2, 3, and 4; inflammation through IL-1 β , IL-6, and TNF- α ; activation of poly (ADP-ribose) polymerase and ubiquitin protease system; interaction with the MAPK pathway, within others (13,14). Thus, the study of all processes involved in the disease was not feasible to address in a single thesis.

Irrespective of which mechanisms were involved in the improvement of heart morphological and hemodynamic parameters, herein, we demonstrated a new alternative for cardiovascular cell therapy, which demonstrates substantial advantages in comparison to the conventional intramyocardial approach. Our technique not only protects the heart from myocardial injury, which is followed by inflammation and arrhythmias (15), but is also capable of keeping cells surrounding the heart for long periods. When considering the clinical translation of the procedure, it is worth to mention that the pericardial route is particularly interesting for dilated,

multi-chambered, cardiomyopathies, besides allowing repeated injections by minimally invasive approaches, protecting the heart from tissue trauma.

When looking at future perspectives, we understand that, before proceeding, a few adjustments need to be made, particularly regarding the conditioned medium production. We need to understand better the specific components of mesenchymal stromal cells secretome and how the relevance of each factor varies according to the different methods of conditioned medium collection. Literature is not unanimous on how cells' secretome should be collected, with different researchers performing very diverse protocols. Some differences related to the stages of cell maturation, the amount of medium used per cm² of cell culture, the frequency of cell medium refreshment, and the time cells have to rest before another harvest cycle. In this regard, we are already performing studies to investigate what is the optimal protocol to derive the maximum concentration of anti-fibrotic and anti-inflammatory factors, while keeping the presence of inflammatory cytokines low. Once an optimized protocol is designed, the next step would be to proceed with larger animal models, such as pigs, to validate the findings of the present thesis and allow performing clinical trials.

With conviction, we believe this thesis was an essential cornerstone for the use of several innovative techniques, solely or combined, as potential approaches to target cardiac regeneration. These include, for instance, the use of dECM hydrogels as a platform for cells and trophic factors delivery and the intrapericardial route as an alternative for cardiovascular cell therapy.

REFERENCES

1. Jackson AO, Zhang J, Jiang Z, Yin K. Endothelial-to-mesenchymal transition: A novel therapeutic target for cardiovascular diseases. *Trends Cardiovasc Med*. 2017 Aug;27(6):383–93.
2. Travers JG, Kamal FA, Robbins J, Yutzey KE, Blaxall BC. Cardiac Fibrosis: The Fibroblast Awakens. *Circ Res*. 2016 Mar 18;118(6):1021–40.
3. Almeida SO, Skelton RJ, Adigopula S, Ardehali R. Arrhythmia in stem cell transplantation. *Card Electrophysiol Clin*. 2015 Jun;7(2):357–70.
4. van den Akker F, Feyen DAM, van den Hoogen P, van Laake LW, van Eeuwijk ECM, Hoefler I, et al. Intramyocardial stem cell injection: go(ne) with the flow. *Eur Heart J*. 2017 Jan 14;38(3):184–6.
5. Vagnozzi RJ, Maillet M, Sargent MA, Khalil H, Johansen AKZ, Schwanekamp JA, et al. An acute immune response underlies the benefit of cardiac stem cell therapy. *Nature*. 2020 Jan;577(7790):405–9.
6. de Couto G. Macrophages in cardiac repair: Environmental cues and therapeutic strategies. *Exp Mol Med*. 2019 Dec 19;51(12):1–10.
7. Ramkisoensing AA, de Vries AAF, Atsma DE, Schalij MJ, Pijnappels DA. Interaction between myofibroblasts and stem cells in the fibrotic heart: balancing between deterioration and regeneration. *Cardiovasc Res*. 2014 May 1;102(2):224–31.
8. Plotnikov EY, Khryapenkova TG, Vasileva AK, Marey MV, Galkina SI, Isaev NK, et al. Cell-to-cell cross-talk between mesenchymal stem cells and cardiomyocytes in co-culture. *J Cell Mol Med*. 2008 Sep;12(5A):1622–31.
9. Cselenyák A, Pankotai E, Horváth EM, Kiss L, Lacza Z. Mesenchymal stem cells rescue cardiomyoblasts from cell death in an in vitro ischemia model via direct cell-to-cell connections. *BMC Cell Biol*. 2010 Apr 20;11:29.
10. Li X, Zhao H, Qi C, Zeng Y, Xu F, Du Y. Direct intercellular communications dominate the interaction between adipose-derived MSCs and myofibroblasts against cardiac fibrosis. *Protein Cell*. 2015 Oct;6(10):735–45.
11. Ramkisoensing AA, Pijnappels DA, Swildens J, Goumans MJ, Fibbe WE, Schalij MJ, et al. Gap junctional coupling with cardiomyocytes is necessary but not sufficient for cardiomyogenic differentiation of cocultured human mesenchymal stem cells. *Stem Cells*. 2012 Jun;30(6):1236–45.
12. Lemcke H, Gaebel R, Skorska A, Voronina N, Lux CA, Petters J, et al. Mechanisms of stem cell based cardiac repair-gap junctional signaling promotes

the cardiac lineage specification of mesenchymal stem cells. *Sci Rep*. 2017 Aug 29;7(1):9755.

13. Renu K, V G A, P B TP, Arunachalam S. Molecular mechanism of doxorubicin-induced cardiomyopathy - An update. *Eur J Pharmacol*. 2018 Jan 5;818:241–53.
14. Nebigil CG, Désaubry L. Updates in Anthracycline-Mediated Cardiotoxicity. *Front Pharmacol*. 2018 Nov 12;9:1262.
15. Almeida SO, Skelton RJ, Adigopula S, Ardehali R. Arrhythmia in stem cell transplantation. *Card Electrophysiol Clin*. 2015 Jun;7(2):357–70.